Functional characterization of
B-cell receptor associated protein 31 in cancer cells

Olga Nagło (geb. Chojnacka)

München, 2019

Diese Dissertation wurde angefertigt

unter der Leitung von Prof. Dr. Angelika Vollmar

im Bereich der Pharmazeutischen Biologie

an der Ludwig-Maximilians-Universität München

Erstgutachterin: Prof. Dr. Barbara Conradt

Zweitgutachterin: Prof. Dr. Angelika Vollmar

Tag der Abgabe: 06.06.2019

Tag der mündlichen Prüfung: 13.08.2019

ERKLÄRUNG

Ich versichere hiermit an Eides statt, dass meine Dissertation selbständig und ohne unerlaubte Hilfsmittel angefertigt worden ist.

Die vorliegende Dissertation wurde weder ganz, noch teilweise bei einer anderen Prüfungskommission vorgelegt.

Ich habe noch zu keinem früheren Zeitpunkt versucht, eine Dissertation einzureichen oder

an einer Doktorprüfung teilzunehmen.

München, den 06.06.2019

_____

Olga Nagło

1. TABLE OF CONTENTS

2. INTRODUCTION

2.1 CANCER INCIDENCE AND MORTALITY IN 2018

According to the statistics obtained from the official website of the European Cancer Information System (ECIS) almost 4 million new cancer cases, excluding non-melanoma skin cancer, have been registered in 2018 (ECIS, 2019). These data has been confirmed also by Ferlay et al. in their publication from November 2018. The highest occurrence of cancer was identified in the breast (522 513 cases), followed by colorectal (499 667 cases), lung (470 039 cases) and prostate (449 761 cases) in Europe. Moreover, almost 2 million of deaths due to this disease have been registered. These data show, that cancer is a serious issue and requires scientific interest.

Although cancer is in the interest to the whole scientific world, it is still difficult to make it fully curable. The problem is the variety of cancer types. Each case must be considered individually. Moreover, chemotherapeutic resistances occur, what makes the whole process of treatment even more complicated and challenging. However, every year there are new therapies introduced in this area of medicine. The survival rate in Europe increased significantly in comparison to the previous years. According to Quaresma et al., 10 years survival rate increased from 24% in 1970's to 49.8% in 2010 (Quaresma et al., 2015).

2.2 HALLMARKS OF CANCER

Cancer cells develop a lot of mechanisms to avoid cellular death and to divide infinitely. They can avoid drug induced death, among others, due to self-sufficiency in induction of growth factors release. Moreover, they can ignore anti-proliferative and apoptotic signaling pathways. What is also helpful to survive in a drug environment is unlimited replicative potential. These events lead to infinite growth of those cells.

Cancer cells can also manipulate the environment to force the organism to build a vascular network in their neighborhood, to receive enough cytokines, growth factors, oxygen and nutrients necessary for survival. What is more, cancer cells have the potential to migrate and invade organs through the blood stream (Hanahan & Weinberg, 2000). Those properties are supporting the process of cancer spreading within the organism. Figure 2.1 represents all the

hallmarks of cancer, namely: sustained angiogenesis, limitless growth potential as well as self-sufficiency in growth factors, metastatic and invasive potential and avoidance of the anti-growth and anti-apoptotic signaling.
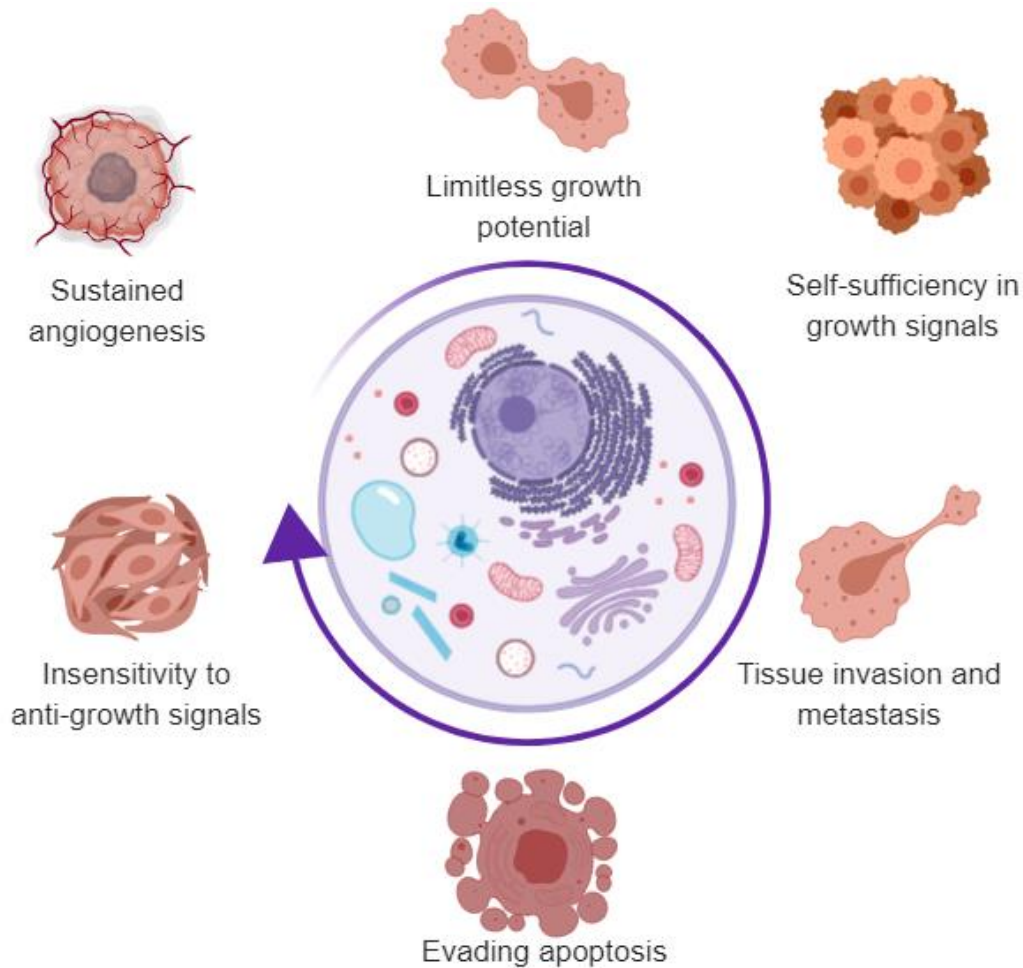
Figure 2.1. Hallmarks of cancer.

2.3 RESISTANCE TO THE COMMON CHEMOTHERAPEUTICS AS A SERIOUS ISSUE

One of the biggest problems in cancer therapy is the ability of cells to form resistance towards chemotherapeutics. A lot of evidence has shown a multitude of drug resistance mechanisms for both - general multi-drug resistance factors and factors specific for one class of drugs (Wijdeven et al., 2016).

Resistance to chemotherapeutics can be divided into two broad categories: intrinsic or acquired. We can assign a resistance to an intrinsic type when cancer cells are resistant towards the chemotherapeutic even before the treatment starts. It can be caused by overexpression of

resistance mediating factors, what results in an ineffective therapy (Holohan et al., 2013). Acquired resistance occurs, when cells form the ability to survive in the presence of a drug. There are many ways for cancer cells to overcome a chemotherapy. Cancer cells can either activate pro-survival signaling or form a mechanism to protect themselves from induction of apoptosis or drug effect. There is a lot of limiting steps before a drug can cause a cellular damage. First limitation is the drug acquirement. Next, it can be either inactivated or the alteration of the drug target can occur. When the drug is already active, the cells can adapt to the new environment or defend themselves through the impairment of apoptosis process (Figure 2.2).
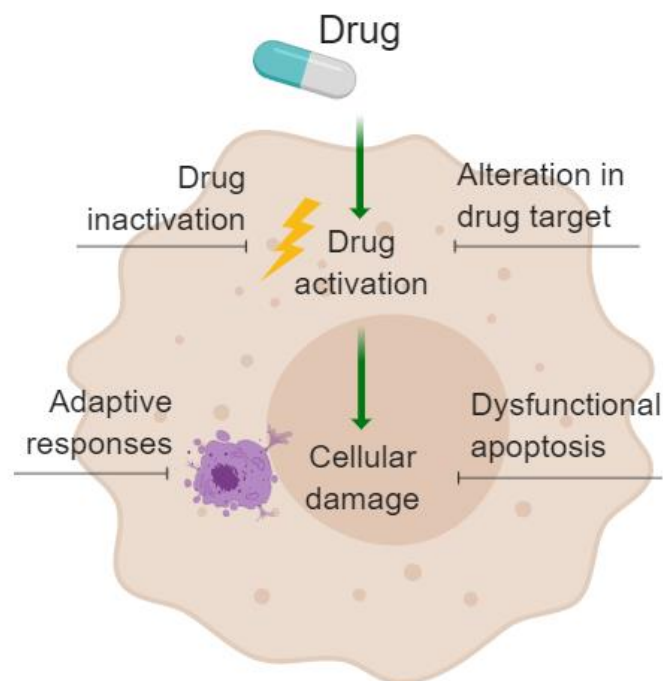
Figure 2.2. General principles of drug resistance. First limiting step of the therapy is the drug acquirement, next factor is a limited drug activation (either through drug inactivation within the cell or alteration in a drug target); even if drug is activated, cells can adapt to the new environment or lead to the dysfunctions in apoptosis process.

Despite a very good development of cancer treatments, there is still a great problem with an insufficient response towards chemotherapeutics. Therefore, combinatorial treatments become more and more popular. The purpose of the combinatorial therapy is either to re-sensitize cancer cells towards common therapeutics or to decrease the dose of drugs to minimalize the side effects. The main rationale behind the combination of more than one drug is to inhibit more than one signaling pathway involved in carcinogenesis, therefore obtaining a synergistic

effect of the treatment. It has been shown before in various cancer types that this approach is successful (Chen & Lahav, 2016). However, the knowledge about the pharmacodynamics, pharmacokinetics and the drugs mechanism of action often remain not fully elucidated. Thus, there is a need to investigate those processes and to deepen the knowledge in this certain topic.

2.4 RE-SENSITIZATION OF CANCEROUS CELLS TOWARDS TREATMENT THROUGH INDUCTION OF ER-STRESS

The endoplasmic reticulum is an organelle in eukaryotic cells, which takes part in the process of protein synthesis, folding, modification and secretion. It is broadly known, that ER homeostasis is impaired when carcinogenesis occurs. When the function of ER is blocked the ER overflows with immature and defective proteins. This situation is called ER stress. This leads to the activation of the unfolded protein response (UPR). The aim of this process is to reduce the amount of defective proteins. UPR consist of three defense mechanisms. The first one is the arrest of further protein synthesis in the ribosomes. The second one is the repair of defective proteins by ER-resident molecular chaperone mobilization. The third one is the elimination and degradation of defective proteins from the ER what is called ER-associated degradation (ERAD) (Kaneko et al., 2017).

It has been shown previously, that targeting the UPR and the ER stress gives good results in re-sensitization of resistant cancerous cells towards the chemotherapeutics (Dufey et al., 2015). Therefore, there is the need to look for drugs targeting the proteins connected to ER homeostasis maintenance and to apply them in combinatorial therapies.

2.5 SMALL MOLECULES – T8 AND PS89

A screening of the commercially available compound library, in terms of chemo-sensitization of cancer cells towards Etoposide treatment, has identified T8 as a promising candidate. A subsequent proteomic analysis has revealed, that the main target of T8 is the protein disulfate isomerase (PDI). The family of PDIs is known as the chaperone proteins and they are involved in the maintenance of the ER homeostasis (Lee & Lee, 2017). Moreover, the interaction between T8 and PDI was reversible, what made this drug very attractive for further investigation (Eirich et al., 2014).

As PDI is a protein required for ER homeostasis maintenance, it has been already shown as an interesting target for chemo-sensitization of cancer cells towards Etoposide induced apoptosis (Xu et al, 2012; Vatolin et al., 2016). However, the interaction of investigated compounds with PDI was not reversible, what reduced their potential in combinatorial treatment approach. Therefore, there was a need for further analysis of substances that are able to interact with PDI.

PS89 has been synthesized as an analogue of T8. The modification has been introduced within two benzene rings (R^1 and R^2). The structures of all derivatives are shown in Figure 2.3 Out of six synthesized molecules PS89 has shown the highest potential in induction of Etoposide mediated apoptosis in Acute Lymphoblastic Leukemia (ALL) cell line - Jurkat. The modification in this molecule consisted of a replacement of fluorine in R^1 by an azide group (Eirich et al., 2014).

Compound		T8	
IC_{50} [µM]		> 300	
Compound	PS83	PS84	PS85
IC_{50} [µM]	240 ± 20	215 ± 17	164 ± 22
Compound	PS86	PS88	PS89
IC_{50} [µM]	203 ± 42	182 ± 48	78 ± 17
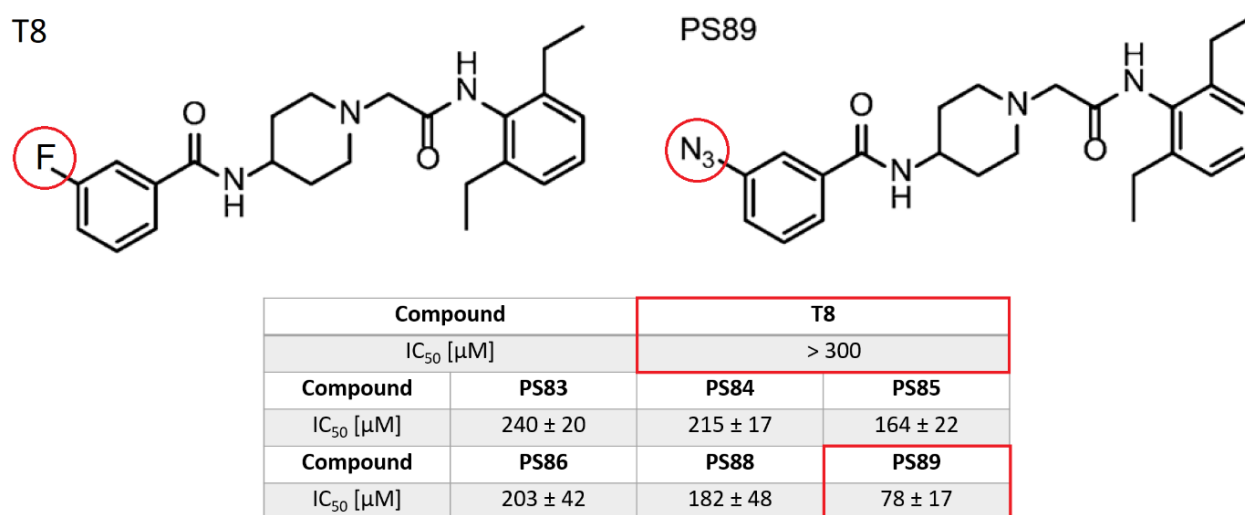
Figure 2.3. The structures of T8 derivatives and the IC50 values in µM in comparison to T8 itself. The figure has been adapted from Eirich et al., 2014.

Surprisingly, what was shown by Dr. Fabian Koczian in his doctoral thesis, PDI was not involved in the chemo-sensitizing effect of PS89. Therefore, the Activity-based Protein Profiling (ABPP) was conduct and identified a B cell receptor - associated protein (BAP31) as one of the interaction partners of PS89.

2.6 FUNCTION OF B CELL RECEPTOR - ASSOCIATED PROTEIN (BAP31) PROTEIN

Bap31 and its homologue Bap29 were originally discovered as B cell receptor-associated proteins. It is an integral ER membrane protein with one cytoplasmic and three transmembrane domains. It has two identical caspase recognition sites at D164 and D238 that are preferentially cleaved by caspase-8. Therefore, upon the apoptotic stimuli, BAP31 can be cleaved into its p20 form which remains in the cellular membrane. (Kim et al., 1994; Breckenridge et al., 2003; Figure 2.4.).
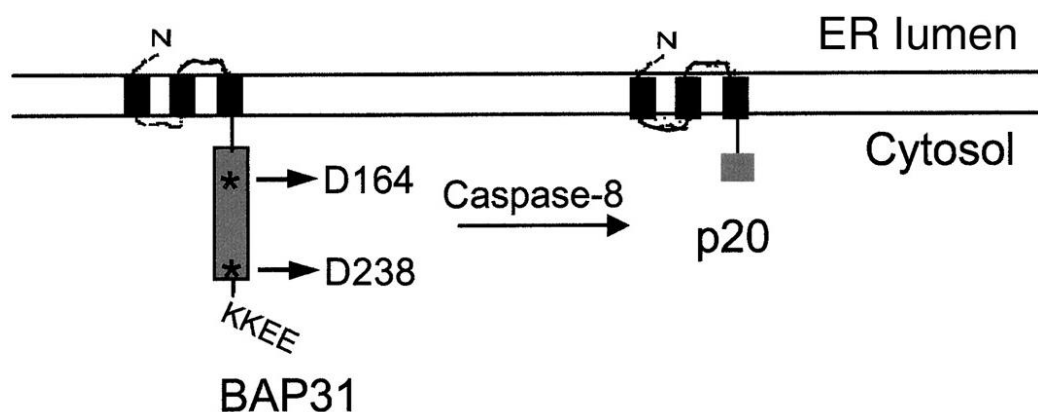
Figure 2.4. The putative structure of BAP31 and its cleavage product upon the apoptotic stimuli and Caspase-8 cleavage. Figure adapted from Breckenridge et al., 2003.

BAP31 is a protein broadly expressed within a cell. According to the GeneCards the subcellular localizations shown in green are derived from database annotations, automatic text mining of the biomedical literature, and sequence-based predictions. The confidence of each association is signified by stars, where 5 is the highest confidence and 1 is the lowest. Therefore, we can conclude that it is very likely to find BAP31 in the plasma membrane as well as in the ER and cytosol. However, so far BAP31 was not seen in the nucleus, lysosomes, endosomes or peroxisomes (Figure 2.5.).

Compartment	Confidence
plasma membrane	5
endoplasmic reticulum	5
cytosol	5
mitochondrion	3
golgi apparatus	3
extracellular	2
cytoskeleton	1
peroxisome	1
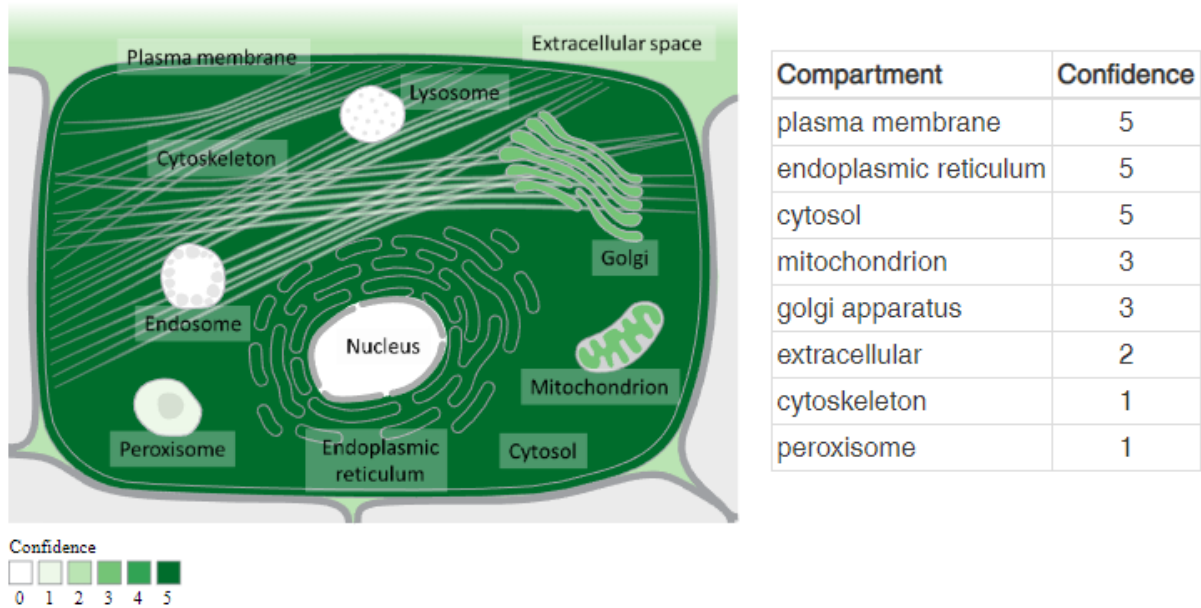
Figure 2.5. BAP31 expression within the mammalian cell. Figure adapted from GeneCards (https://www.genecards.org/cgi-bin/carddisp.pl?gene=BCAP31)

According to the function of BAP31, it was shown to be involved in the process of induction of apoptosis. Wang et al. have shown that a mitochondrial fission protein - Fission 1 homologue (Fis1), transduces the apoptotic signal from ER to mitochondria through an interaction with BAP31 (Wang et al., 2011). Moreover, Nguyen et al. proved, that the induction of Fas - mediated apoptosis leads to the activation of Caspase-8, what results in the cleavage of BAP31, loss of mitochondrial membrane potential ($\Delta\Psi$m) and, finally, cytochrome c release to the cytoplasm (Nguyen et al., 2000; Figure 2.6.). The same schema has been confirmed in the different settings and elucidated to the detail (Breckenridge et al., 2003; Iwasawa et al., 2011, Grimm, 2012).
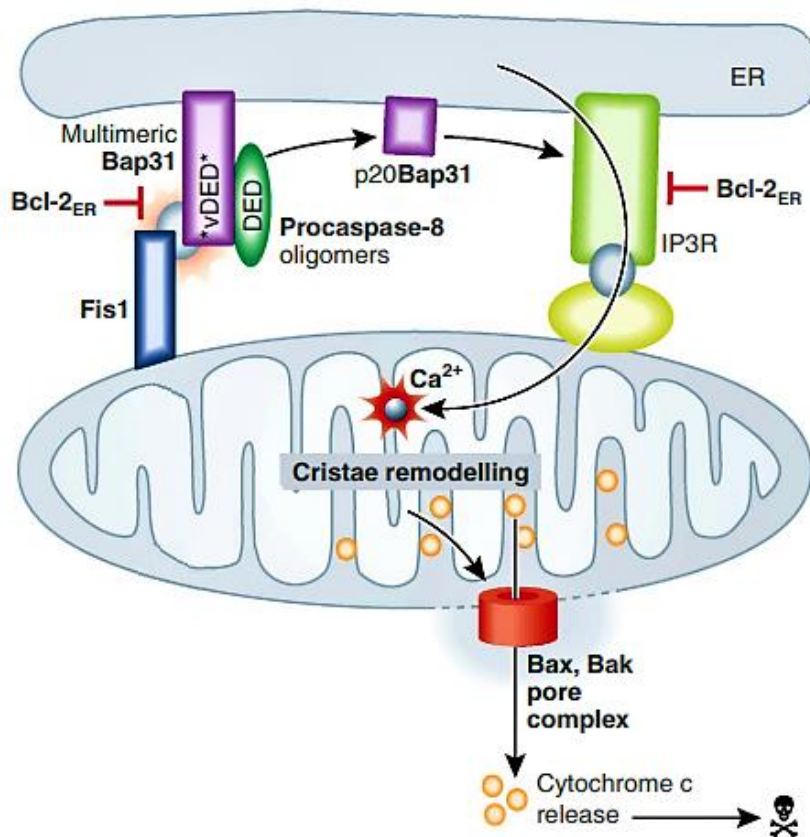
Figure 2.6. Model for the involvement of the Fis1/Bap31/procaspase-8 platform in Bax/Bak-mediated permeabilization of the mitochondrial outer membrane. Additional opportunities for regulation involve pro-survival members of the Bcl-2 family operating at the ER, as well as other targets of p20Bap31 that might influence the ER membrane protein trafficking machinery. Figure adapted from Wang et al., 2011.

Moreover, BAP31 expression has been shown to be connected to the various cancer types. However, this data remains controversial. Namely, Ma et al. have shown that low expression of BAP31 is associated with unfavorable prognosis in human colorectal cancer, when Seo et al. describe that enhanced expression of cell-surface B-cell receptor-associated protein 31 contributes to poor survival of non-small cell lung carcinoma cells. Xu et al., investigating colorectal cancer, could show that suppression of BAP31 via MiR-451a leads to decrease in the proliferation and increase of apoptosis via ER-stress induction. The same was true for Chen et al., who focused on gastric cancer. These data show, that function of BAP31 could be different in various cancer types and also stress out the idea to deepen the knowledge concerning the function of BAP31 in cancer.

3. MATERIALS AND METHODS

3.1 MATERIALS

3.1.1 Cells

Cell line	Supplier
CCRF-CEM	M. Kavallaris, Sydney, Australia
HL-60	ATCC, Manassas, VA, USA
MCF10a	ATCC, Manassas, VA, USA
MDA-MB-231	Cell line Services (CLS), Eppelheim, Germany
SKBR3	Cell line Services (CLS), Eppelheim, Germany

Table 3.1. List of used cell lines.

Patient Derived Xenograft (PDX) cells were kindly provided by PhD Binje Vick, group of Prof. Dr. med. Jeremias (Helmholtz Center Munich, Germany) either from murine bone marrow or spleen. Peripheral blood mononuclear cells (PBMCs) have been freshly obtained from the blood of healthy volunteers as described in section 3.2.3.

RIL175 were kindly provided by Prof. Dr. med. Simon Rothenfußer from the Center of Integrated Protein Science Munich and Division of Clinical Pharmacology, Department of Internal Medicine IV, Hospital of the Ludwig Maximilian University of Munich.

3.1.2 Compounds

Substance	Solvent	Storage (ºC)	Supplier
Brefeldin A	DMSO	-20ºC	Sigma-Aldrich, St Louis, MO, USA
Cerulenin	Ethanol	-20ºC	Sigma-Aldrich, St Louis, MO, USA
CP-640,186	Ethanol	-20ºC	Sigma-Aldrich, St Louis, MO, USA
Daunorubicin	DMSO	-20ºC	Sigma-Aldrich, St Louis, MO, USA
Etoposide	DMSO	-20ºC	Sigma-Aldrich, St Louis, MO, USA

PS89	DMSO	-20ºC	University of Saarland, Saarbrücken, Germany
Soraphen A	Ethanol	-20ºC	University of Saarland, Saarbrücken, Germany
TOFA	DMSO	-20ºC	Sigma-Aldrich, St Louis, MO, USA
UCM05	Ethanol	-20ºC	Sigma-Aldrich, St Louis, MO, USA
Vincristine	DMSO	-20ºC	Sigma-Aldrich, St Louis, MO, USA

Table 3.2. List of used compounds.

3.1.3   Chemicals and Reagents

Reagent	Supplier
2,2,2 - Trichloroethanol (TCE)	Sigma Aldrich, St Louis, MO, USA
Adenine	Sigma Aldrich, Taufkirchen, Germany
Ammonium persulfate (APS)	Sigma Aldrich, St Louis, MO, USA
Aureobasidin A	Takara Bio USA, Inc., Mountain View, CA, USA
BamHI	New England BioLabs, Ipswich, MA, USA
Blasticidin	Thermo Fisher, Waltham, MA, USA
Bovine Serum Albumine (BSA)	Sigma Aldrich, Taufkirchen, Germany
Cal-520 AM	AAT Bioquest, Sunnyvale, CA, USA
Calcium chloride	Sigma Aldrich, Taufkirchen, Germany
Carboxy-H2DCFDA	Thermo Fisher, Waltham, MA, USA
Cell-Titer Blue (CTB)	Promega, Madison, WI, USA
Cholera toxin from *Vibrio cholerae*	Sigma Aldrich, Taufkirchen, Germany
Complete® mini EDTA free	Sigma Aldrich, Taufkirchen, Germany
Coumaric acid	Fluka, Buchs, Switzerland
Crystal Violet	Carl Roth, Karlsruhe, Germany

D-glucose	Merck, Darmstadt, Germany
DharmaFECT transfection reagent	GE Dharmacon, Lafayette, CO, USA
Dimethyl sulfoxide (DMSO)	AppliChem, Darmstadt, Germany
Disodium hydrogen phosphate	Grüssing GmbH, Filsum, Germany
Dithiothreitol (DTT)	Sigma Aldrich, Taufkirchen, Germany
Dulbecco's modified Eagle's medium (DMEM)	PAN Biotech, Aidenbach, Germany
Dulbecco's Modified Eagle Medium/Nutrient Mixture F-12 (DMEM/F12)	PAN Biotech, Aidenbach, Germany
EcoRI	New England BioLabs, Ipswich, MA, USA
EGF tetramethylrhodamine conjugate	Life Technologies, Carlsbad, CA, USA
Epidermal Growth Factor (EGF)	PeproTech Inc., Rocky Hill, NJ, USA
Ethylenediaminetetraacetic acid (EDTA)	Carl Roth, Karlsruhe, Germany
Fetal calf serum (FCS)	PAN Biotech, Aidenbach, Germany
Ficoll-Paque PLUS	GE Healthcare, Chicago, IL, USA
FluorSave^{TM} Reagent mounting medium	Merck, Darmstadt, Germany
Formaldehyde 16%, ultrapure	Polysciences, Warrington, PA, USA
Glycerol	Sigma Aldrich, Taufkirchen, Germany
Glycine	ORG Laborchemie, Bunde, Germany
HEPES	Sigma Aldrich, Taufkirchen, Germany
Hoechst 33342	Sigma Aldrich, St Louis, MO, USA
Horse serum	Invitrogen, Karlsruhe, Germany
Human Methylcellulose Complete Media	R&D Systems, Inc., Minneapolis, MN, USA
Hydrocortisone	Sigma Aldrich, Taufkirchen, Germany

Hydrogen Peroxide	Sigma Aldrich, Taufkirchen, Germany
Insulin from bovine pancreas	Sigma Aldrich, Taufkirchen, Germany
Leucine	Sigma Aldrich, Taufkirchen, Germany
Lipofectamine 3000	Thermo Fisher, Waltham, MA, USA
L-Tryptophan	Sigma Aldrich, Taufkirchen, Germany
Luminol	AppliChem, Darmstadt, Germany
L-α-Phosphatidylinositol ammonium salt solution from bovine liver – PI mix	Sigma Aldrich, Taufkirchen, Germany
Magnesium chloride hexahydrate	Grüssing GmbH, Filsum, Germany
Magnesium sulfate heptahydrate	Grüssing GmbH, Filsum, Germany
Matchmaker Gold Yeast Two-Hybrid System	Takara Bio USA, Inc., Mountain View, CA, USA
Methanol	Sigma Aldrich, Taufkirchen, Germany
Monopotassium phosphate (KH_2PO_4)	Sigma Aldrich, Taufkirchen, Germany
N,N,N′,N′-Tetrametyloetylenodiamina (TEMED)	VWR, Radnor, PA, USA
Nonfat powdered milk (Blotto)	Carl Roth, Karlsruhe, Germany
ON-TARGETplus siRNA against: ACC1, BAP31 and TRA2B	GE Dharmacon, Lafayette, CO, USA
Opti-MEM™	Thermo Fisher, Waltham, MA, USA
Page Ruler ™ Prestained Protein Ladder	Thermo Fisher, Waltham, MA, USA
Penicillin/Streptomycin 100x	PAA Laboratories, Pasching, Austria
Phenylmethylsulfonyl fluoride (PMSF)	Sigma Aldrich, Taufkirchen, Germany
Pierce™ BCA Protein Assay Kit	Thermo Fischer Scientific, Waltham, MA, USA

Polyacrylamide (Rotiphorese® Gel A 30%)	Carl Roth, Karlsruhe, Germany
Potassium chloride	AppliChem GmbH, Darmstadt, Germany
Propidium iodide	Sigma Aldrich, Taufkirchen, Germany
Puromycin	Thermo Fisher, Waltham, MA, USA
Pyronin Y	Sigma Aldrich, Taufkirchen, Germany
Pyruvate	Merck, Darmstadt, Germany
Roswell Park Memorial Institute (RPMI) 1640 Medium	PAN Biotech, Aidenbach, Germany
siRNA buffer (5x)	GE Dharmacon, Lafayette, CO, USA
Sodium bicarbonate	Grüssing GmbH, Filsum, Germany
Sodium chloride (NaCl)	Sigma Aldrich, Taufkirchen, Germany
Sodium citrate	Carl Roth, Karlsruhe, Germany
Sodium dodecyl sulfate (SDS)	AppliChem, Darmstadt, Germany
T7 Endonuclease I	New England BioLabs, Ipswich, MA, USA
Transferrin from human serum tetramethylrhodamine conjugate	Invitrogen, Karlsruhe, Germany
Tris	Sigma Aldrich, Taufkirchen, Germany
Tris-HCl	Sigma Aldrich, Taufkirchen, Germany
Triton X-100	Merck, Darmstadt, Germany
Trypsin	PAN Biotech, Aidenbach, Germany
Tween® 20	BDH/Prolabo®, Ismaning, Germany
X-α-Gal	Takara Bio USA, Inc., Mountain View, CA, USA

Yeast Synthetic Drop-out Medium Supplements without histidine, leucine, tryptophan and uracil (QDO)	Sigma Aldrich, Taufkirchen, Germany
Yeast Synthetic Drop-out Medium Supplements without Leucine and Tryptophan (DDO)	Sigma Aldrich, Taufkirchen, Germany

Table 3.3. List of chemicals, reagents, inhibitors and kits used during experiments.

All commonly used acids, bases, buffer salts and organic solvents were either purchased from Merck (Darmstadt, Germany) or Sigma-Aldrich (St Louis, MO, USA).

3.1.4 Primary antibodies

Antibody	Product No.	Origin	Supplier
ACC1	#4190	Rabbit	Cell Signaling, Danvers, MA, USA
BAP31 (B-10)	sc-365347	Mouse	Santa Cruz, Dallas, TX, USA
BCAP31	HPA003906	Rabbit	Sigma Aldrich, St Louis, MO, USA
BiP	610978	Mouse	BD, Franklin Lakes, NJ, USA
Caspase-3	C8487	Rabbit	Sigma Aldrich, St Louis, MO, USA
Caspase-8	#9746	Mouse	Cell Signaling, Danvers, MA, USA
CD34	555821	Mouse	BD, Franklin Lakes, NJ, USA
Cytochrome c	#4272	Rabbit	Cell Signaling, Danvers, MA, USA
EGFR	#2239	Mouse	Cell Signaling, Danvers, MA, USA
EGFR pTyr1068	#2234	Rabbit	Cell Signaling, Danvers, MA, USA
HER2	#2156	Rabbit	Cell Signaling, Danvers, MA, USA
HER2 pTyr1221/1222	#2243	Rabbit	Cell Signaling, Danvers, MA, USA

Histone 3	ab1791	Rabbit	Abcam, Berlin, Germany
LC3 I/II	#4108	Rabbit	Cell Signaling, Danvers, MA, USA
NF-kB p65	sc-372	Rabbit	Santa Cruz, Dallas, TX, USA
PARP	#9542	Rabbit	Cell Signaling, Danvers, MA, USA
PRMT2	AV40196	Rabbit	Sigma Aldrich, St Louis, MO, USA
SQSTM1/p62	#5114	Rabbit	Cell Signaling, Danvers, MA, USA
TRA2B	ab31353	Rabbit	Abcam, Berlin, Germany
VDAC	#4866	Rabbit	Cell Signaling, Danvers, MA, USA

Table 3.4. List of primary antibodies used in experiments.

3.1.5 Secondary antibodies

Antibody	Product No.	Origin	Supplier
Alexa Fluor 488-conjugated mAb18	A-11008	Goat	Invitrogen, Karlsruhe, Germany
Alexa Fluor 546-conjugated mAb18	A-11003	Goat	Invitrogen, Karlsruhe, Germany
Alexa Fluor 633-conjugated mAb18	A - 21050	Goat	Invitrogen, Karlsruhe, Germany
HRP, Anti-Mouse IgG1	ab97240	Goat	Abcam, Berlin, Germany
HRP, Anti-Rabbit	111-035-144	Goat	Dianova, Hamburg, Germany
HRP, Anti-Rabbit IgG	172-1019	Goat	Bio-Rad, Hercules, CA, USA

Table 3.5. List of secondary antibodies used in experiments.

3.1.6 Technical equipment

Device	Function	Manufacturer
Abbocath-T 14 G, 2,2 x 51 mm	Cannula	ICU Medical Germany GmbH, Lüdenscheid, Germany
Amersham NC/PVDF (0,2μM, 0,45μM)	Blotting membrane	GE Healthcare, Chicago, IL, USA
BD Discardit 5ml Eccentric Tip Syringe	Syringe	BD Biosciences, Heilderberg, Germany
BD FACS Canto^{TM} II	Flow cytometer	BD Biosciences, Heilderberg, Germany
Canon EOS 450C	Camera	Canon, Tokyo, Japan
Cell culture flasks, tubes and plates	Disposable cell culture material	Nunc, Thermo Fisher, Waltham, MA, USA
Chemidoc^{TM} Touch Imaging System	Immunoblot Imaging	Bio-Rad, Hercules, CA, USA
Consort power supply E835	Electrophoresis	Sigma Aldrich, St Louis, MO, USA
HBT 130-2	Thermoblock	Haep Labor Consult, Bovenden, Germany
HeraCell	Incubator	Heraeus, Hanau, Germany
ibiTreat μ-slide	Microscopy 8-well slide	Ibidi, Planegg, Germany
Mikro 22R	Microcentrifuge	Hettich, Tuttlingen, Germany
Mini Protean 3	Electrophoretic transfer	Bio-Rad, Hercules, CA, USA
Nucleofector^{TM} II Device	Transfection through electroporation	Lonza, Basel, Switzerland
Olympus CK30	Inverted microscope	Olympus, Tokyo, Japan

Rotina 46R	Centrifuge	Hettich, Tuttlingen, Germany
SP8 LSM system	Confocal microscope	Leica, Wetzlar, Germany
SpectraFluor Plus	Fluorescence reader	Tecan, Ma nnedorf, Switzerland
Tecan Sunrise	Absorbance reader	Tecan, Ma nnedorf, Switzerland
Thermoshake, Laboshake	Thermoshaker	Gerhard Analytical Systems, Königswinter, Germany
Tube 4ml, 75x12mm, K3E	Blood collection	SARSTEDT AG & Co. KG, Nümbrecht, Germany
Vi-Cell^{TM} XR	Cell viability analyzer	Beckman Coulter, Brea, CA, USA
Zeiss LSM 510	Confocal microscope	Zeiss, Oberkochen, Germany

Table 3.6. List of technical equipment necessary for cell culture and analytics.

3.1.7 Software

Software name and version	Supplier
BioRender	BioRender, Toronto, Ontario, USA
BLAST	NCBI, U.S. National Library of Medicine, Bethesda, MD, USA
DNAMAN	Lynnon LLC., San Ramon, CA, USA
FlowJo v7.6.5	Tree Star, Ashland, OR, USA
GraphPad Prism 7/8	GraphPad Software, San Diego, CA, USA
Image Lab v5.2	Bio-Rad, Hercules, CA, USA
ImageJ	National Institutes of Health, LOCI, University of Wisconsin, USA
Leica LAS X	Leica, Wetzlar, Germany
Microsoft Office 2016	Microsoft, Redmont, WA, USA

Table 3.7. Software used for the evaluation and analysis of the data.

3.2 CELL CULTURE

3.2.1 Maintenance of cell lines

SKBR3, MDA-MB-231 as well as RIL-175 cancer cell lines were cultivated in DMEM culture medium supplemented with 10% fetal calf serum (FCS) and 1% Penicillin/Streptomycin (P/S). MCF10A mammary epithelial cells were cultivated in DMEM/F12 Mix 1:1 supplemented with 5% horse serum, 20 µg/l EGF, 10 mg/l insulin, 0,5 mg/l hydrocortisone, 0,1 mg/l cholera toxin and 1% P/S. HL-60 and CCRF-CEM cell lines were cultivated in RPMI 1640 medium with 2 mM glutamine supplemented with 10% FCS and 1% of P/S. All the cell lines were kept in a humidified incubator at 37°C under a 5% CO_2 atmosphere.

Cells were passaged twice a week before they reached 90% confluence. To detach them from the culture dish, after washing flask twice with PBS (Table 3.8.), 1ml of Trypsin/EDTA (T/E) solution (Table 3.8.) was added. Cells were incubated together with T/E at 37ºC until all of them lost their adhesion to the bottom of the culture dish. The trypsinization process was stopped with 10ml of complete culture medium. Cell density was determined using Vi-Cell^{TM} XR device. One million of either SKBR3 or MDA-MB-231, two million of MCF10A or 0,5 million of RIL-175 were seeded back in the culture flask for further cultivation.

Suspension cell lines were split by using one million of cells per 10 ml of fresh medium.

Phosphate-buffered saline (PBS), pH 7,4		Trypsin/EDTA	
NaCl	123,3 mM	Trypsin	0,05%
Na_2HPO_4	10,4 mM	EDTA	0,02%
KH_2PO_4	3,2 mM	PBS	
H_2O			

Table 3.8. Buffers and solutions commonly used in cell culture.

24

3.2.2 Freezing and thawing process

To store the cells for a long term, they were frozen in liquid nitrogen. For the cryopreservation purpose, the cultivation medium was supplemented with 20% FCS, 1% P/S and 10% DMSO. One milliliter of cell suspension in concentration of $1 \cdot 10^6$/ml was transferred into each cryovial. Cells were frozen at -80ºC for 24 hours and, subsequently, transferred to the tanks with liquid nitrogen.

To thaw the cell line, cells were taken from the storage tank and quickly thawed in a water bath at 37ºC. Once the suspension of cells became liquid, it was transferred to the falcon tube containing 10 ml of fresh, complete medium. Cells were centrifuged for 5 minutes at 1000 rpm. Supernatant was discarded and cells were re-suspended in 5 ml of complete culture medium. Next, they were transferred into a T25 cell culture flask.

3.2.3 Isolation of Peripheral Blood Mononuclear Cells (PBMCs)

Blood samples were collected from healthy volunteers to EDTA-coated vials. Subsequently, blood was diluted 1:1 with PBS and layered on top of Ficoll-Paque PLUS density gradient media in 50ml plastic tubes. Next, tubes were centrifuged for 40 minutes at 1490 rpm. Both parameters – accel and decel – were set to 1, to avoid disruption of layers through rapid start or stop of the centrifuge. The layer of PBMCs (Figure 3.1.) was collected using a big needle and a syringe and washed once with PBS. Cells were re-suspended in RPMI 1640 medium supplemented with 1 mM pyruvate, 20% FCS and 1% P/S, seeded in appropriate plates and stimulated with compounds of choice.
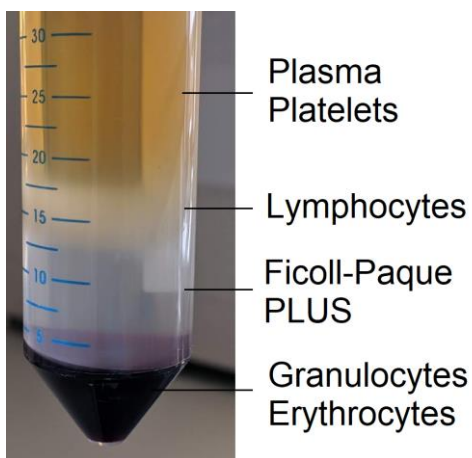
Figure 3.1. Layers obtained after gradient centrifugation using a Ficoll-Paque PLUS reagent.

3.2.4 Generation and isolation of patient derived xenograft cells (PDX)

Cultivation of Patient Derived Xenograft (PDX) cells in vivo was described by Terziyska N. et al., 2012 and Vick B. et al., 2015. For the purpose of experiments, cells were freshly separated from either spleen or bone marrow of NOD *scid* gamma (NSG) mice. Subsequently, they were cultivated in RPMI 1640 medium supplemented with 4µg/l Na Selen, 6mg/l Insulin, 3mg/lTransferin, 1 mM Natrium Pyruvat and 50 µM a-Thioglycerol (a-TG) in the presence of compounds or with the mock.

3.2.5 Stimulation with compounds

Cells were seeded one day before stimulation and left overnight to appropriately attach to the experimental dish. Compounds were dissolved in culture medium. Controls were treated with the highest volume of solvent used for stimulation during the experiment. DMSO, as a solvent, did not exceed 0,5% of experimental volume of medium. A list of compounds is provided in Table 3.2.

3.3 PROLIFERATION AND ATTACHMENT ASSAYS

3.3.1 Cell-Titer Blue® viability assay

Cell-Titer-Blue® (CTB) viability assay (Promega, Madison, WI, USA) was used to determine proliferation rate of experimental cells. This assay relays on the ability of living cells to metabolize a redox dye – Resazurin – into a fluorescent product – Resorufin. As dying cells are losing their metabolic capability, they do not generate any fluorescent singal.

To determine the proliferation capacity, cells were seeded in 96-well plates in a number of 1000 cells/well. On the next day, cells were treated with compounds of our choice (Em experimental) or mock (Em control), and further cultivated in complete medium in a total amount of 200µl. After 72 or 96 hours of proliferation, 40µl of CTB reagent was added to each well. Cells were incubated for 2 hours at 37ºC. The fluorescent signal was recorded at 595nm, with an excitation at 550 nm, using a Tecan SpectraFluor Plus microplate reader. The signal assessed at day 0 served as a reference (Em reference). The proliferation of cells was calculated as follows:

$$\frac{Em\ experimental - Em\ reference}{Em\ control - Em\ reference} \times 100\% = proliferation$$

3.3.2 ViCell – counting of the cell number

Cells were seeded in 24-well plates in the number of $0,5 \cdot 10^5$ cells/well in 400 µl of culture medium in triplicates. They were cultivated for 72 hours and, subsequently, trypsinized, diluted in 2ml of culture medium and counted using ViCell device. The data has been normalized to 100% for the wild type control.

3.3.3 xCELLigence – the real-time analysis of the cellular growth and attachment

Cells have been seeded in the number of $4 \cdot 10^3$ cells/well in the special plate. Right after the seeding, the plate was installed in the xCELLigence device and the real-time measurement was conducted for the next 72 hours. Subsequently, the data were analyzed using the RTCA 2.0 software, which allows the calculation of the doubling time for each sample.

Out of this data, we were able to compare also the attachment ability of the cells. For this purpose, we analyzed a change in the cell index just for the first 120 minutes.

3.3.4 Attachment analysis – crystal violet staining

To verify the attachment capability of the cells, they were seeded in the number of $0,5 \cdot 10^6$ cells/well in 6-well plates and left for 30 minutes, 37ºC to attach to the bottom of the well. Next, not attached cells were washed out with PBS. Remaining cells were stained using 500 µl of crystal violet solution for 5 minutes with shaking. Next, the crystal violet was washed out and the number of cells attached to the bottom was counted.

3.3.5 Colony formation assay

Leukemia HL-60 cells pre-treated for 24h with either single treatment with PS89 25µM, Mercaptopurine 100µM, or combination of those compounds were seeded in the amount of $1 \cdot 10^4$

/well in 1ml of Human Methylcellulose Complete Media in triplicates into 12-well plate. Single cells were distributed equally over the well and incubated for 7 days at 37°C to check their ability to form the colonies out of the single cell. After 7 days, the pictures were captured, and the number of colonies was counted using Image J software.

3.4 IMMUNOBLOTTING

3.4.1 Preparation of samples

Cells, after an appropriate treatment, were washed twice with PBS and lysed using Triton X-100 lysis buffer (Table 3.9.), 200µl/well in 6-well plate. Immediately, plates were frozen at -20°C for at least 1 hour to improve lysis of all the cellular membranes. Subsequently, samples were thawed on ice for 30 minutes. Next, they were scratched from the plates and transferred to the 1,5 ml plastic tubes. Samples were centrifuged for 10 minutes at 14 000 rpm. Supernatant was used for further determination of protein concentration.

Triton X-100 lysis buffer (pH 8,0)	
NaCl	150mM
Tris-HCl	50mM
Triton X-100	1%
Complete 25x	4%

Table 3.9. Tritron X-100 lysis buffer used to prepare samples for immunoblotting.

3.4.2 Preparation of samples for the cytosol/mitochondrial fractionation

Cells were seeded in 10 cm petri dishes in a number of 1 million in 10 ml of medium. To isolate the fractions of cytoplasm and mitochondria, cells after the required stimulation were lysed with Digitonin lysis buffer (Table 3.10) for 20 minutes on ice. Next, cells were collected to the 1,5ml plastic tubes and centrifuged for 10 minutes at 13 000 rpm. The supernatant was collected to the fresh tube as the cytosolic fraction. The pellet was subjected to the lysis with Triton X-100 lysis

buffer (Table 3.9) for 30 minutes on ice. Subsequently, the mixture was centrifuged for 10 minutes at 14 000 rpm and the supernatant was collected as the mitochondrial fraction.

Digitonin Lysis buffer (pH 7,2)	
Hepes 7,2 pH	10mM
Na_2EGTA	0,2 mM
Succinate	5 mM
Sucrose	200 mM
BSA	0,15% (w/v)
Mannitol	210 mM
Digitonin	80 µg/ml
H_2O	

Table 3.10. Digitonin lysis buffer used to prepare samples for immunoblotting.

3.4.3   Preparation of samples for the cytosol/nuclear fractionation.

Cells were seeded in 10 cm petri dishes in a number of 1 million in 10 ml of medium. To isolate the fractions of cytoplasm and nucleus, cells were detached using T/E, centrifuged for 5 minutes at 1000 rpm and the medium was discarded. Cells were washed with PBS and lysed with 5 pellet volumes of Cytoplasmic Extract (CE) Buffer (Table 3.11) for 3 minutes on ice. Next, cells were centrifuged for 10 minutes at 13 000 rpm. The collected supernatant was transferred to the fresh tube as the cytosolic fraction. The pellet was subjected to the lysis with 2 pellet volumes of Nuclear Extract (NE) buffer and 30 µl of 5 M NaCl (Table 3.11) for 20 minutes on ice. Subsequently, the mixture was centrifuged for 10 minutes at 14 000 rpm and the supernatant was collected as the nuclear fraction. Both supernatants were centrifuged once again to discard the remaining pollution.

Cytoplasmic Extract buffer (pH 7,6)		Nuclear Extract buffer (pH 8,0)	
Hepes pH 7,6	10 mM	Tris-HCl pH 8,0	20 mM
KCl	60 mM	NaCl	420 mM
EDTA	1 mM	EDTA	200 µM
NP40	0,075% (v/v)	$MgCl_2$	1,5 mM
DTT	1 mM	PMSF	1 mM
PMSF	1 mM	Glycerol	25% (v/v)
Complete protease inhibitor		Complete protease inhibitor	
H_2O		H_2O	

Table 3.11. Cytoplasmic Extract and Nuclear extract buffers used to prepare samples for immunoblotting.

3.4.4 Determination of protein concentration

Pierce™ BCA Protein Assay Kit relays on the reduction of Cu^{2+} to Cu^+. In the first step copper is chelated by a protein. This reaction leads to the formation of light blue complex. In the second step of the reaction, bicinchoninic acid (BCA) reacts with the reduced (cuprous) cation that was formed in step one. The intense purple-colored reaction product results from the chelation of two molecules of BCA with one cuprous ion. The absorbance is measured at 550 nm wave length.

To ensure that the same amount of the protein is loaded, each sample was diluted 1:5 with water and triplicates of the dilution, 10 µl each, were transferred onto 96-well plate. Bovine Serum Albumin (BSA) standards were used to create a standard curve. To each well 190 µl of Pierce™ BCA Protein Assay Kit solution was added, and the plate was incubated for 40 minutes, room temperature, shaking in dark. Subsequently, absorbance was measured with Tecan Sunrise reader and the protein concentration was determined by linear regression using GraphPad Prism 7/8 software. Samples for western blot were prepared using 40 µg of protein mixed with SDS sample buffer (Table 3.12.). Samples were boiled for 5 minutes at 95ºC.

5x SDS sample buffer		1x SDS sample buffer	
Tris-HCl (pH 6,8)	3.125 M	5x SDS sample buffer	20%
Glycerol	50 %	H_2O	
SDS	5 %		
DTT	2 %		
Pyronin Y	0,025%		
H_2O			

Table 3.12. Sample buffers used for western blot.

3.4.5   Sodium dodecyl sulfate – polyacrylamide gel electrophoresis (SDS-PAGE)

To separate the proteins according to their size, polyacrylamide gels were used (Table 3.13.). The density of the gel was adjusted to the protein size, mostly 12%. The chamber of a Mini Protean 3 system from Bio-Rad was filled with electrophoresis buffer (Table 3.13.) and prepared samples were loaded. A Page Ruler Pre-stained protein ladder was used as a reference for a protein size. Electrophoresis was performed for 20 min at 100V and 40 min at 200 V. Subsequently, gels were imaged using ChemiDoc^TM Touch Imaging system for further evaluation of samples loading. The "stain free" setting allows to detect trichloroethanol (TCE), which is added to the separation gel.

Stacking gel		Separation gel 12%		Electrophoresis buffer	
Rotiphorese Gel 30	17 %	Rotiphorese Gel 30	40 %	Tris	4,9 mM
Tris-HCl (pH 6,8)	125 mM	Tris-HCl (pH 8,8)	375 mM	Glycine	38 mM
SDS	0,1 %	SDS	0,1 %	SDS	0,1 %
TEMED	0,2 %	TEMED	0,1 %	H_2O	
APS	0,1 %	APS	0,05 %		
H_2O		TCE	0,5 %		
		H_2O			

Table 3.13. Recipes for electrophoresis and gels used for western blot.

3.4.6 Blotting process

To transfer proteins onto the membrane of choice (depending on the protein size either PVDF or Nitrocellulose), in order to make them accessible for the detection, a "sandwich" was carefully composed of blotting paper, gel, membrane and sponge filters. This complex composition was transferred into the blotting tank supplemented with ice pack and 1x tank buffer (Table 3.14.). The blotting process was performed for 1,5 hours at 100 V at 4ºC. To cool the tank buffer more efficiently a magnetic stirrer was used.

Tank buffer 5x		Tank buffer 1x
Tris-Base	240 mM	Tank buffer 5x 20 %
Glycine	195 mM	Methanol 20 %
H_2O		H_2O

Table 3.14. Buffer used for blotting process.

3.4.7 Protein detection

To avoid unspecific binding of antibodies, the membrane was blocked using 5% Blotto solution (Table 3.15.) for at least 1 hour. Next, primary antibody diluted 1:1000 in 5% BSA was applied and membrane was incubated overnight at 4ºC. Subsequently, the membrane was washed 3 times for 5 minutes with the PBS-T buffer (Table 3.15.). Following, the membrane was incubated with a secondary antibody diluted 1:1000 in 1% Blotto solution for next 2 hours, room temperature. After that, membrane was washed once again as described above.

To detect a signal from enhanced chemiluminescence (ECL), an ECL solution (Table 3.15.) was applied for 1 minute. In this type of detection, horseradish peroxidase (HRP) conjugated to the secondary antibody oxidizes luminol. Chemiluminescent signal was visualized using ChemiDoc^{TM} Touch Imaging system. Evaluation of Western Blots was performed using Image Lab^{TM} software.

PBS-T (pH 7,6)	
NaCl	123,3 mM
Na_2HPO_4	10,4 mM
KH_2PO_4	3,2 mM
Tween20	0,1 %
H_2O	

ECL buffer	
Tris (pH 8,5) 100 mM	
Luminol 2,5 mM	
Coumaric acid 1mM	
H_2O_2 17 µM	
H_2O	

Blotto 5%	
Milk Powder	5%
PBS-T	

Table 3.15. Buffers used for the membrane development.

3.5 FLOW CYTOMETRY

3.5.1 Analysis of apoptosis

Loss of the nuclear DNA due to the DNA fragmentation is characteristic for the apoptosis process. The usage of the fluorochrome like propidium iodide (PI), which binds to the DNA, enables a rapid and precise evaluation of the cellular DNA content. Using flow cytometry enables

identification of the population of the cells which are hypodiploid (Nicoletti et al., 1991). Therefore, propidium iodide staining can be applied to analyze a sub-G1 population of the cells, which are containing less DNA in comparison to the cells in the normal state, what indicates that they are apoptotic.

To analyze the apoptosis rate, cells were seeded and treated with compounds as depicted. Next, the cells were harvested and put to the plastic FACS tubes (detached with T/E, if applicable) and centrifuged 5 minutes, 1000 rpm, 4ºC. The supernatant was discarded. Cells were washed with 1ml of PBS and centrifuged as described above. PBS was discarded and 200µl of HFS solution (Table 3.16.) was added to each tube. FACS measurement was performed not earlier than 30 minutes after staining.

For the analysis of apoptosis Flow-Jo 7.6 software was used. It was assessed as a percent of sub-G1 population out of all events. To analyze the cell cycle frequency, the PI stained cells were recorded on the linear x-axis and analyzed applying Watson Pragmatic univariate model.

Hypotonic Fluorochrome Solution (HFS)
Propidium iodide 50 µg/ml
Sodium citrate 0.1% (w/v)
Triton X-100 0.1% (v/v)
PBS

Table 3.16. Hypotonic Fluorochrome Solution (HFS).

3.5.2 Measurement of cytosolic calcium level

Cal-520 AM dye can easily cross the cellular membrane. Once it is inside a living cell, its lipophilic blocking groups are cleaved by esterases. This leads to a change of the molecular charge from positive to negative, what prevents the dye to cross the cellular membrane back. When the imprisoned dye binds to the calcium ions, its fluorescence is greatly enhanced.

To measure the level of calcium ions in the cytoplasm, the cells were loaded with 1µM solution of Cal-520 AM dye in Hanks and Hepes Buffer (HHBS, Table 3.17.) for 90 minutes at 37ºC and 30

minutes at room temperature. To load the cells with the dye, they were harvested to plastic FACS tubes, centrifuged (1000 rpm, RT, 5min) and the supernatant was discarded. The Cal-520 AM dye solution was applied. Next, the cells were washed with HHBS and re-suspended in 200µl of propidium iodide solution in HBSS. The FACS measurement was performed immediately after staining.

Propidium iodide staining was used to distinguish between dead and living cells. Compensation calculation was applied to define each dye. Using Flow Jo 7.6 software, PI positive cells were excluded and the living cells were evaluated for Cal-520 AM fluorescent signal intensity using the FACSCanto II device at Ex 488 nm and Em 530/30 nm.

HHBS (pH 7,2)					
$CaCl_2$	1,26 mM	KCl	5,33 mM	$MgSO_4$ x 7 H_2O	0,41 mM
D-glucose	5,56 mM	KH_2PO_4	0,44 mM	Na_2HPO_4	0,34 mM
Hepes	20 mM	$MgCl_2$ x 6 H_2O	0,49 mM	NaCl	137,9 mM
$NaHCO_3$	4,17 mM	H_2O			

Table 3.17. Hanks and Hepes Buffer.

3.5.3   Measurement of Reactive Oxygen Species (ROS) level

Carboxy-H2DCFDA (6-carboxy-2',7'-dichlorodihydrofluorescein diacetate) is an acetated form of fluorescein, which is used to measure cellular levels of reactive oxygen species. Carboxy-H2DCFDA is a non-fluorescent dye and the esterase cleavage of its lipophilic blocking groups yields a charged form of the dye that is much better retained by cells than is the parent compound. Once the carboxy-H2DCFDA diffuses into the cell, esterases cleave the dye what makes it impossible to escape from the cell. Next, the Reactive Oxygen Species (ROS) - present in the cytoplasm when the apoptosis occurs, can oxidize the dye, what results in the fluorescence. Oxidation of these probes can be detected by monitoring the increase in fluorescence with a flow cytometer, fluorometer, microplate reader, or fluorescence microscope, using excitation sources and filters appropriate for fluorescein (FITC).

Cells harvested into plastic FACS tubes were centrifuged and the supernatant was discarded. The cells were washed with PBS and loaded with dye (20 µM in PBS) for 45 min at 37°C in the dark. After the incubation, excess of the dye was removed. Cells were washed once again and re-suspended in 200µl of PBS. FACS measurement was conducted immediately after the staining, using a FACS Canto II device at Ex 488 nm and Em 530/30 nm.

Propidium iodide staining was used as a counterstaining as described in the section 3.5.2.

3.5.4 Identification of apoptosis in the CD34+ cells

To identify CD34$^+$ cells, PBMCs were isolated as described in the section 3.2.3. Appropriate treatment was applied. Next, the cells were centrifuged for 5 minutes at 1000 rpm. Culture medium was discarded, and cells were washed with PBS. For the immuno-staining cells were re-suspended in PBS containing FITC-conjugated antibody directed against CD34 antigen (BD Pharmingen™, Heidelberg, Germany) and incubated for 1 hour, shaking in the dark, RT. After the incubation, cells were washed and re-suspended in PBS-Propidium iodide mixture.

FACS Canto II flow cytometer was used for the measurement. The gating was set according to the Fukuda et al. (1998). FITC-positive population in a number of 25 000 events was used as a stopping gate. PI-positive values were used to calculate the specific apoptosis rate as depicted here:

$$specific\ apoptosis\ [\%] = \frac{Apoptosis\ of\ treated\ cells[\%] - Apoptosis\ in\ control\ [\%]}{100\% - Apoptosis\ in\ control[\%]} \times 100$$

3.6 TRANSIENT TRANSFECTION OF CELLS

3.6.1 Transfection with siRNA

First, the cells were seeded in the amount that gave about 80-90% of confluence on the other day. For the transfection purpose, culture medium was changed to one without P/S. Silencing RNA (siRNA) was prepared as described by a supplier (Dharmacon GE, Lafayette, CO, USA). DharmaFECT Transfection Reagent was used according to the manufacturer's instruction. Briefly,

2,5µl of 20µM siRNA was mixed with 197,5µl of the medium without FCS and without P/S in tube 1, and 5µl of DharmaFECT reagent with 195µl of the same medium in tube 2. After 5 minutes of incubation the content of both tubes was combined into one. After additional 20 minutes of incubation the mixture was added to cells for at least 24 hours in the incubator.

3.6.2 Transfection with plasmid

For the transient transfection with plasmid, a Lipofectamine$^®$ 3000 kit (Thermo Fisher, Waltham, MA, USA) was used according to manufacturer instructions. Briefly, cells were seeded a day before transfection in amount that result in 80-90% of confluence on the other day. The culture medium was changed to 2ml of one without P/S. Plasmid DNA was diluted with Opti-MEM^{TM} medium in one tube with P3000^{TM} reagent. In another tube Lipofectamine^{TM} 3000 was diluted with Opti-MEM^{TM} medium. The content of the tubes was combined, vortexed and incubated for 10 minutes in room temperature. The mixture was added to the cells and incubated at least 24 hours in the incubator.

3.7 GENOME EDITING USING THE CRISPR-CAS9 TECHNIQUE

3.7.1 Design of targeting components.

To generate a knock-out of BAP31 in RIL-175 cancer cell line, we decided to use the CRIPSR/Cas9 technique as described before (Ran et al., 2013). To design the guide RNA (gRNA), the sequence of BAP31 protein was checked on the website http://www.ensembl.org. We decided to remove exon 3, what should result in a truncated protein, which further will be subjected to the nonsense mediated mRNA decay (NMD). Sequence used for the design of gRNA was depicted as Figure 3.2. Exon 3 sequence was shown in green, where bold part represents the coding region.

```
Sequence of mBCAP31, Exon 3: 1301 bp;

1       CATGATCAGC CGAGCTTGCT GATTTTTAAC AGCATGAAAC TCCTCCCGAA GGCTCTTTAG
61      ATGATATAGC TAAATTATTT GTTCATAGAA ATGATGGAGA GTCTAGATTC CTTTTCATAA
121     CCTAGGGTGG TAGGAGTCTA GACCAAAAAA AAAAAAAGTA TCACATTTTA AACAAAGGGG
181     AGCCAGGAAT AGTGGTGGCA CACTTCTTTA ATCCTGCCAT TGTGAGACAG GCAAGCGGAT
241     CTTTGCGAGC TTGAGGCTAG CCTCATCTAC ATAGTGAGAC CCTGCCTGTC TCAAAACCAT
301     GTTTGTAGCA GGTGTTTTAT CTACTACAAA GGGAAGTATG ATGAAAAGTA AGTTACCCTT
361     ACTGGAAACT GCCAGGATTT TAAAGATTGA CTTTCCAGGT GTTTCTGCAT ATGCATAAAC
421     ATCTTTTTCT AAATCCTTTT GAAGTTAATG AATAGGAAAG GCATAGCAGT AGCTGAGACT
481     GATTTTTGTA TGGGGCCTCG TAGCCACTGC AGAAGAGCAC CAAGTTGTCC TTAAATTTTG
541     CTTAGGGTTT GGATTGCAAA AGTTCATTTT CTTCAATATC TGTCTTCATT TCTTTCACAG
601     ATGGCAGAAG GTTTTTAAAT CCCGGCTGGT GGAGTTGGTA GTGACCTATG GCAACACTTT
661     CTTTGTGGTT CTCATCGTCA TCCTTGTACT GTTGGTTATT GGTGAGTGAG CTGTAGCAGG
721     AGGTTGCTAT CTGACCAGAT CCTGTGTCAT GGCTTCTAAA GCTCTGTGCC ACATTGGAAA
781     ATAAGCATTC TCAGAATCAA ACTCAATAAG TGCCCTTTGA TAATCTGTTA AGGAAGTGCT
841     TGCTATTAGC AGGACCTTCA TTTCAAGATG TTCCTATAGC AGTCCATATG GACTTAAACT
901     CAATGGCCTT TATATACTCT TATGACCACA TTTGTTACCA AGATACCCTA CCCTAGTTAT
961     TTTAGAACTG GTACTAAGAG AAGCTAATGG TCTGTGACCC TGATTCAAAT AGTGGTGTTT
1021    ATTAGTCATG TGGATCAGAC TTCTTTTTTA AGAAATTATT TTGTCTTTTA TTTGTCATTG
1081    TTATTATTTT GTTTTTTTGA GACAATGTCT CTATGTGGCC CTGGATGTCA TGGCACTTGC
1141    TCTGTAGACC AGGCTGGCCT TGAATTTATA GAGATCCATC TGCTGCTTTC TAAGTTCTGA
1201    GATTAAAAAG GTGTGCACTG GGCTGCTTTT GTTATCTTAA AAATGTTGTT TTCTTAATCT
       1261   TAAAAAGAC ACCTGAGTTT GTTTGTTTGT TTGTTTGTTT G
```

Figure 3.2. A sequence of mBCAP31 gene. Includes Exon 3 (green) and parts of introns (black).

To design the guide RNAs we used website http://crispor.tefor.net as described before (Haeussler et al., 2016). Three of the most specific suggestions were picked for each: forward and revers gRNAs (Hsu et al., 2013) as depicted in table 3.18.

Guide RNAs sequences

Forward	Reverse
88 / fw: TGTTCCTATAGCAGTCCATA *TGG*	**137 / rev:** ATAACTAGGGTAGGGTATCT *TGG*
50 / fw: CAGCATGAAACTCCTCCCGA *AGG*	**145 / rev:** GTTCTAAAATAACTAGGGTA *GGG*
363 / fw: GAAAAGTAAGTTACCCTTAC *TGG*	**42 / rev:** TCATCTAAAGAGCCTTCGGG *AGG*

Table 3.18. Sequences of gRNA designed for generation of BAP31 knock out cells.

3.7.2 Cloning of oligos into Cas9 plasmid

Designed DNA oligos were cloned into eCas9_Puro2.0 Plasmid. First, all designed oligos were annealed using a PCR cycler for 5 minutes at 95°C and then ramping down to 25°C for another 20 minutes (Table 3.19).

Reagent	Volume (µl)
sgRNA fwd (100 µM)	1
sgRNA rev (100 µM)	1
T4 ligation buffer 10x	1
H2O	7

Table 3.19. PCR reaction for annealing of oligos.

Subsequently, oligos were diluted 1:200 with water. Next, the restriction digestion of plasmid backbone was performed at 37°C for 30 minutes as depicted in Table 3.20.

Reagent	Volume (µl)
eCas9_Puro2.0 Plasmid 150 ng	x
FD Buffer colorless 10x	1,5
FD BbsI bzw BpiI	1
H2O	Ad 15

Table 3.20. Digestion of plasmid backbone with restriction enzymes.

Ligation of digested plasmid backbone and designed oligos was performed for 30 minutes at room temperature (Table 3.21.).

Reagent	Volume (µl)
Digested plasmid	10
Oligos diluted	2
T4 ligation buffer 10x	2
T4 DNA Ligase	1
H_2O	5

Table 3.21. Ligation of plasmid backbone with oligos.

The last step was to digest the not ligated plasmid. For this purpose, the ligation mixture was combined with Plasmid Safe exonuclease and incubated for 30 minutes at 37°C and 30 minutes at 70°C. The reaction components are shown in the table 3.22.

Reagent	Volume (µl)
Ligation mix (see above)	11
PlasmidSafe buffer 10x	1,5
ATP 25 mM	0,6
PlasmidSafe Exonuclease	1
H2O	Ad 15

Table 3.22. Digestion of not ligated plasmid.

3.7.3 Transformation of plasmids into E. Coli

To introduce the previously prepared plasmids into *E. coli,* 100 µl of competent DH5α strain were thawed for each plasmid. Subsequently, 3 µl of appropriate plasmid were added to each vial and the mixture was incubated for 10 minutes on ice. Next, incubation for 45 seconds at 42°C and another 2 minutes on ice was conducted. Transformed bacteria were plated onto agar plates containing Ampicillin and incubated overnight at 37°C.

For each plasmid 3-6 colonies were inoculated into 5 ml of liquid LB medium containing Ampicillin in the concentration of 100 µg/ml and incubated at 37°C overnight. On the following day the isolation of DNA was performed using QIAprep Spin Miniprep Kit (Qiagen, Hilden, Germany) according to the manufacturer's instruction.

To check if the insert was cloned properly, EheI restriction enzyme digestion was performed. Two suitable clones were sent for sequencing. The obtained results were compared with reference sequence using DNAMAN software. Suitable plasmids were used for the subsequent experiments.

3.7.4 Determining Genome Targeting Efficiency using T7 Endonuclease I

This approach is used to determine the targeting efficiency of previously designed gRNAs. T7 Endonuclease I recognize and cleaves non-perfectly matched DNA. Mismatches may occur, when the double DNA strand is cut and repaired through the non-homologous end joining (NHEJ) repair.

Determination of efficiency was performed according to the manufacturer's instruction (New England BioLabs, Ipswich, MA, USA). Briefly, 100ng of genomic DNA, either from cells transfected with oligos or the control cells, was used for each PCR reaction together with primers depicted in Table 3.23. Small amounts of PCR product were checked for the proper amplification and the residue was cleaned. Next, T7 Endonuclease I digestion was performed. The gRNAs with the highest targeting capacity were used during the next steps.

Primer name	Sequence	Binding site
5'-1/2 T7 fwd	TAAAGGGCATGCACCACCAT	5'-1: 75, 460
5'-1/2/3 T7 rev	TGCTCTTCTGCAGTGGCTAC	5'-2: 73, 462
5'-3 T7 fwd	ACAGCATGAAACTCCTCCCG	5'-3: 159, 331
3'-1/2 T7 fwd	TTAAATCCCGGCTGGTGGAG	3'-1: 197, 329
3'-1/2/3 T7 rev	AGCAAGTGCCATGACATCCA	3'-2: 189 ,337
3'-3 T7 fwd	GGTGAGTGAGCTGTAGCAGG	3'-3: 185, 255

Table 3.23. Primers used for the PCR reaction to determine efficiency of Cas9 plasmids.

3.7.5   Transfection and selection of clones.

Two plasmids were identified for the usage in further genome editing:

- ✓ 363 / fw: GAAAAGTAAGTTACCCTTAC TGG
- ✓ 145 / rev: GTTCTAAAATAACTAGGGTA GGG.

RIL-175 cells were transfected with both plasmids, using Lipofectamine 3000™ reagent, according to the manufacturer's instructions. Subsequently, cells were selected using 2μg/mL Puromycin and 5 µg/mL Blasticidin for 48 hours. After selection, cells were incubated in culture medium until confluence was achieved. Next, cells were diluted to the concentration of 0,6 cell/well and seeded into 96-well plates. To avoid cell aggregates, before seeding they were separated using a cell strainer. Single clones were grown until confluence. The gene expression was checked using PCR and the protein expression using western blot approach.

3.7.6   2.8. The polymerase chain reaction (PCR)

To identify the knockout of BAP31, generated clones were subjected to the PCR. I used a forward primer: 5'ACAGCATGAAACTCCTCCCG3'   and   the   reverse   primer:

5'AGCAAGTGCCATGACATCCA3'. The cells were lysed with a QuickExtract DNA extraction reagent. I used the high fidelity DNA polymerase (Thermoscientific, Germany) according to the manufacturer's instructions.

For the colony PCR the *Taq* DNA Polymerase (ThermoFisher, Germany) was used according to the manufacturer's instructions. A small amount of the fresh yeast was used as the template.

3.8 MIGRATION OF CANCER CELLS

3.8.1 The Boyden Chambers

To analyze the migratory capacity of cancer cells they were cultivated in 6-well plates and starved for 24 hours before the experiment. Next, cells were trypsinized, counted and transferred to the upper chamber (8 µm pores) in a number of $1 \cdot 10^5$ cells/chamber in 200 µl of starvation medium. The lower chamber was filled with 600 µl of complete medium. Cells were allowed to migrate for 5 hours. The number of migrating cells was calculated with ImageJ software using the "Cell Counter" plugin.

3.8.2 Wound healing assay

Cells were seeded in the 12-well plates in a number of $8 \cdot 10^5$ cells. On the next day, when the cells achieved the confluence, the scratch with the yellow tip was made in the middle of the well. Cells were washed twice with PBS and the hunger medium was added for the negative control and the complete medium in duplicates to the rest of the cells. The migration capability was verified after 16 hours.

3.9 LUCIFERASE DOUBLE REPORTER GENE ASSAY - SPLICING

To verify the splicing capability of the cells, I transfected them with either Luc plasmid, which contained sequence for the Firefly luciferase, or Luc-I plasmid, which contained the insert between the coding sequence for the Firefly luciferase. As the control of the transfection efficiency we used the plasmid for the expression of Renilla luciferase. The transfection was conducted using Lipofectamine 3000 reagent as described in the section 2.6.2. Two days after the transfection, cells were lysed using passive lysis buffer provided within the Dual-Luciferase® Reporter Assay

System (Promega, Germany) kit. Cells were collected to the plastic 1,5ml tubes and centrifuged 10 minutes at 14 000 rpm. 20 µl of supernatant was transferred onto the 96-well white plate. The measurement was conducted according to the manufacturer's instructions using Orion II microplate luminometer (Titertek Berthold, Bad Wildbad, Germany).

3.10 IMMUNOSTAINING AND CONFOCAL MICROSCOPY

Cells were seeded into 8-well µ-Slide (Ibidi, Martinsried, Germany) in a number of $1 \cdot 10^4$ cells/well in culture medium and incubated at 37°C until about 60-70% of confluence. Next, cells were washed 3x with PBS+ (PBS solution containing Mg^{2+} and Ca^{2+} ions), fixed with 4% paraformaldehyde (PFA) in PBS for 10 minutes in room temperature. Once again cells were washed 3x with PBS and permeabilized with 0,1% Triton-X solution for another 10 minutes. Next, unspecific binding sites were blocked using 5% BSA in PBS solution for 30 minutes. An appropriate antibody was diluted 1:1000 in 1% BSA, applied onto the cells and incubated overnight at 4°C with shaking. On the following day, the samples were washed 3x, 5 minutes with 1% BSA solution with shaking. Subsequently, appropriate Alexa Fluor® secondary antibodies were added in a concentration of 1:1000 in 1% BSA for another 2 hours in room temperature, shaking in the dark. After incubation time, cells were washed 3x with 1% BSA for 5 minutes in room temperature, shaking in dark. Before the end of the incubation, Hoechst33342 (Sigma-Aldrich) in a 1:200 dilution was added to the cells. Next, cells were mounted with FluorSave™ mounting medium and the samples were covered with glass cover slides. Prepared samples were incubated overnight at 4°C, shaking in the dark. On the following day, pictures were acquired with either Zeiss LSM 510 Meta Confocal Microscope (Zeiss, Oberkochen, Germany) or Leica SP8 Inverted scanning confocal microscope (Leica, Wetzlar, Germany).

3.11 RECYCLING OF THE TRANSFERRIN RECEPTOR IN CANCER CELLS.

To check the ability of cancer cells to recycle the transferrin receptor upon Soraphen A treatment, cells were seeded into 8-well µ-Slide (Ibidi, Martinsried, Germany). Following appropriate treatment, 100ng/ml of rhodamine-conjugated transferrin was applied onto the cells for 1h. Subsequently, cells were washed 3x with PBS+ and fixed with 4% PFA solution in PBS for 10 minutes. Cells were washed 3x with PBS. Hoechst33342 (Sigma-Aldrich) in dilution 1:200 was added to the cells for 10 minutes. After additional 3 washing steps with PBS, FluorSave™ medium

was added into each well and covered with glass cover slides. Prepared samples were incubated overnight at 4°C, shaking in the dark. On the following day pictures were acquired with Zeiss LSM 510 Meta Confocal Microscope (Zeiss, Oberkochen, Germany).

3.12 FORMATION OF LIPOSOMES CONTAINING PHOSPHATIDYLINOSITOL (PI) MIX

First, 50µM of L-α-Phosphatidylinositol ammonium salt solution from bovine liver – PI mix (Sigma) dissolved in chlorophorm was added to a falcon. Next, the chlorophorm was evaporated with the stream of N2. The falcon was left for 30 minutes under the flow without the lid, to remove remains of chlorophorm. HEPES buffer (20µM, Table 3.24.) was added and the mixture was kept for 30minutes in water bath (37ºC) to hydrate PIs, from time to time vortexed. Appropriate volume of medium (with 2% FCS and 1% P/S) was added and incubated for additional 30 minutes in wather bath at 37ºC. Afterwards, PIs mixture was sonicated at room temperature for 30 minutes to reduce the size of liposomes formed during the phase of hydratation. Immediately after the sonication, the prepared PI mix was put on the cells.

1 M HEPES, pH = 7.0	
HEPES	119.15 g
NaOH	to adjust pH
H_2O	

Table 3.24. HEPES buffer composition.

3.13 RESCUE OF THE SORAPHEN A TREATMENT EFFECT

Cells were seeded in 24-well plates $(0,5 \cdot 10^5$/well) in DMEM medium with 10% FCS and 1% P/S. After the attachment of the cells, they were stimulated with 10µM of Soraphen A for 24 hours in DMEM with 2% of FCS and 1% of P/S at 37ºC. Subsequently, PI mix mentioned above was prepared for stimulation.

Cells were treated with the PI mix for 16 hours. After this time, PI was removed from the cells, medium with 2% FCS and 1% P/S was added and the cells were left for additional 2 days to freely

proliferate. The rate of proliferation was checked with the CellTiter-Blue® reagent (Promega, Madison, WI, USA).

3.14 IDENTIFICATION OF BAP31 INTERACTION PARTNERS APPLYING YEAST 2 HYBRID APPROACH

To identify BAP31 interaction partners we decided to apply the Yeast 2 Hybrid approach as described before (Chien et al., 1991). For this purpose, we used the Matchmaker Gold Yeast Two-Hybrid System (Takara Bio Group, CA, USA) according to the manufacturer's instruction. Briefly, we cloned a bait insert – sequence for BAP31 – into pGBKT7 vector provided with the kit, using BamHI and EcoRI restriction enzymes. Next, the obtained plasmids were sequenced to confirm that the insert is in-frame with the vector.

Subsequently, the bait-plasmid was transformed into the Yeast strain – Y2HGold. After the selection on DDO (Double Dropout, SD/-Leu/-Trp) plates, a prominent yeast colony was inoculated into liquid DDO medium and incubated overnight, shaking at 30ºC. On the following day the culture was harvested and the bait-containing Y2HGold strain was mated with the library in Y187 Yeast Strain. Next, mated yeast were seeded on plates with increasing selectivity, namely: DDO, DDO/X (DDO + X-α-Gal) ending up on DDO/X/A (DDO/X + Aureobasidin A). Colonies, which grew on DDO/X/A plates and turned blue were diluted in water and stamped onto each selection plate – DDO, DDO/X and DDO/X/A. Yest colonies which were growing and turning blue on DDO/X/A but not at DDO and DDO/X plates were used for the colony PCR.

The size of PCR product was compared using agarose gel electrophoresis and plasmids which seemed to contain the inserts of a different size were selected, purified and sent for the sequencing. The results were checked using BLAST tool. Hits were tested towards auto-activation. The interaction partner of BAP31 protein was identified.

4. AIMS OF THE STUDY

Following the promising results of work of Dr. Fabian Koczian in his doctoral thesis, I decided to extend the topic of PS89 driven chemo-sensitization by different types of leukemia applying various cytostatics and combining them with PS89. Moreover, following promising results of previous work, I wanted to focus on the function of BAP31 in cancer cells.

In my opinion the most interesting points were:

1. To show the potential of combination therapy using cytostatics with the chemo-sensitizing compound – PS89 in different types of leukemia models.
2. To elucidate the mechanism of induction of apoptosis in different leukemia models treated with combination of PS89 with various cytostatics.
3. To investigate the functional results of lack of BAP31 expression on cancer cells.

5. RESULTS

5.1 INVOLVEMENT OF BAP31 IN THE CHEMO-SENSITIZATION OF VARIOUS LEUKEMIA TYPES TOWARDS COMMONLY USED CHEMOTHERAPEUTICS

5.1.1 Combination of various cytostatics with PS89 enhances their anti-cancer properties in different leukemia types but not in hematopoietic cells.

Treatment of leukemia is difficult due to the formation of chemo-resistance. Moreover, there is a great spectrum of side effects which occur upon the chemotherapy. Thus, it is of a great importance to focus on combinatorial therapies, which can decrease the side effects of common treatments and re-sensitize cell which have formed a resistance towards the chemotherapeutics. Accordingly, I decided to test various cytostatics in combination with the small molecule – PS89, to introduce a new approach for the treatment of various types of leukemia.

To test the capability of proliferation of the acute myeloid leukemia (AML) cell line out of the single cell, I applied the colony formation assay (Figure 5.1.). We decided to use one of the drugs commonly used in the AML treatment – 6-Mercaptopurine (6-MP). Cells treated with DMSO as well as PS89 did not show a decrease in the colony number. The treatment with 6-MP alone was more effective. What is interesting, after the addition of PS89 together with 6-MP (+/+), we can observe a synergistic effect on the inhibition of colony formation. The significance was tested using the BLISS independence model with the result value of 1,78.
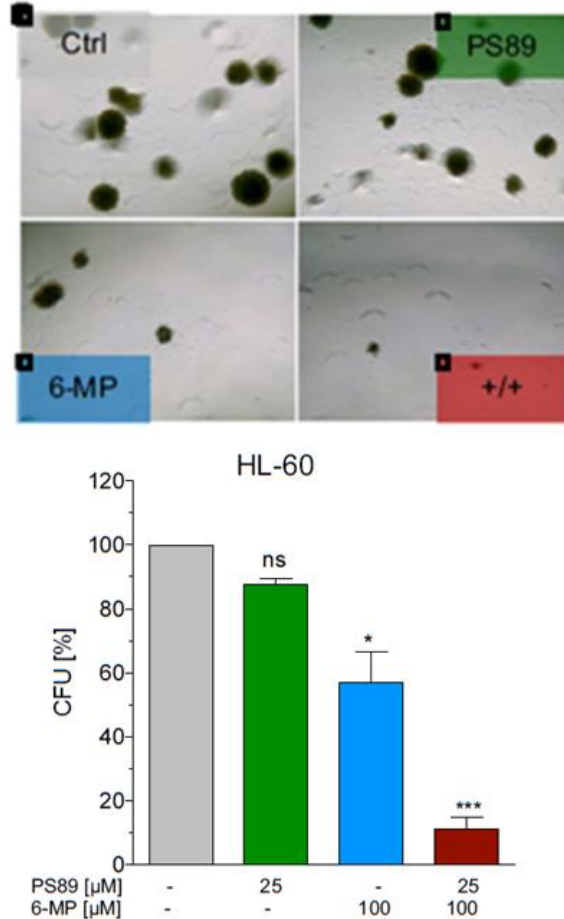
Figure 5.1. The effect of the combinatorial treatment on the colony formation capability of the AML cell line HL-60. Cells were pre-treated for 24 hours with either 25 µM of PS89, 100 µM of 6-Mercaptopurine (6-MP) or the combination. Next, cells were seeded in the number of $1 \cdot 10^4$/well and left to proliferate for 7 days. The data are presented as colony formation units (CFU). The graph shows three independent experiments. The error bar shows standard deviation. Data were tested applying one-way ANOVA statistic.

I also checked the influence of combinatorial treatment on the induction of apoptosis in various leukemia cell lines. Therefore, we treated Jurkat (ALL) and HL-60 (AML) cells with increasing doses of 6-MP and 25µM of PS89 for 48 hours to test the half maximal effective concentration (EC50) value for the drug alone and in the combination with the potential chemo-sensitizer (Figure 5.2). We could show, that combination of Mercaptopurine (6-MP) with PS89 led to the decrease of the EC50 value of Mercaptopurine in Jurkat cells from 2,9µM to 1,3µM and in HL-60 from

511,8 µM to 128,8 µM. These values have been obtained through the application of a nonlinear regression model.
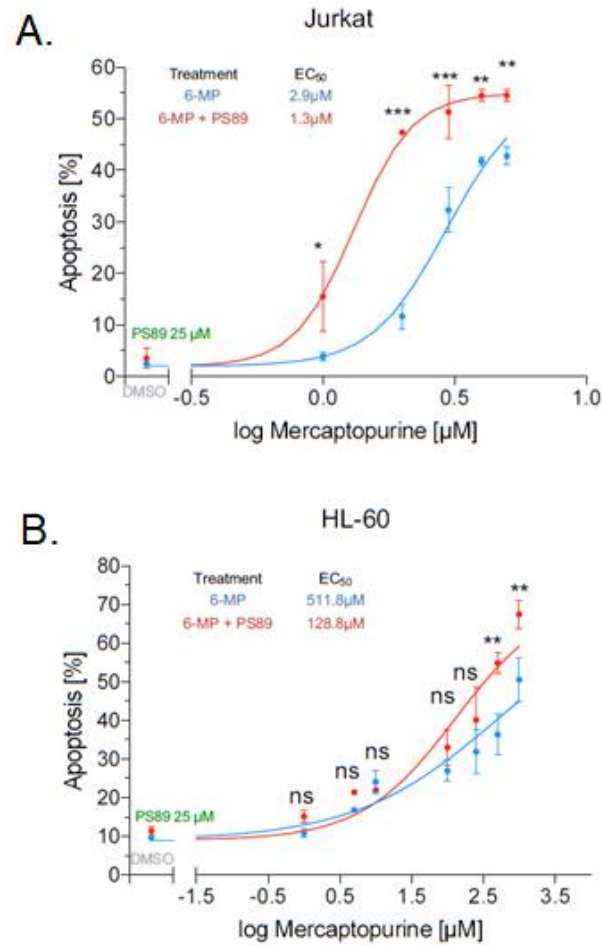
Figure 5.2. Chemo-sensitizing effect of PS89. Combination of Mercaptopurine (6-MP) with PS89 leads to the decrease of the EC50 value in comparison to Mercaptopurine alone in Jurkat cells (A) as well as in HL-60 (B). Cells were treated with increasing doses of Mercaptopurine with or without addition of 25µM of PS89 for 48 hours. Graphs show three independent experiments. The error bars show standard deviation. EC50 value was calculated applying nonlinear regression model.

I analyzed also the combination of PS89 with Dexamethasone (DEX). DEX is a corticosteroid commonly used for the treatment of various cancer types, including ALL and AML. Figure 5.3. presents the effect of the combinatorial treatment on the induction of apoptosis in HL-60 and Jurkat cell lines. Stimulation of cells for 48 hours with combination of cytostatic with putative chemo-

sensitizer led to the significant increase in the apoptosis rate in comparison to the treatment with PS89 or DEX alone.
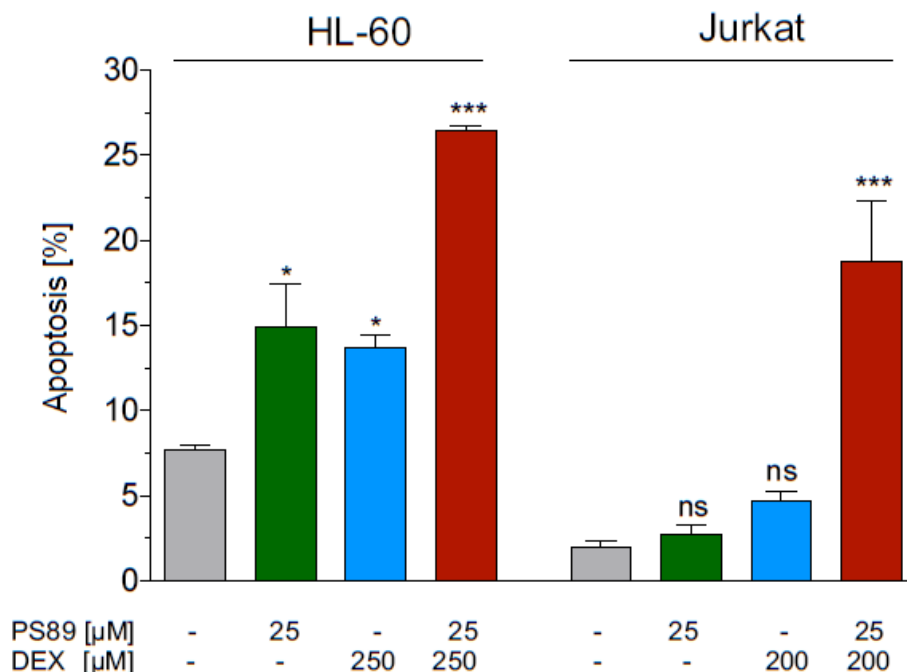
Figure 5.3. Induction of apoptosis in cells treated with combination of PS89 and Dexamethasone (DEX). HL-60 as well as Jurkat cells were treated with either 25µM of PS89, 250 µM of DEX or combination of those two for 48 hours. The percent of apoptosis was assessed as the PI-positive percent of acquired events. Graph shows three independent experiments. Error bars show the standard deviation. Data was tested applying one-way ANOVA statistic.

As the potential of the therapy is connected also to generated side effects, I asked ourselves if combinatorial treatment could be harmful for CD34^{+} cells. This protein is a marker for early hematopoietic cells, which are crucial in the formation of blood cells, therefore very important in the process of recovery after chemotherapy.

To show that combinatorial treatment is not harmful for hematopoietic cells, I isolated the Peripheral Blood Mononuclear Cells (PBMCs), where about 0,1% of cells are CD34+, from the blood of healthy volunteers as described in the section 3.2.3 and treated them with the combination of cytostatic and chemosensitizer.

It has been tested before and showed in the doctoral thesis of Dr. Fabian Koczian, that combination of 20 µM of DNR and 25 µM PS89 leads to a synergistic effect in the induction of apoptosis in

PDX cells with BLISS values of 1,1 – 1,7 depending on the patient. Therefore, I showed that the same setting is not harmful for the cells expressing CD34 protein (Figure 5.4). The induction of specific apoptosis oscillated between 0% and 3% in cells treated either with PS89, Daunorubicin or combination. Therefore, we can conclude that this treatment is not harmful for hemopoietic cells characterized by CD34 expression.
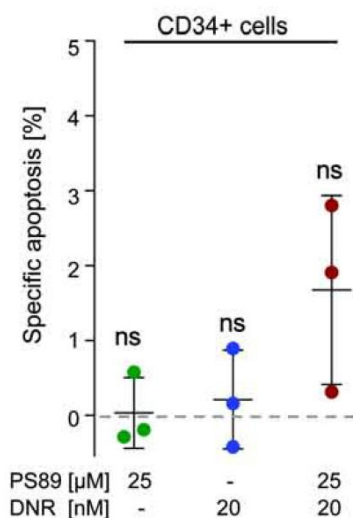
Figure 5.4. The influence of the treatment with Daunorubicin and PS89 on CD34+ cells. Cells were treated for 48 hours with 25 µM of PS89, 20µM of Daunorubicin or the combination. The stopping gate was set to 25 000 of FITC-positive cells. The graph shows three independent experiments. The error bars show standard deviation. Data was tested applying one-way ANOVA statistic.

5.1.2 Caspase-8 and BAP31 activation constitutes a platform for the induction of apoptosis in leukemia cells upon the treatment with the combination of PS89 and cytostatic.

It was shown that PS89 targets PDI (Eirich et al., 2014). However, the research of Dr. Fabian Koczian, which is shown in his doctoral thesis, has indicated that silencing of PDI is not mimicking the effect of PS89 treatment. Moreover, in his thesis, he has shown further proteomics analysis, applying the Activity Based Protein Profiling (ABPP) approach. These data revealed that BAP31 is another promising target of PS89, which is also involved in ER homeostasis. Therefore, our further research focused on this protein.

As described before, Caspase-8 and BAP31 constitute a platform for the induction of apoptosis (Wang et al., 2011). Therefore, I tested the activation of BAP31, which is expressed in the amount

of cleaved protein, and Caspase-8 in an ALL cell line - CCRF-CEM (Figure 5.5). The treatment was applied for either 24 or 48 hours. Already after 24 hours we could observe a decrease in the total form of both BAP31 and Caspase-8 when cells were treated with the combination of Vincristine (VCR) and PS89. However, the effect was the most prominent after 48 hours of treatment with the combination. Then we could see also the cleavage product of BAP31, what was not possible in 24 hours setting. This confirms, that the addition of PS89 and the cytostatic, but not the substances alone, led to the activation of both – Caspase-8 and BAP31.
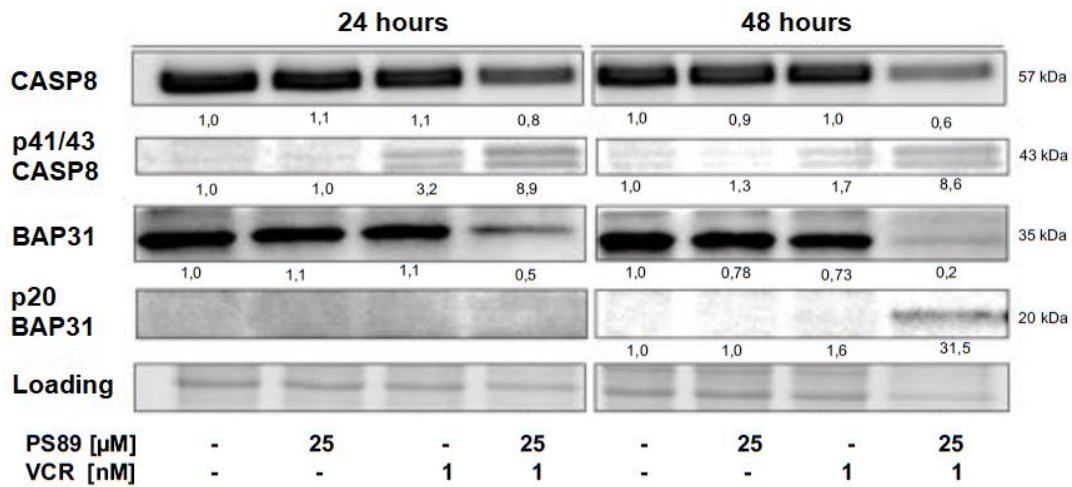
Figure 5.5. CCRF-CEM cells were treated with 1 nM of Vincristine (VCR), 25 μM of PS89 or the combination for either 24 or 48 hours. Next, they were subjected to western blot to analyze activation of Caspase-8 and BAP31. The experiment was performed three times, independently. Figure shows one, representative blot.

I could confirm that the mode of action is the same when we apply PS89 and VCR treatment to the Patient Derived Xenograft (PDX) cells. This type of cells is obtained from human patients and cultivated in immuno-deficient mice. To isolate the human cells for the experiments, it is necessary to use either spleen or bone marrow of mouse. This approach allows us to test our setting in a primary environment in comparison to the regular cell lines growing *in vitro*. Already 24 hours of exposition to the combination of substances was sufficient to show the decrease in the total form of both Caspase-8 and BAP31 (Figure 5.6). This decrease shows indirect proof for the cleavage of those two proteins. Therefore, we can conclude that also in this cell line treatment with combination of PS89 and Vincristine induced activation of Caspase-8 as well as BAP31.
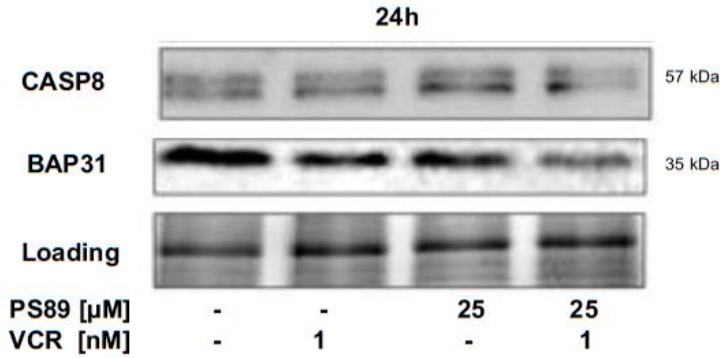
Figure 5.6. Activation of Caspase-8 and BAP31 in Patient Derived Xenograft (PDX) cells. PDX cells were treated with 1nM of Vincristine (VCR), PS89 or the combination for 24 hours. Next, they were subjected to western blot to validate activation of Caspase-8 and BAP31. This experiment was performed three times. The figure shows one, representative blot.

5.1.3 The pro-apoptotic cross-talk between Endoplasmic Reticulum (ER) and mitochondria.

According to the literature the Caspase-8 and BAP31 cleavage is followed by the release of calcium from the ER leading to the transfer of apoptotic signal further to the mitochondria (Wang et al., 2011; Iwasawa et al., 2011; Grimm, 2012). Therefore, we tested the combination of PS89 with DNR or VCR in the HL-60 (Figure 5.7. A) and CCRF-CEM (Figure 5.7. B) cells for 24 and 48 hours, and in PDX (Figure 5.7. C) cells for 24 hours. We showed, that the treatment with PS89 and drugs alone was not very effective concerning the induction of a calcium release. However, after the treatment of both HL-60 and CCRF-CEM cells for 48 hours with the combination, we observe a significant increase in the cytosolic calcium level. The same is true already after 24 hours treatment of the PDX cells with VCR and PS89. It means, that the activation of Caspase-8 and BAP31 leads to subsequent calcium release from ER to cytoplasm, what is an important signaling event concerning induction of apoptosis, as described above.
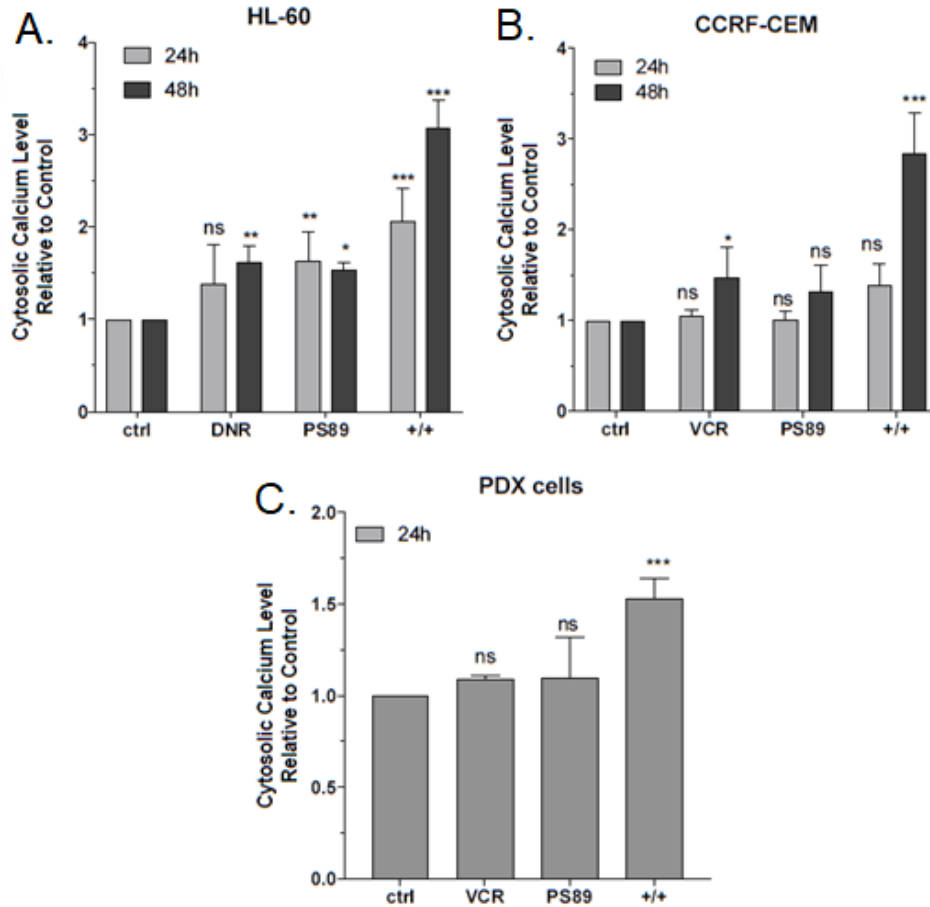
Figure 5.7. The treatment of AML (A), ALL (B) and PDX (C) cells with combination of PS89 with cytostatic led to the increase in the level of cytosolic calcium. Cells were treated for 24 or 48 hours. Next, loaded with fluorescent dye Cal-520. Data were assessed by flow cytometry. A. Treatment of HL-60 cells with combination of Daunorubicin (20µM) and PS89 (25µM) of HL-60 for 24 (grey) and 48 (dark grey) hours. B. Treatment of CCRF-CEM cells with combination of PS89 (25µM) and VCR (1nM) for 24 (grey) and 48 (dark grey) hours. C. PDX were treated with combination of VCR (1nM) and PS89 (25µM) for 24 hours. The graph shows three independent experiments. Error bars represent standard deviation. Data was tested applying one-way ANOVA statistic.

Following described mechanism of induction of apoptosis, calcium release triggers apoptotic events in the mitochondria. The mitochondrial membrane potential ($\Delta\Psi$m) is linked to the outer mitochondrial membrane permeabilization, what leads to cell death induction through the release of the cytochrome c (Wang et al., 2011). Therefore, we checked if our treatment induces a release of the mentioned protein from mitochondria to the cytoplasm.

For the purpose of this experiment, we used the CCRF-CEM cell line and the mitochondrial/cytoplasmic fractionation approach. As it is shown in Figure 5.8, the treatment with both PS89 and VCR for 48 hours led to the release of cytochrome c to the cytoplasm. The Voltage-Dependent Anion Channel (VDAC) was used as a mitochondrial marker. We can observe, that the cytoplasmic fraction was not contaminated with mitochondria, but still cytochrome C is present in the cytoplasmic fraction in cells treated with combination of PS89 and VCR. We can conclude, that cytochrome C is released to the cytoplasm as the result of calcium release and loss of mitochondrial membrane potential.
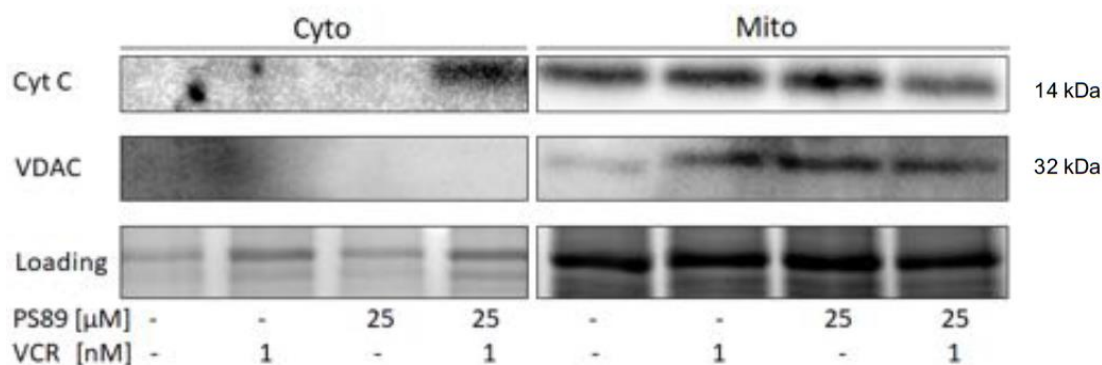
Figure 5.8. Release of cytochrome C to cytoplasm. CCRF-CEM cells were treated with the combination of PS89 (25µM) and Vincristine (VCR, 1nM) for 48 hours. Next, they were subjected to cytoplasm/mitochondria fractionation and western blot. Fractions of cytoplasm and mitochondria were checked for the cytochrome C expression. VDAC was used as a marker for mitochondrial fraction. Experiment was performed 3 times, independently. Graph shows one, representative blot.

The loss of the mitochondrial membrane potential induced through Ca^{2+} signalling, leads also to the release of Reactive Oxygen Species (ROS) (Tait et al., 2010; Yaday et al., 2015). Therefore, we tested cytosolic ROS concentration in CCRF-CEM and HL-60 cell lines (Figure 5.9.). Once again, the data were consistent. The most prominent release of ROS was observed upon a combinatorial treatment for 48 hours in both tested cell lines. This leads us to the conclusion, that the mitochondrial damage occurring after the treatment with combination of potential chemo-sensitizer with cytostatics results in accumulation of ROS, what provokes further disturbance of ER redox homeostasis, closing the feedback loop.
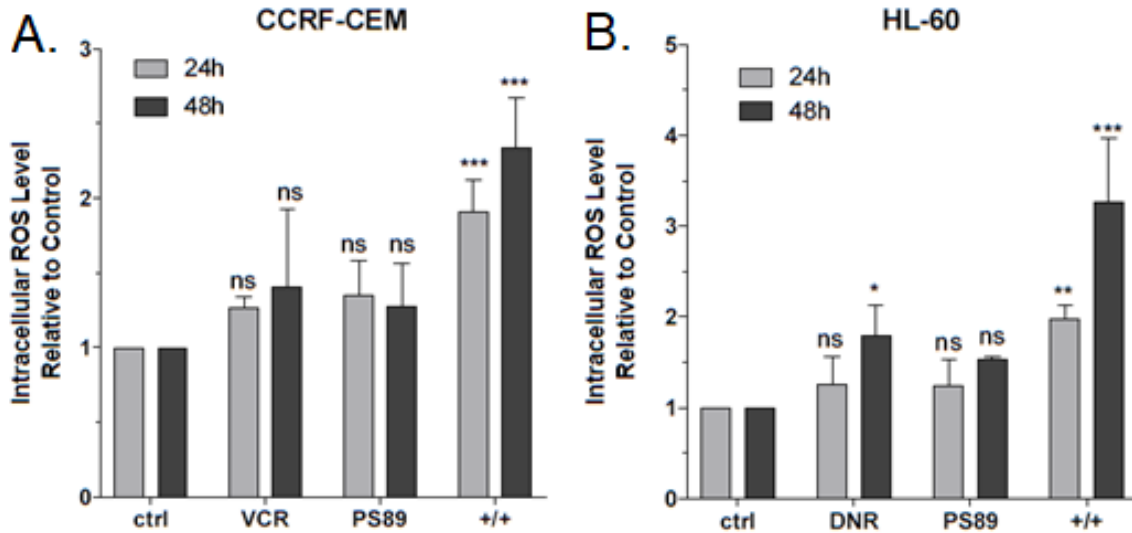
Figure 5.9. Accumulation of Reactive Oxygen Species (ROS) upon treatment with combination. Cells were treated for either 24 (grey) or 48 (dark grey) hours, next loaded with the redox sensitive dye Carboxy-H2DCFDA and analyzed by flow cytometry. The values represent the mean of fluorescence intensity normalized towards control. A. treatment of CCRF-CEM cells with combination of 1nM of VCR and 25 µM of PS89. B. Treatment of HL-60 with combination of 20 µM of DNR and 25 µM of PS89. Error bars show standard deviation. Experiment was performed three times, independently. Data was tested applying one-way ANOVA statistic.

5.1.4 The cytochrome c release induces an activation of the death protease.

The release of cytochrome c to the cytoplasm triggers the activation of the death protease – Caspase-3 (Zou et al., 1997; Li et al., 1997) and further leads to the cleavage of Poly(ADP-Ribose)-Polymerase (PARP) enabling apoptosis (Decker et al., 2000). Therefore, we tested CCRF-CEM and HL-60 cell lines treating them with either VCR or 6-MP in combination with PS89 for 24 hours (Figure 5.10). We showed, that already after this period of stimulation with combinatorial treatment both PARP and Caspase 3 are cleaved. These data confirm that treatment with the combination of potential chemo-sensitizer and cytostatic, but not the drugs alone, leads to the activation of the apoptotic pathway.
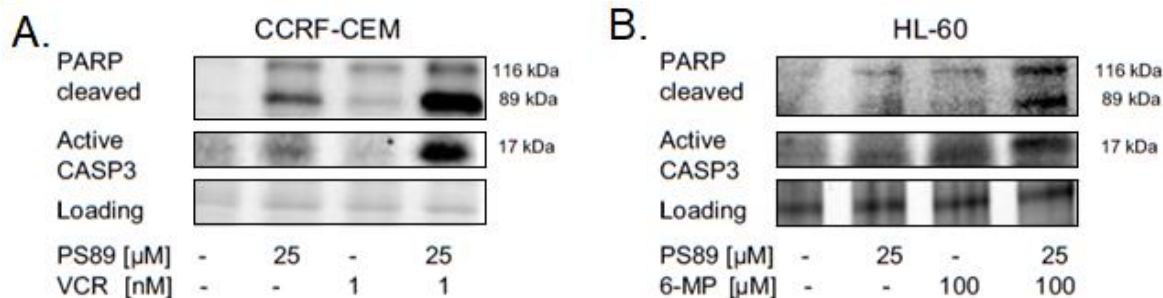
Figure 5.10. Treatment of leukemic cells leads to the activation of apoptotic pathway. Cells were treated with cytostatics, PS89 alone or combination for 24 hours. Next, they were subjected for western blot analysis for PAPRP and Caspase-3 activation. A. Treatment of CCRF-CEM cells with combination of 1nM of VCR and 25 µM of PS89 leads to the activation of apoptotic pathway. B. Treatment of HL-60 cells with combination of 100µM of 6-MP and 25µM of PS89 induces activation of PARP and Caspase-3.

5.1.5   The summary of the effect of BAP31 activation on the chemo-sensitization of leukemic cells towards cytostatic treatment.

In summary, we proved that the activation of Caspase-8 and further BAP31 cleavage led to an increase in the cytosolic calcium level and loss of mitochondrial membrane potential. The latter one enabled release of Reactive Oxygen Species and cytochrome C to the cytoplasm. When the ROS release triggered further ER-stress in a positive feedback loop, cytochrome c present in the cytoplasm activated the apoptotic stimuli like caspase-3, leading to the PARP cleavage. All these events resulted in the induction of apoptosis.

We proved, that chemo-sensitization of cells with PS89 gave significantly better results in induction of apoptosis in comparison to the treatment with the estabilished chemotherapeutics alone. Therefore, we believe that this substance is a great candidate for further testing concerning the combinatorial treatment. These data could be confirmed regardless of the cell line or the cytostatic used during the experiments. It confirms, that the mechanism of action is the same in all the tested settings.

These data have been published in *Haematologica* on October 2018 under the title: Targeting The ER-Mitochondria Interface Sensitizes Leukemia Cells Towards Cytostatics by: Fabian Koczian, Olga Nagło, Jan Vomacka, Binje Vick, Phil Servatius, Themistoklis Zisis, Britta Hettich, Uli

Kazmaier, Stephan A Sieber, Irmela Jeremias, Stefan Zahler and Simone Braig (Doi: 10.3324/haematol.2018.197368).

5.2   THE FUNCTION OF BAP31 IN HEPATOCELLULAR CARCINOMA

Inspired by the results of investigation of the effect of PS89 on BAP31, we asked ourselves what kind of function this protein has in cancer. As the literature focus on BAP31 as a chaperon protein present in the ER and the inducer of apoptosis, we decided to go deeper into its function in cancer cells which is not elucidated to the detail, yet. Therefore, we generated a stable knockout of BAP31 in the hepatocellular carcinoma mouse cell line – RIL-175, using CRISPR/Cas9 technique. This provided us a tool for a deeper understanding of the function of BAP31.

5.2.1   Generation of the BAP31 deficient cell line.

To establish a stable BAP31 knockout in RIL-175 cell line, we followed the literature (Ran et al., 2013). We decided to remove exon 3 to obtain the mRNA for the truncated protein, which would be subsequently subjected to the nonsense-mediated decay (NMD) pathway. This should result in the knock out of the protein of our interest.

For our further investigation, we decided to use two controls: the wild type cell line (WT) and the cell line generated out of the clone which went through the CRISPR/Cas9 technique, but the knockout was not successful (crWT). Moreover, to exclude the off-target effects, we used two different cell lines generated out of the knock out clones – KO1 and KO2.

To be certain, that the knock out was successful, we confirmed it applying three methods. First, we compared the size of the PCR products and observed that the size of the PCR product for the knockout cells was twice smaller than one of the wild type cells (Figure 5.11.A). Second, we sequenced this product and compared with the reference sequence. This has shown, that almost half of the sequence is missing in clones declared as the knockouts. Third, we checked the protein expression applying western blot approach and saw, that there is no more expression of BAP31 in knockout cell lines (Figure 5.11.B).

Figure 5.11. The confirmation of BAP31 knockout in RIL-175. In further investigation we used four cell lines: wild type (WT) and the unsuccessfully CRISPR-ed clone (crWT) as the controls, and two BAP31 knock out clones to exclude the effect of the off-targets (KO1 and KO2). A. The PCR product of the wild type and BAP31 knockout. B. Expression of BAP31 in the wild type and knockout cell lines evaluated by western blot.

5.2.2 Knock out of BAP31 had no influence on the morphology of cancer cells.

Our first concern was the morphology of the generated cell lines. Any changes in the appearance of the cells could give us a hint if e.g. BAP31 is important for the cytoskeleton composition or cell attachment. Therefore, we took a closer look into the shape and behaviour of RIL-175 cells in comparison to the generated clones in culture, but we could not see any morphological changes between the cell lines (Figure 5.12).
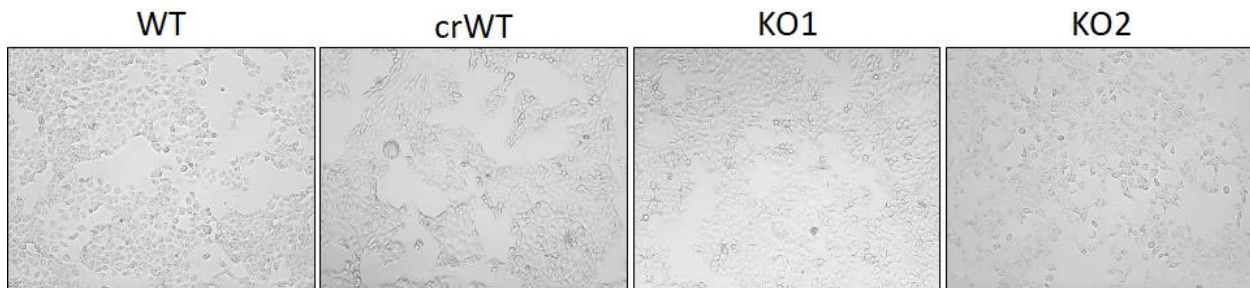
Figure 5.12. The morphology of RIL-175 cells is not affected by knockout of BAP31. Pictures were taken using light microscope.

5.2.3 There is no influence of BAP31 deficiency on the proliferation of cancer cells.

High proliferation capacity of cells is one of the hallmarks of cancer. Therefore, we wanted to know if the knockout of BAP31 has an influence on the growth of RIL-175.

We started with CellTiter-Blue, which relays on the metabolic activity of cells (Figure 5.13.A). In this assay we could not see any changes in the proliferation of wild type and knockout cells. To exclude the possibility that we could not see an effect on the proliferation because the cellular metabolism was changed, we used ViCell device to count the cells (Figure 5.13.B). After 72 hours of proliferation, cells were detached and counted with ViCell device. Once again, we could not observe any changes in the number of BAP31 knockout in comparison to wild type cells. The last approach – using an xCELLigence device – relayed on the disruption of the transduction of electrical impulses through the plate (Figure 5.13.C). Also, this experiment showed, that there is no difference in the proliferation capacity between cells expressing and lacking BAP31. In summary, even though we have checked the metabolism, number of cells and the growth area, we could not notice any significant changes in the proliferation capability of tested cells.
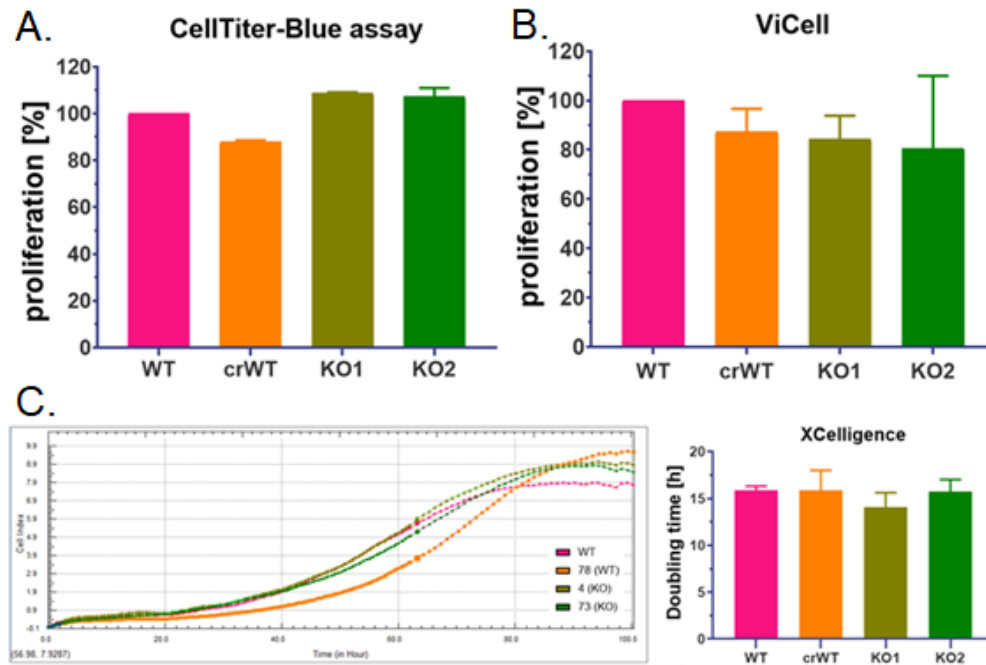
Figure 5.13. BAP31 knockout has no influence on the proliferation of RIL-175 cells. A. The proliferation rate of WT and KO cells was quantified with CellTiter-Blue reagent after 72 hours. Data was normalized towards the "Day 0" control. B. Cell were proliferating for 72 hours. The number of cells was assessed using the ViCell device at the end of the experiment. Data is shown as a percent of control. C. An electronic readout called impedance non-invasively quantify adherent cell proliferation and viability in real time. The cells are seeded in standard microplates that contain microelectronic sensor arrays. The interaction of cells with the electronic biosensors generates a cell-electrode impedance response that not only indicates cell viability but also correlates with the number of the cells seeded in the well.

We confirmed these data testing the cell cycle frequency of generated cell lines (Figure 5.14). Using the FlowJo software, we applied the Watson Pragmatic univariate model. Fitting the curves to the appropriate cell cycle phase returned the values of each cell cycle phase. We could not observe any cell cycle arrest neither in the wild type nor knockout cells. These data are consistent with the experiments testing the proliferation capability of cancer cells upon the BAP31 knockout, supporting the statement that depletion of BAP31 has no influence on the proliferation of cancer cells.
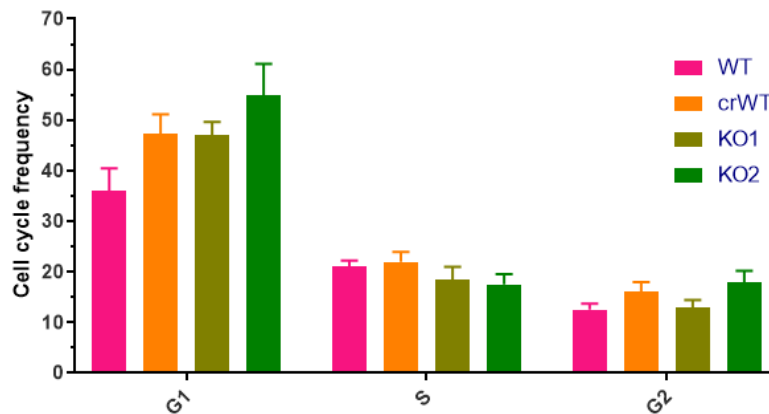
Figure 5.14. Comparison of the cell cycle frequency in the wild type and knock out BAP31 in RIL-175 cancer cells. The DNA content was measured by flow cytometry, assessing the signal from propidium iodide. Cell cycle frequency was analyzed applying the Watson pragmatic model using FlowJo software.

5.2.4 The migration is also not affected by BAP31 knockout.

Next to the high growth capacity, migration is a hallmark of cancer as well. Therefore, we applied two approaches to test the capability of cancer cells expressing and lacking the BAP31 protein to migrate. Figure 5.15.A shows the result of the experiment using Boyden Chambers, when Figure 5.15.B shows the simple scratch assay. Both experiments confirm the same conclusion – there are no consistent results of knock out of BAP31 in cancer cells on their migratory abilities.
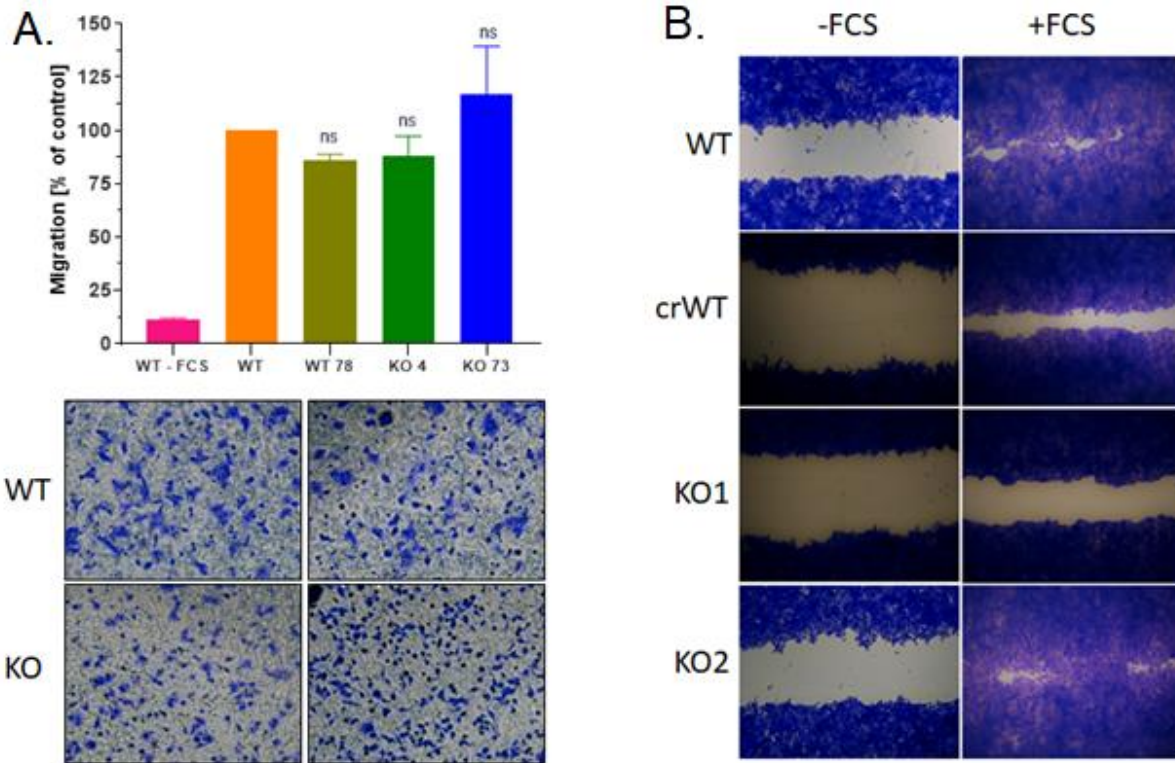
Figure 5.15. BAP31 knockout does not influence the capability of cancer cell line RIL-175 to migrate. A. Cell movement abilities have been tested with Boyden Chambers approach. Boyden chambers with 5µm pores were used. Cells were migrating for 5 hours. Cell number was assessed with ImageJ software. B. The wound healing assay has been performed to check the migration capability of cells expressing and lacking BAP31. When confluence was achieved, a scratch was done with a pipet tip. Cells were allowed to "heal the wound" for 16 hours. Next, cells were stained for the contrast with crystal violet. Pictures were taken under the light microscope. Data was tested using one-way ANOVA statistic.

5.2.5 Knock out of BAP31 does not affect the attachment of cancer cells.

We also tested the attachment of the cells. To compare the ability of wild type and knockout cells, we decided to use two different approaches – a crystal violet staining after 30 minutes of attachment (Figure 5.16.A) and the xCELLigence up to 120 minutes (Figure 5.16.B). However, the knockout of BAP31 had no significant influence also on this function of RIL-175 cell line.

63
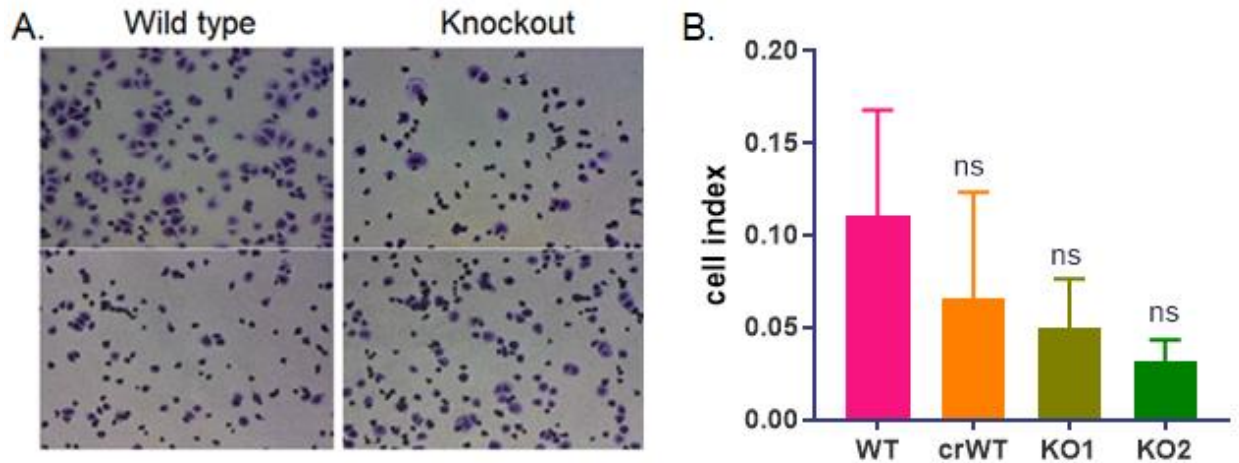
Figure 5.16. The attachment of RIL-175 cells expressing BAP31 in comparison to the BAP31 knockout cells. A. Cells stained with crystal violet after 30 minutes of attachment. B. xCELLigence analysis of the attachment 30 minutes after the seeding.

5.2.6 Identification of BAP31 interaction partners.

As we could not observe any functional differences between cells expressing and lacking BAP31, we decided to check for the proteins which interact with the one of our interest. To identify BAP31 interaction partners, we used a Yeast Two Hybrid technique.

In this approach a bait protein is expressed as a fusion to the Gal4 DNA-binding domain (DNA-BD; pGBKT7 vector; Figure 5.17.B), while libraries of prey proteins are expressed as fusions to the Gal4 activation domain (AD; pGADT7 vector; Figure 5.17.B; Fields & Song, 1989; Chien et al. 1991). When the bait and the prey proteins interact, the AD and DNA-BD domains are in the proximity (Figure 5.17.A). This results in the activation of transcription of four independent reporter genes: *AUR1-C*, *ADE2*, *HIS3*, and *MEL1*. In the yeast strain Y2HGold, activation of the reporters occurs only in a cell that contains proteins which interact and bind to the Gal4-responsive promoter. Therefore, it is possible to select the colonies in which the interaction occurs, seeding them on the plates with increasing selection capacity.
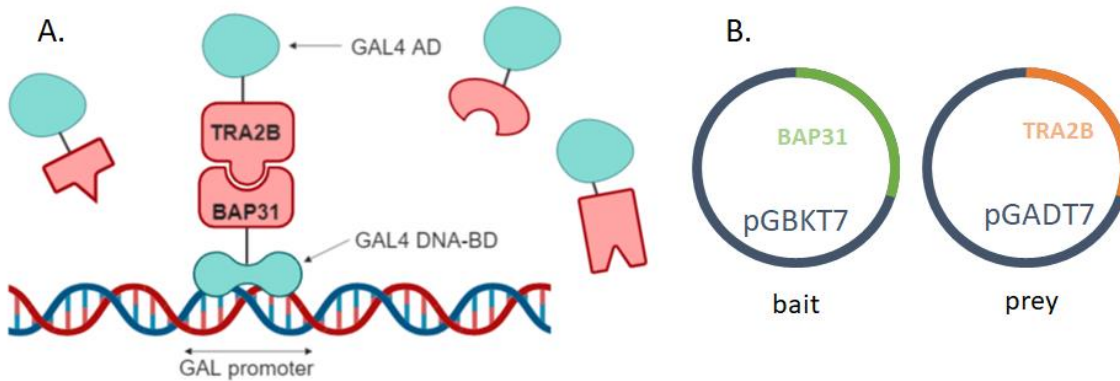
Figure 5.17. The Yeast Two Hybrid technique. A. The interaction between the bait (BAP31) and a prey (TRA2B) leads to the activation of transcription of reporter genes, as the GAL4 DNA binding domain (DNA-BD) and the GAL4 activation domain (AD) are in the proximity. B. Plasmids illustrating the bait and the prey cloned into the appropriate vectors.

In our investigation, I used BAP31 as a bait. Seeding the yeast on the selective plates allowed us to identify the colonies with the potential interaction of BAP31 with a prey. Those colonies were subjected to colony PCR and the bands of a different size were identified and sequenced. Out of 25 sequenced colonies, I obtained two hits: Transformer 2 Beta Homolog (TRA2B) and SNARE-associated protein Snapin (SNAPIN). Next, we needed to confirm that the prey plasmid does not autonomously activate the reporter genes in Y2HGold, in the absence of the bait protein.

Figure 5.18. shows two settings which we applied to test our prey plasmids towards auto-activation. In one setting we have just the prey expression (pGBKT) and in the second expression of both bait and prey proteins (pGBKT-BAP31). This interaction between bait and prey should activate the reporter genes. One of those is *MEL1* coding α-Galactosidase which can hydrolize X-α-Galactose (X). This reaction results in the blue product. One more reporter gene is a resistance to Aureobasidin A (A). There are two more reporter genes – Adenine and Histidine. Yeast cannot grow on the medium without these amino acids. As QDO plate is lacking Tryptophan and Leucine (which are coded on the vectors) as well as Adenine and Histidine which are reporter genes, yeast is not able to grow on this plate if there is no expression of reporter genes. If the reaction between prey and bait occurs, we can observe growing colonies which turn blue. Unfortunately, the plasmid for SNAPIN, even if there is no interaction with bait, seems to activate the reporter genes.

Therefore, we need to assume that there was no interaction between SNAPIN and BAP31 and had to exclude SNAPIN from our investigation.
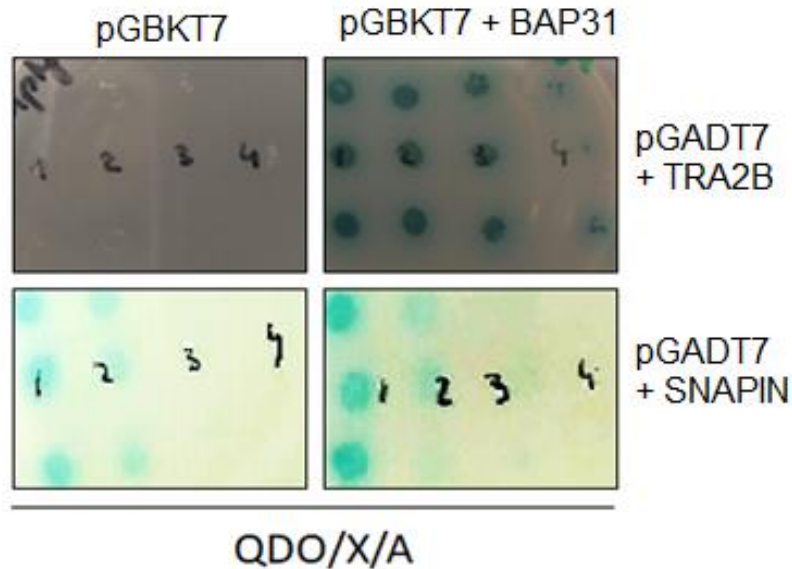
Figure 5.18. Test of the prey vector for the autoactivation. Prey plasmids were transformed into yeast together with empty bait vector (pGBKT7) or bait plasmid containing sequence for BAP31 (pGBKT7-BAP31). Only, when the interaction between bait and prey proteins occurs, the yeast should be able to grow on the selective plate, due to the activation of reporter genes. As prey plasmid containing sequence for SNAPIN was able to activate reporter genes when there was no bait, we call it auto-activation. It was not possible to go on with this hit, because there was most likely no interaction between BAP31 and SNAPIN.

Applying co-immunoprecipitation assay we could confirm, that BAP31 interacts with TRA2B. Figure 5.19. shows the result of immunoprecipitation of BAP31. The immune-precipitate of BAP31 was next subjected to western blot. We were successful to show, that in the mixture of proteins which interact with BAP31 we could also show presence of TRA2B. It re-confirmed the results obtained in yeast and established that interaction between BAP31 and TRA2B occurs also in mammalian cells.
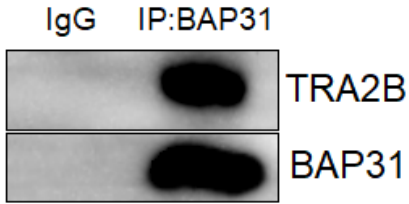
Figure 5.19. BAP31 and TRA2B interact also in mammalian cells. Cytoplasmic fraction of RIL-175 cells was incubated with μMACS^{TM} Protein G MicroBeads and BAP31 antibody. BAP31precipitate was subjected to western blot and analyzed for TRA2B expression. IgG control for rabbit was used to exclude bands representing light and heavy chain of antibody used for immunoprecipitation of BAP31.

5.2.7 The functional result of lack of the interaction between BAP31 and TRA2B.

Following our discovery, that BAP31 interacts with TRA2B, we decided to check the function regulated by TRA2B. This protein has been reported as an activator of splicing (Grellscheid et al., 2011; Elliott et al., 2012) as well as the alternative splicing regulator (Daoud et al., 1999; Matlin et al. 2005; Watermann 2006). We hypothesize that BAP31 captures TRA2B in the cytoplasm, what inhibits its function preventing its nuclear translocation. Following this hypothesis, lack of BAP31 expression should result in increase of TRA2B activity. Therefore, we decided to check the splicing capacity of the generated BAP31 knockouts.

To investigate if the changes in splicing occur in cells lacking BAP31 we used the Luciferase Reporter Gene Assay. Cells were transfected with the plasmid containing the sequence coding luciferase interrupted via an intron (Figure 5.20. A). To normalize the data between the cell lines to the normal transcription level, we used the plasmid which coded luciferase without any additional inserts.

In this experiment we could show, that cells which are not expressing BAP31 show higher splicing capacity (Figure 5.20.B). To confirm, that this function is affected due to TRA2B activity, we silenced this protein by siRNA in the experimental cells and normalized data to the wild type control expressing TRA2B. Clearly, knock out of TRA2B rescued the increase in splicing capability of cells lacking BAP31 (Figure 5.20.C). Therefore, we can state that knock out of BAP31 in RIL-175 led to the increase in splicing capacity, what is connected to TRA2B protein.
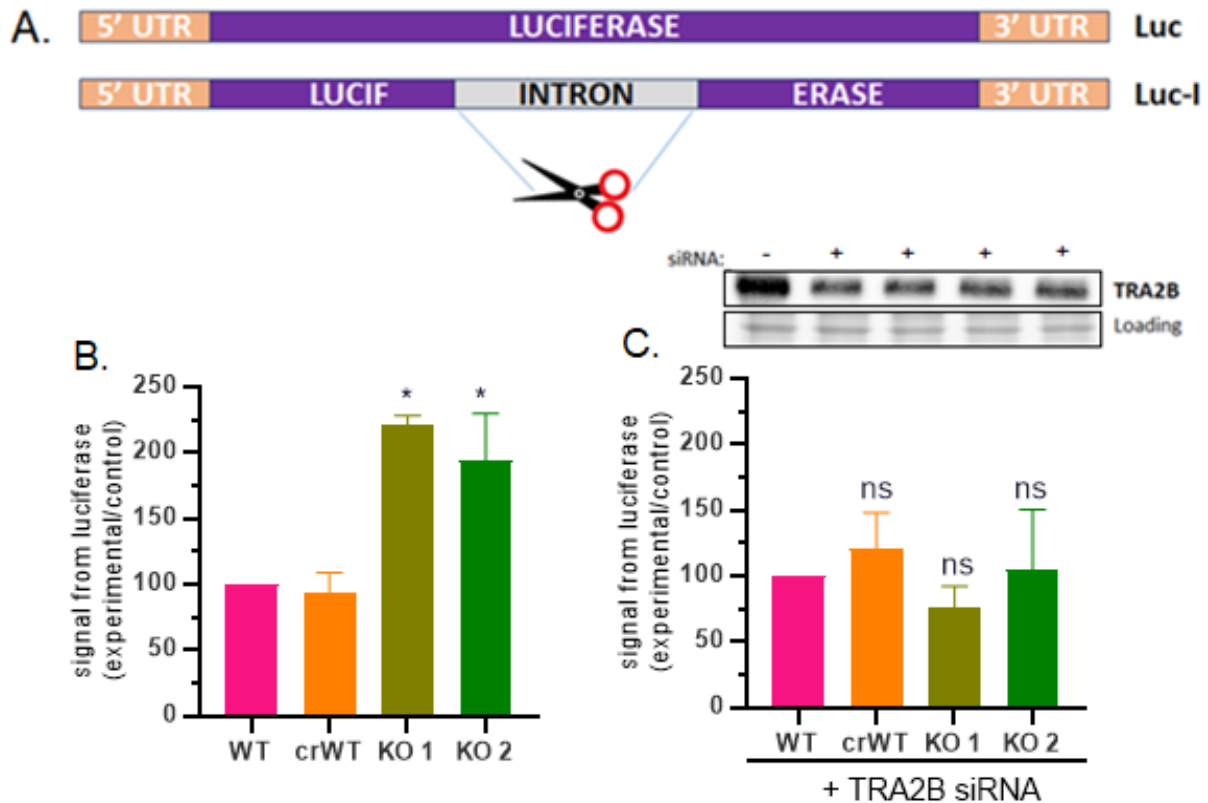
Figure 5.20. Knock out of BAP31 leads to the increase in splicing capacity of RIL-175 cells. A. The schema of plasmids used in luciferase reporter gene assay. B. Cells lacking BAP31 show increased splicing. Data was assessed with Luciferase reporter gene assay and normalized towards basal transcription level of each cell line. C. Silencing of TRA2B rescues the increase in splicing ability of BAP31 knockout cells. First, cells were transfected with siRNA for 24 hours, next transfected with plasmids for another 48 hours. After this time luciferase content was verified. Data was tested using one-way ANOVA statistic.

5.2.8 Influence of increased splicing on the signaling in cancer cells.

As described above, we investigated that the splicing capacity of RIL-175 cells is affected due to the lack of BAP31 expression. Therefore, we wanted to elucidate the signaling consequences of this change. Best et al. (2014), have investigated the Tra2-dependent genes and identified 53 proteins which were associated with Tra2 expression. Out of those genes Protein Arginine Methyltransferase 2 (PRMT2) seemed to be interesting concerning the cancer, as it is a regulator of Nuclear Factor κB (NFκB). Therefore, we have checked the expression of PRMT2 in cells expressing and lacking BAP31 (Figure 5.21A). We could confirm, that the expression of PRMT2 was increased in BAP31 knockout cells. This was consistent with the increase in splicing capacity

of cells lacking the protein of our interest. Moreover, we silenced TRA2B in all the cell lines and checked the expression of PRMT2 (Figure 5.21B). Treatment of cells with siRNA directed against TRA2B led to the rescue of increase in PRMT2 expression in BAP31 knockout cells.
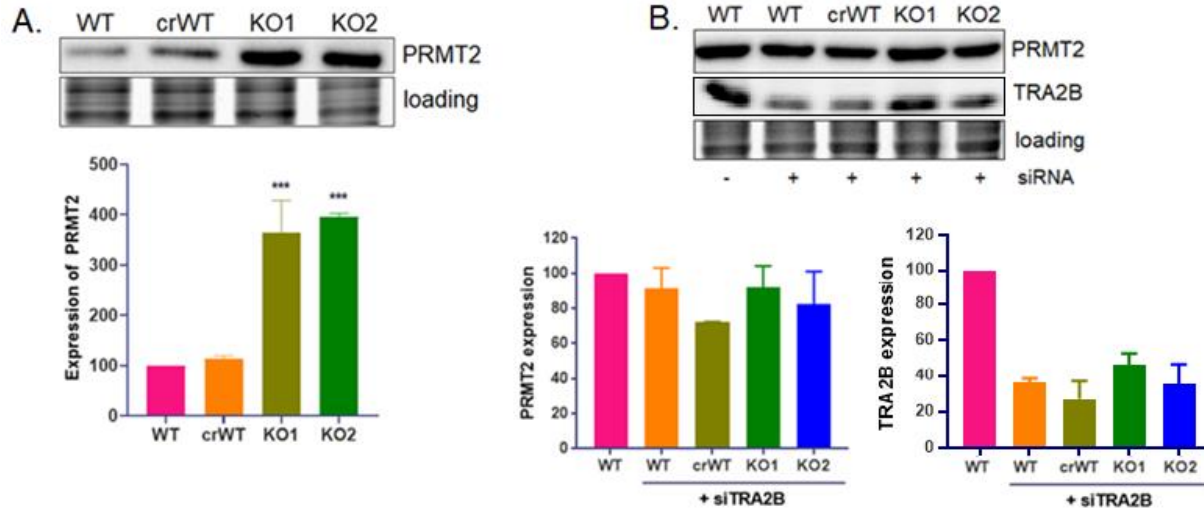
Figure 5.21. The expression of PRMT2 protein in RIL-175 expressing and lacking BAP31. A. Knock out of BAP31 leads to the significant increase in the expression of PRMT2. Expression was validated by western blot and quantified using Image Lab software. B. Silencing of TRA2B rescues the increase in expression of PRMT2. Cells were transfected with siRNA for 72 hours. After this time the expression of PRMT2 was verified by western blot and quantified with Image Lab software. Data was tested using one-way ANOVA statistic.

Following these hints, we examined the downstream of PRMT2 protein, namely NFκB signaling. According to the literature, PRMT2 regulates the NFκB signaling pathway through the nuclear accumulation of IkBα (Ganesh et al., 2006; Dalloneau et al., 2011).

To confirm our hypothesis that increased expression of PRMT2 leads to changes in the NFκB signaling also in our setting, we decided to check the nuclear accumulation of IkBα in the nucleus (Figure 5.22). The mechanism of regulation of NFκB by PRMT2 involves the accumulation of IkBα in the nucleus, therefore we applied the cytosol/nuclear fractionation approach to visualize this increase. As it is shown in the BAP31 knockout cells there is an increase of IkBα in the nucleus. Histone 3 (H3) was used as a marker for the nuclear and Tubulin for the cytoplasmic fraction. These data confirm that in cells lacking BAP31 more IkBα accumulates in the nucleus in comparison to the control, wild type cells.
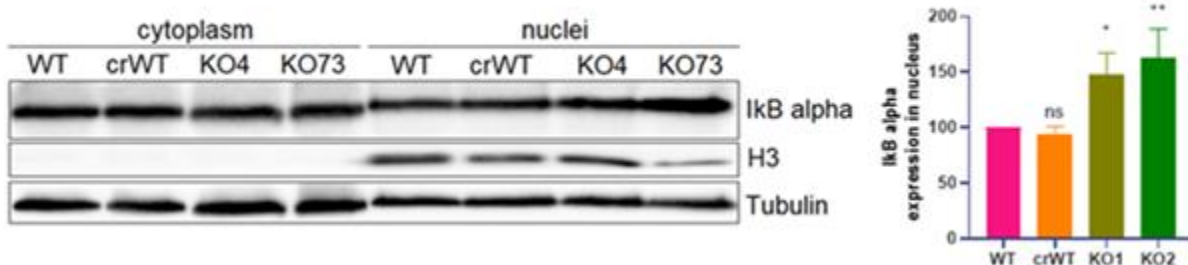
Figure 5.22. NFκB signaling in wild type vs knockout cells. Cytoplasm/nucleus fractionation was applied to check the expression of IkBα in the nucleus. Histone 3 (H3) was used as a nuclear marker to verify the quality of fractionation. Tubulin α was used as a cytoplasmic marker. Quantification was performed using Image Lab software. Data was tested using one-way ANOVA statistic.

As NFκB is connected to the autophagy process in cancer cells (Zhu et al., 2017), we investigated if also in our model we can observe the difference between the wild type and BAP31 knockout cells. It is known, that autophagy is a very dynamic process, therefore it is not possible to just check the expression of the proteins associated with autophagy. Zhang et al. (2018) provide an instruction how to properly evaluate the autophagic flux. Rephrasing this article, state of the art method requires to use the inhibitor of autophagy (we used Concanamycin) next to the control cells. Subsequently, it is recommended to subtract the amount of expressed control protein from the one treated with the inhibitor. Then, the result of the equation gives the amount of autophagic flux.

I decided to check the expression of LC3-II as well as p62. Both proteins, upon described analysis, showed decreased autophagic flux in cells with BAP31 knockout in comparison to the wild type (Figure 5.23 A and B). Moreover, I overexpressed LC3-II conjugated with EGPF, what enabled us to show the decrease in the formation of autophagosomes in cells lacking BAP31 (Figure 5.23. C). These data show, that a decrease in NFκB signaling leads to the inhibition of autophagy in our setting.
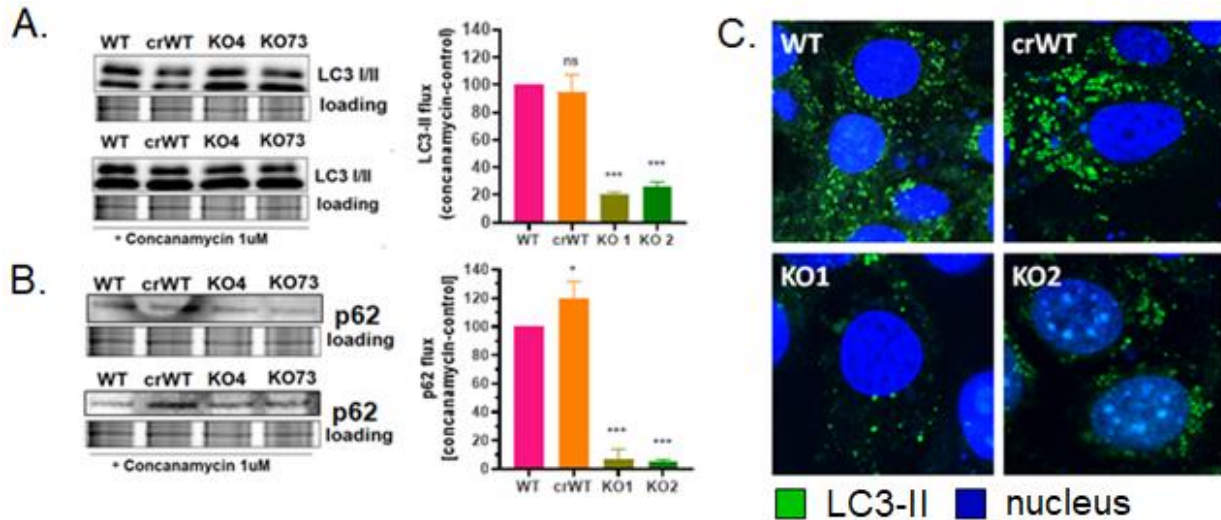
Figure 5.23. Knock out of BAP31 leads to the decrease in autophagic flux. A. Expression of LC3-II protein with and without inhibitor of autophagy. Data show the difference between expression in treated and not treated cells, which value indicates autophagic flux. B. Expression of p62, another indicator of autophagic flux, also with and without treatment with inhibitor of autophagy. C. Expression of LC3-II-EGFP via plasmid transfection in mammalian cell. Green dots indicate the number of autophagosomes. Data was tested applying one-way ANOVA statistic.

5.2.9 The knockout of BAP31 in cancer cells leads to the decrease in autophagic flux – summary.

In summary, we proved that lack of the interaction between BAP31 and TRA2B leads to the increase in the splicing capacity of cancer cells (Figure 5.24.). We hypothesize, that BAP31 captures TRA2B in cytoplasm, therefore preventing nuclear translocation of this protein. It explains that lack of BAP31 results in increase of TRA2B activity what leads to the increase in splicing capacity in cells lacking BAP31. Next, increased splicing results in the higher expression of PRMT2, which has been shown as one of the genes regulated via Tra2 proteins. Subsequently, PRMT2 negatively regulates NFκB signaling, causing the accumulation of IkBα in the nucleus, what leads to the decreased activation of NFκB and in the reduction of autophagy.

Our discovery introduces a new function of BAP31 in cancer cells. This novel mode of action for the first time shows BAP31 as a protein regulating the process of autophagy. Moreover, the interaction of BAP31 and TRA2B is not known so far. Therefore, it gives a new point of view on BAP31 in respect to the cancer treatment.

71
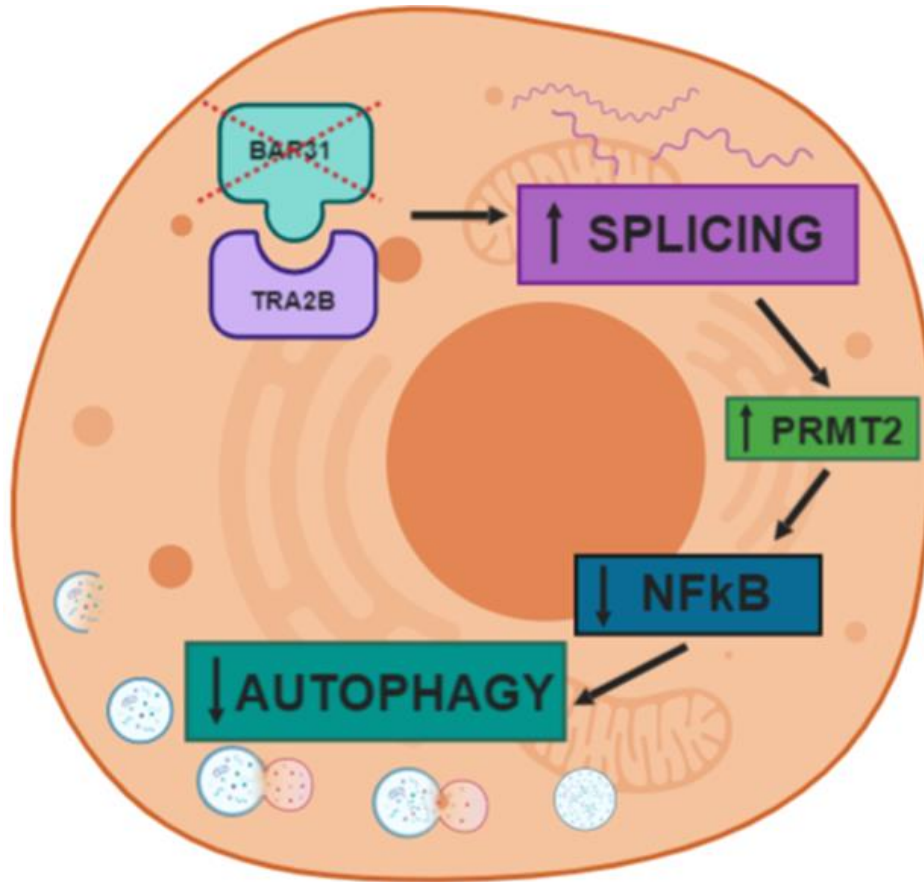
Figure 5.24. Functional result of BAP31 knockout in cancer cells. BAP31 knockout leads to the absence of BAP31 protein, therefore BAP31 and TRA2B cannot interact. It results in increased splicing capacity of BAP31 knockout cells. As PRMT2 is one of the proteins which gene is regulated via TRA2B activity, increase in splicing leads to the increase in PRMT2 expression. PRMT2 is known to enhance nuclear accumulation of IkBα, what results in decreased nuclear translocation of NFκB-p65, what leads to decreased NFκB signaling pathway. All these events end with disturbed process of autophagy.

6. DISCUSSION

6.1 PS89 – A POTENT CHEMO-SENSITIZER

Chemo-resistance is still the main contributor to chemotherapy failure and relapse, due to cancer cells adaptation to chemotherapeutic stress for survival through genetic and epigenetic alterations (Zhou et al., 2012). As one of the mechanisms inducing chemo-resistance of cancer cells is ability to avoid apoptosis (Zheng 2017) it is a common approach to combine chemotherapeutics to achieve a better effect of anti-cancer therapy (Zhang et al., 2017; Ma et al., 2019). Our work reveals PS89 as a very prominent chemo-sensitizer. As shown in the results part, we were able to show, that combination of PS89 with commonly used cytostatics results in significant increase in induction of apoptosis in comparison to treatment with drugs alone.

We could show, that the treatment with 25µM of PS89 was not toxic for the cells, but in the combination with chemotherapeutics like Etoposide, Vincristine, Daunorubicin or 6-Mercaptopurine it was highly effective in induction of ER-mitochondrial mediated apoptosis. In all used cell lines, we were able to show that the mechanism of induction of apoptosis is consistent. Moreover, the EC50 value for each of these drugs was significantly decreased when combined with PS89.

As the used dose of PS89 was sub toxic for the cells, but worked well in combination with other drugs, we decided to characterize this substance as a chemo-sensitizer.

6.1.1 Induction of ER-stress by T8 derivative - PS89

The small molecule PS89 was synthesized as an analogue of T8. Out of six synthesized molecules PS89 was shown to have the highest potential in induction of Etoposide mediated apoptosis in the Acute Lymphoblastic Leukemia (ALL) cell line Jurkat. In the proteomics analysis it showed to target and inhibit the Protein Disulfide Isomerase (PDI) (Eirich et al., 2014). This protein is known as a key player concerning the maintenance of ER homeostasis (Zhang et al., 2018). As the ER stress is a common reason for the chemo-resistance of cancer cells (Lingjing et al., 2018; Madden et al., 2019), ER homeostasis is an attractive target concerning re-sensitization of cancer cells (Janczar et al., 2017; Shah et al., 2018; Clarke et al., 2019). However, the approach of silencing

73

PDI revealed, that this protein is not the only target of PS89. Dr. Fabian Koczian in his doctoral thesis has shown, that the knockout of PDI does not rescue the effect of combinatorial treatment. Therefore, it was necessary to look for another target of the small molecule. Activity Based Protein Profiling (ABPP) conducted by group of Prof. Dr. Stephan Sieber (Department of Chemistry, Technical University of Munich) characterized BAP31 as another target of PS89 next to PDI, which is also connected to the ER homeostasis. Thus, BAP31 and its function became our focus in further research.

Following the function of PS89 targets we asked the question if the ER function is impaired in cell treated with PS89 or the combination. We could show, that treatment of leukemic cells with PS89 alone did not induce any ER stress or Unfolded Protein Response. However, in the combination with chemotherapeutics we observed a very prominent increase in signaling connected to disturbed ER homeostasis. This indicates, that activation of all the events connected to the ER stress response results from the impaired ER function and defect in resolving the stress condition induced via treatment with cytostatics (Eirich et al., 2014).

6.1.2 Chemo-sensitization of leukemic cells towards cytostatics – the mechanism of action

It is well known, that the induction of apoptosis via cytostatics involves the mitochondria-mediated mechanism of apoptosis (Chonghaile et al., 2011). Moreover, it is of increasing interest how the ER-mitochondrial communication is involved in the cell fate (Shore et al., 2011; Bhat et al., 2016; Simmen & Herrera-Cruz, 2017).

Our work reveals a potential crosstalk between ER and mitochondria triggered via PS89. As mentioned above, the conducted ABPP has identified BAP31, next to the PDI, as the target of PS89. BAP31 has been described already as the target of caspase-8. Interestingly, caspase-8 is one of essential players in apoptosis mediated by the unfolded protein response (UPR), upon chronic ER stress (Estornes et al., 2015; Cano-González et al., 2018; Muñoz-Pinedo & López-Rivas, 2018) what links ER chaperone function of BAP31 to apoptosis. Reaching to the work of Iwasawa et al., we can learn, that the apoptotic stimuli from Etoposide activates caspase-8, what leads to the cleavage of BAP31 to its pro-apoptotic form – p20. Activated BAP31 triggers the release of ER calcium to cytoplasm, what results in the induction of mitochondrial apoptosis (Iwasawa et al.,

2011). Therefore, we investigated if this mechanism of action is applicable also for PS89-cytostatic induced apoptosis.

To show what an important role the interaction of caspase-8 and BAP31 plays in the treatment with PS89 as the chemo-sensitizer, we investigated the key proteins involved in this signaling pathway. We were able to show, that cleavage of Caspase-8 as well as BAP31 in the combinatorial treatment led to the prominent calcium release from ER in comparison to the treatment with cytostatics alone. The subsequent event was mitochondrial outer membrane permeabilization (MOMP), what led to the release of cytochrome c and Reactive Oxygen Species (ROS) to cytoplasm. When ROS seems to induce the ER stress in a positive loop, cytochrome c present in cytoplasm triggers further apoptotic stimuli (Shore et al., 2011; Grimm, 2012).

6.1.3   The potential of PS89 as a chemo-sensitizer in the treatment of leukemia cells

We were able to prove, that the addition of PS89 as a chemo-sensitizer next to the commonly used cytostatics, significantly decreases the EC50 value of used drug. This supports the idea of application of combinatorial therapies to lower the required dose of the chemotherapeutics (Bayat-Mokhtari et al., 2017). Moreover, as it was shown in the doctoral thesis of Dr. Fabian Koczian, applying combination of PS89 and Vincristine re-sensitized Vincristine resistant CCRF-CEM cells. Once again, it supports the idea of the application of combinatorial therapies in respect of re-sensitization of drug-resistant cancer cells. This is why the potential of this small molecule should be further tested in vivo and, in the future, subjected to the clinical trials.

6.2 THE FUNCTIONAL RESPONSE TO BAP31 KNOCK OUT IN HEPATOCELLULAR CARCINOMA

Motivated by the success of PS89 combinatorial therapy, we wanted to focus on the function of BAP31. As this protein seemed to be not well investigated in the context of cancer, we created a stable BAP31 knockout in the murine hepatocellular carcinoma cell line – RIL-175, what gave us a tool to investigate the function of this protein.

However, as shown in the result part, BAP31 knockout had no influence on main functions of cancer cells, like proliferation, migration or attachment. To learn more about the protein of our interest, we decided to use the Yeast 2 Hybrid (Y2H) approach to identify the interaction partners of BAP31. Using this technique, we were able to show a novel association of BAP31 with Transformer 2 β homolog (TRA2B). We could confirm the co-localization of these two proteins applying confocal microscopy imaging as well as fractionation approach. Moreover, we were able to show the interaction between BAP31 and TRA2B in mammalian cells using co-immunoprecipitation approach.

6.2.1 Transformer 2 β homolog protein – the functional consequences of the lack of interaction with BAP31

Transformer 2 β homolog (TRA2B) is known as the enhancer of splicing as well as the regulator of alternative splicing (Dauwalder et al., 1996). Nowadays, TRA2B was also shown to be connected to cancer growth and senescence in different types of cancer (Kajita et al., 2016; Chen et al., 2018; Satake et al., 2018) as well as connected to neoplasia and metastasis (Best et al., 2013). Following the function of TRA2B in the cell, we validated the splicing capability of cells expressing and lacking BAP31. We could show, that in cell lines which are not expressing BAP31 the splicing level is twice amount of the control. Therefore, we concluded that the interruption of interaction between BAP31 and TRA2B leads to an increased activity of TRA2B.

BAP31 was shown as a chaperon protein (Schamel et al., 2003; Ladasky et al., 2006) thus, we hypothesize that TRA2B associate with BAP31 in the cytoplasm, where they are both localized, what prevents too frequent translocation of TRA2B to the nucleus. If there is no BAP31 in the cell, TRA2B can freely migrate to the nucleus where it acts as the splicing factor increasing the splicing

capacity of cancer cells. However, we were not able to show the higher expression of TRA2B in the nucleus in cells lacking BAP31. It could be, that these changes are not high enough to be shown via regular immunoblotting approach. Therefore, the mechanism that leads to the increased splicing capacity in cells lacking the interaction between TRA2B and BAP31 needs to be further investigated.

6.2.2   Increase in PRMT2 expression due to the increase in TRA2B-dependent splicing

Transformer 2 (TRA2) proteins play a role in the regulation of pre-mRNA splicing. Human *TRA2* gene has two separate gene paralogs encoding TRA2A and TRA2B proteins (Ghosh et al., 2016). Best et al. have identified 53 genes which were regulated via double-knockout of TRA2α and TRA2β (Best et al., 2014). Out of those we focused on Protein Arginine Methyltransferase 2 (PRMT2), which is known to regulate the Nuclear Factor κB (NFκB) signaling. PRMT2 is involved in the regulation of NFκB activation via accumulation of IkBα in the nucleus (Ganesh et al., 2006; Dalloneau et al., 2011). This accumulation prevents further translocation of p65 to the nucleus decreasing the activity of NFκB.

In the canonical signaling pathway, upon the activation of the NFκB receptor, the signal is transduced to the IκB kinase (IKK) complex. The IKK is the core element of the NFκB cascade. It is essentially made of two kinases (IKKα and IKKβ) and a regulatory subunit, NEMO/IKKγ (Israël, 2010). Subsequently, the Inhibitor of κB (IkB) protein is phosphorylated by IKK, what leads to the release of NFκB from the inhibitory complex. Once this transcription factor is free, it can translocate to the nucleus and fulfill its function.

We were able to show, that the expression of PRMT2 is almost four-fold higher in cells lacking BAP31. Moreover, applying the nuclear-cytoplasm fractionation we could show, that the accumulation of IkBα in nucleus occurs in BAP31 knockout cell lines but not in the wild type. We also showed, that the translocation of p65 to the nucleus is lower in cells lacking BAP31, what is consistent with increased expression of PRMT2 in those cells. Moreover, we also showed that the phosphorylation of IkBα was affected in cells lacking BAP31 expression. All these data prove, that NFκB signaling is decreased in cell lines lacking BAP31-TRA2B interaction (Figure 6.1.).
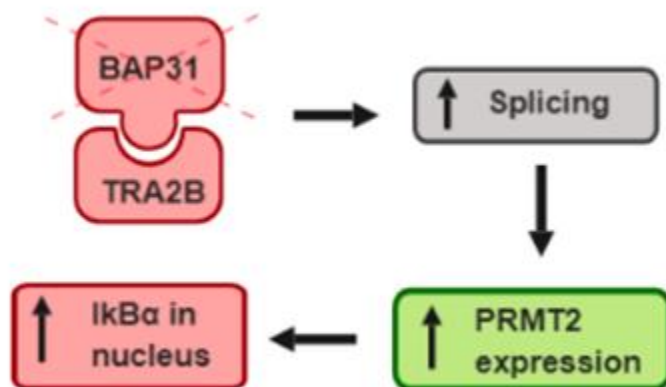
Figure 6.1. Influence of lack of BAP31 on NFκB signaling. Lack of interaction between BAP31 and TRA2B leads to the increase in splicing, what results in increased PRMT2 expression. As PRMT2 is a protein which blocks nuclear export of IkBα, it leads to nuclear accumulation of IkBα. All these events result in decreased activation of NFκB signaling pathway.

6.2.3 The result of changes in NFκB signaling – decrease in autophagy

NFκB is a protein involved in carcinogenesis in almost every aspect (Xia et al., 2014; Park & Hong, 2016). NFκB can be activated through a broad spectrum of stimuli like growth factors (Epidermal Growth Factor (EGF)), lipopolysaccharides (LPS) produced by bacteria, cytokines (TNF-α, IL-6, ect.), UV light, reactive oxygen species (ROS), DNA damage or oncogenic stress (Xia et al., 2014).

According to Xia et al. NFκB signaling supports proliferation of cancerous cells, angiogenesis, promotes metastasis, influences the metabolism of the cell as well as helps cancer cells to escape apoptosis (Xia et al., 2014). Moreover, NFκB signaling has been connected to autophagy, which is in a focus of science nowadays (Trocoli & Djavaheri-Mergny, 2011; Zhu et al., 2017). As we could not see a difference in proliferation or migration of cells lacking BAP31 expression, we decided to investigate a potential role of BAP31 in autophagy.

To prove that autophagy is affected in our setting, we checked the expression of LC3-II as well as p62 with and without treatment with Concanamycin, a known inhibitor of autophagy. Following the instructions contained in the article of Zhang et al., we verified the level of autophagy (Zhang et al., 2017). Evaluation of both proteins showed that this process is decreased in BAP31 knockout cells. We could re-confirm that via overexpression of LC3-II conjugated with GFP. Using confocal

78

microscopy, we showed that the number of autophagosomes is lower in cells lacking BAP31 expression.

6.2.4 Autophagy as the therapeutic target in cancer

Autophagy is a process of capturing the intracellular components in autophagosomes and delivers them to the lysosomes for the degradation and recycling (Levine & Kroeme, 2008; Mizushima, 2010). Selective autophagy recognizes, captures and eliminates the unfolded proteins induced by stress and damaged organelles. This helps to protect normal cellular components. To ensure, that the cargo is recognized properly, it is tagged via ubiquitination. Subsequently, ubiquitin is recognized by the autophagy receptors and the cargo is subjected to the autophagy machinery (Clague & Urbe, 2010). Under normal conditions, autophagy functions at a constitutive, low basal level to maintain protein and organelle quality, quantity, and functionality. However, this process is dramatically induced by starvation and other stressors, which enable cellular and organismal survival. Autophagy upregulation is part of a survival mechanism under the nutrient stress, which is conserved from yeast to mammals (Amaravadi et al., 2016).

Nowadays, it is known that autophagy has opposing, context-dependent roles in cancer. Therefore, both - stimulation and inhibition of autophagy have been proposed as cancer therapies (Levy et al., 2017). It was shown, that once cancer is established, increased autophagic flux often enables tumor cell survival and growth (White, 2012; Amaravadi et al., 2016). This supports the idea, that inhibition of autophagy would be a good therapeutic approach.

It is important to keep in mind, that many of current cancer treatments are affecting autophagy. For example, those which are impairing the mTOR signaling pathway like Rapamycin (Jung et al., 2010; Paquette et al., 2018). Also, the physiological changes in cancer environment like hypoxia or nutrient depletion have an influence on the autophagy (Levy et al., 2017). Therefore, it is impossible to ignore this process in the context of cancer.

As we shown in our work, knockout of BAP31 leads to the decrease of autophagy in mice hepatocellular carcinoma cell line. However, we did not observe any influence of decreased autophagy on the proliferation capacity or migratory potential of used cells. This could be explained via different roles of autophagy in different types of cancer as discussed above. It would

be necessary to investigate the role of BAP31 on the autophagy induction in different types of cancer to understand in which setting BAP31 expression would have a survival and therapeutic meaning.

6.2.5 The consequences of BAP31 deregulation in different types of cancer

The role of BAP31 inhibition or overexpression is very controversial. Tan et al. Showed that the low expression of BAP31 in human primary hepatocellular carcinoma (Tan et al., 2016) as well as in human colorectal cancer (Ma et al., 2018) correlates with poor prognosis. Also, Seo et al. showed that the overexpression of BAP31 is connected to poor survival of non-small cell lung carcinoma cells (Seo et al., 2017). However, there are also statements, that inhibition of BAP31 is supporting cell death and inhibiting cancer growth (Xu et al., 2019) as well as suppressing metastasis of malignant cells (Yu et al., 2015; Dang et al., 2018; Wang et al., 2019).

As mentioned above, autophagy also seems to contribute to the survival, growth and metastasis of cancer (Mowers et al., 2017), however depending on the type of cancer inhibition or induction of this process can have a different role. The confusion about BAP31 expression in cancer seems to be the same. Therefore, the contribution of BAP31 in the process of autophagy could be a missing puzzle piece concerning the function of the investigated protein in cancer.

Our research is first to report involvement of BAP31 in autophagy. Moreover, it introduces a new perspective concerning the role of BAP31 and shed a light on its function in cancer cells.

7. Summary

BAP31 is an interesting protein investigated more intensively nowadays. Its function in induction of apoptosis has been broadly described in literature. Here, using state-of-the-art molecular biology methods, we checked the chemo-sensitizing effect of a small molecule targeting BAP31 – PS89, on different leukemia types in combination with commonly used cytostatics and showed very prominent results concerning chemo-resistance and induction of apoptosis in leukemia in vitro models. Moreover, we were able to confirm the involvement of BAP31 activation in mitochondriadriven apoptotic signaling pathway.

The promising results of combination treatment led us to focus on this interesting protein. From the literature it is clear that the induction of apoptosis is not the only influence that BAP31 exerts on cancer cells. Therefore, it was of our interest to explore the function of BAP31 in this regard. For this purpose, we applied a novel CRISPR/Cas9 technique to create a tool for further investigation – a stable knockout of BAP31 in murine hepatocellular carcinoma cell line RIL-175.

To overcome the next challenge, which was the identification of BAP31 cooperation partners, we applied the Yeast Two Hybrid method, which was intensively developed over last years. This approach enabled us to identify a novel interaction between BAP31 and TRA2B (a protein engaged in splicing). Dual Luciferase Reporter Gene assay allowed us to show increased splicing capability of BAP31 knockout cells. The literature review helped to identify the protein regulated via TRA2B dependent splicing – PRMT2. We were able to confirm, that the expression of this protein is upregulated in cells lacking BAP31. Mitochondrial/nuclear fractionation approach helped to confirm that increased expression of PRMT2 led to the accumulation of IkBα in the nucleus, what has been described in the literature as the mechanism of action for PRMT2. This accumulation potentially inhibits activity of the NFκB complex what results in decreased autophagy in cells lacking BAP31 expression (Figure 7.1).

Summarizing, we were able to show for the first time the involvement of BAP31 in cellular processes like splicing or autophagy, which are known to be changed in various types of cancer. Our work shed light on the function of BAP31, what is a starting point for further drug development, treatment strategies as well as diagnostic parameter. However, further investigation is needed.
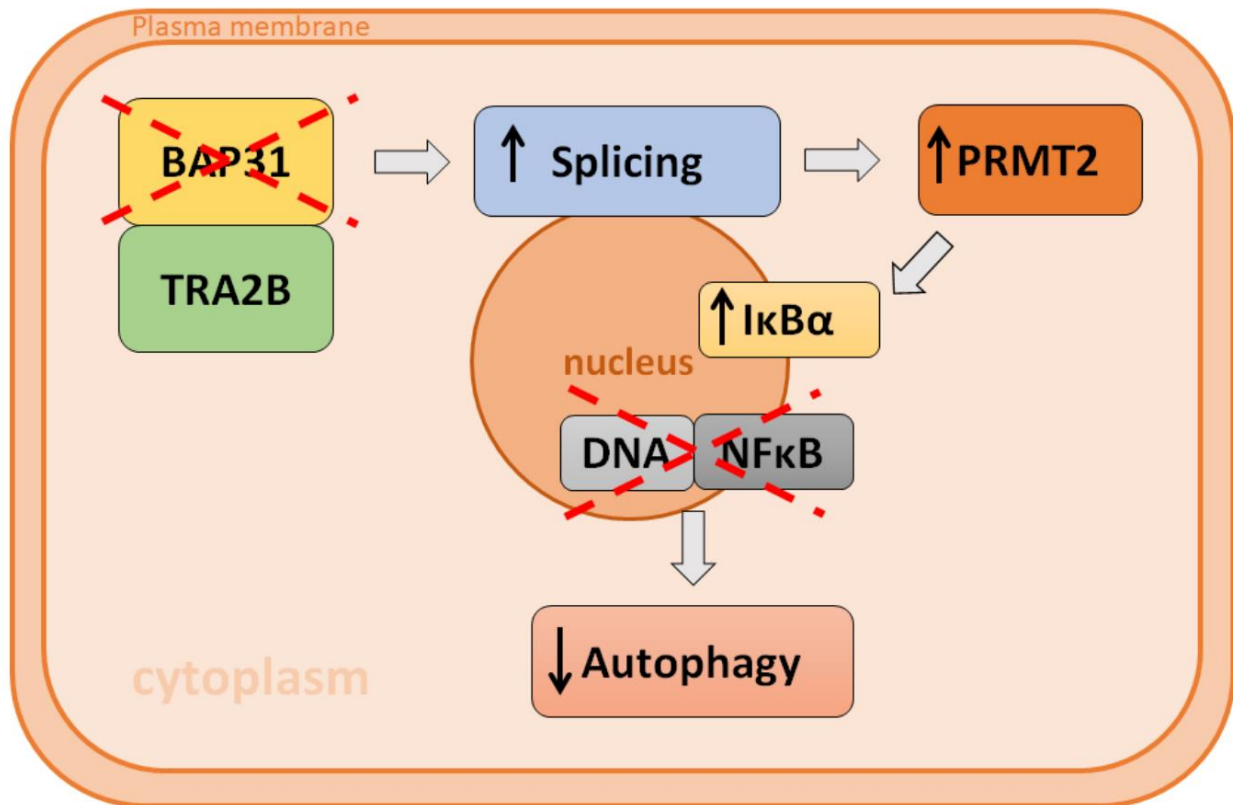
Figure 7.1. Functional result of BAP31 knockout in cancer cells. Lack of BAP31 leads to the increase in splicing capability, what results in increased expression of PRMT2. Activity of PRMT2 affects the transport of IκBα from nucleus. Accumulation of IκBα potentially interferes with NFκBDNA binding affecting its activity. All these events influence autophagy capacity of cells lacking BAP31.

8. SIDE PROJECT

Targeting de novo lipogenesis as a novel approach in anti-cancer therapy

Stoiber K, Nagło O, Pernpeintner C, Zhang S, Koeberle A, Ulrich M, Werz O, Müller R, Zahler S, Lohmüller T, Feldmann J, Braig S. British Journal of Cancer. 2018 Jan; 118(1):43-51;

8.1 INTRODUCTION

Cellular membrane is a very important organelle for each cell. It is not only a selective barrier taking part in the maintenance of cell integrity and compartmentalization but also establishes a signaling platform for the processes like cellular growth, differentiation or migration (Cooper, 2000). Therefore, plasma membrane properties are of great interest of science concerning their contribution to regulation of malignancy and metastatic abilities of cancer cells (Escriba et al., 2015). As the ability of cells to deform plays a quite important role in metastatic potential, this property was proposed as a marker for migratory capability of cancer cells. It is important to keep in mind, that these peculiarities are connected not only to the cellular cytoskeleton but also to the membrane characteristics (Remmerbach et al., 2009; Swaminathan et al., 2011).

So far, all the efforts to target the migratory capacity of the cell focused on the cytoskeleton (Rauscher, 2018; Ilan, 2019; Bryce et al., 2019). However, cellular membrane is also of a great importance concerning this process. The composition of plasma membrane impacts biomechanistic as well as characteristic of the cells (Sherbet. 1989; Nicolson 2015). This has been shown before, that the acetyl-CoA carboxylase (ACC) activity, which is a limiting enzyme of fatty acid synthesis, can influence the phospholipid composition of cellular membrane, what leads to the changes in its composition (Rysman et al., 2010; Braig et al., 2015).

The aim of this study was to investigate the consequences of disturbing plasma membrane physiology by inhibiting ACC. Thereby we investigated of key players of cancer promoting signaling pathways and unrevealed the functional impact of ACC inhibition on proliferation of cancerous cells. We could contribute to the investigation of molecular basis of targeting the plasma membrane properties and introduce it as a promising therapeutic strategy against cancer.

8.2 Results

It was shown in the doctoral thesis of Dr. Katharina Stoiber, that inhibition of ACC activity via Soraphen A treatment of the HER2 overexpressing breast cancer cell line SKBR3 led to changes in plasma membrane composition. ESI tandem mass spectrometry has revealed that the double-bonds in cells treated with Soraphen A changes from the less saturated towards more saturated in all groups of phospholipids, namely: phosphatidylcholine (PC), phosphatidylethanolamine (PE), phosphatidylinositol (PI), phosphatidylserine (PS). Also, it was shown that the chain length of PC as well as PE was increased in cells treated with the ACC inhibitor in comparison to the control cells. This led to the impairment of the plasma membrane rigidity, what was tested applying the Fluorescence Recovery after Photobleaching (FRAP) approach in cells treated with Soraphen A. Another approach which used to confirm changes in the membrane stiffness was the vesicle deformation measurement conducted via Dr. Carla Pernpeintner from the group of Prof. Dr. Jochen Feldmann (Photonics and Optoelectronics Group of Department of Physics and Center for Nanoscience, LMU), which re-confirmed the impairment of plasma membrane properties (Figure 7.1.).
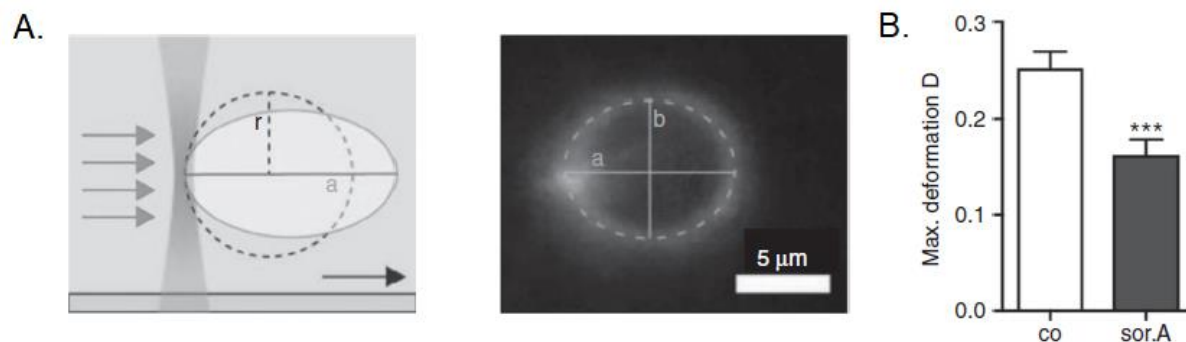
Figure 8.1. A. Experimental setup for vesicle deformation measurements: A single membrane vesicle derived from SKBR3 cells was trapped on one end with a focused laser beam (optical tweezer). Application of flow results in elongation of the vesicle along the flow direction. Right: Dark-field microscopy image of an optically trapped vesicle. The 2D projection of the vesicle is fitted with an ellipse using home-built Matlab and C þ þ routines. A dashed line indicates an elliptic fit of the vesicle cross-section with half axis a and b. B. Comparison of the maximum deformation Dmax of vesicles obtained from cells after treatment with Soraphen A or control. The error bars indicate the s.e.m. for a sample size of 30 and 40 cells, respectively.

As Dr. Katharina Stoiber also shown in her thesis, changes in cellular membrane composition led to the inhibition of interaction between HER2 and EGFR. Activation of these two proteins is an important event in signaling which promotes cancer proliferation (Diermeier et al., 2005). She was also able to show that the phosphorylation of these proteins is decreased in cells treated with increasing doses of Soraphen A.

Next to the signaling, receptor recycling is another process strongly dependent on membrane characteristics. Previous research has indicated that endocytotic recycling of EGFR may be the underlying molecular mechanism for its increase (Tong et al., 2017). Therefore, my role was to investigate the recycling process in cells treated with Soraphen A as well as upon the silencing of ACC1. This experiment could confirm, that treatment with ACC inhibitor led to the disturbance in recycling of transferrin receptor. The same effect was observed in ACC1 knockout cells (Figure 7.2).
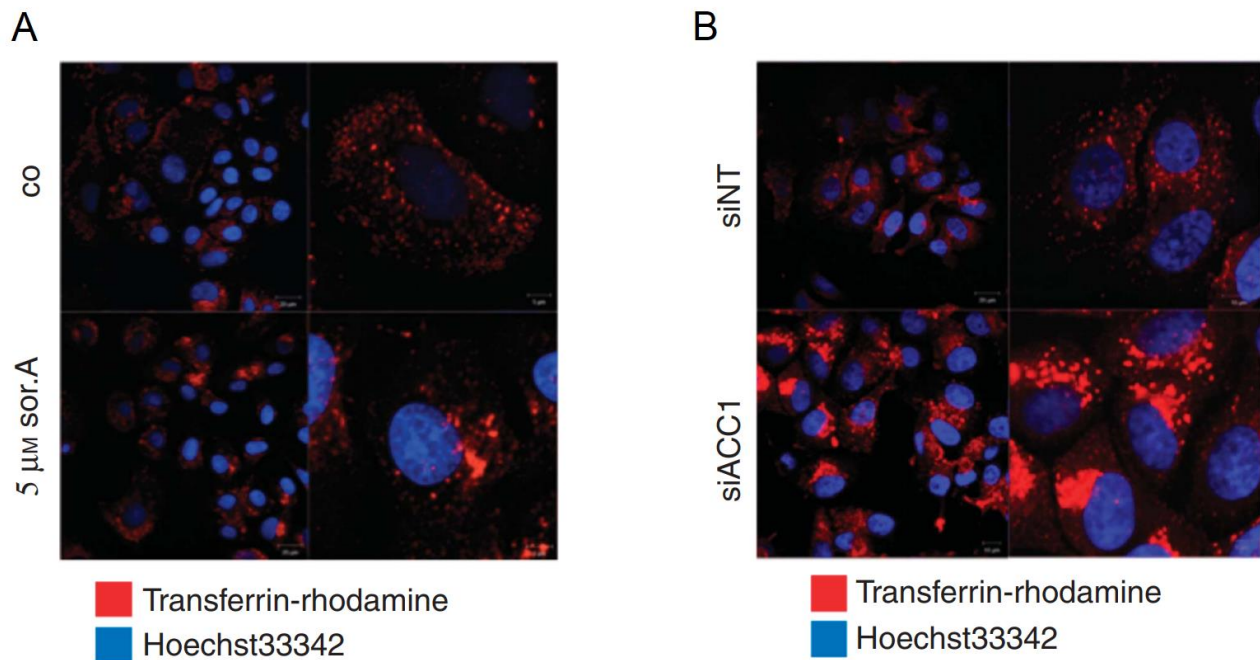
Figure 8.2. Impaired recycling of transmembrane receptors. A: Receptor recycling of soraphen A-treated and B: siACC1-transfected SKBR3 cells was monitored by adding rhodamine-tagged transferrin upon the treatment for 72 hours with either Soraphen A or siACC1.

Metastasis is the leading cause of cancer related death and thus it is crucial that we improve our understanding of the mechanisms that promote this life-threatening phenomenon. Therefore, the migratory capacity of cancer cells upon the treatment with Soraphen A was fully investigated via Dr. Katharina Stoiber. Next to the metastasis, second important property of cancer cells is capability to grow. Thus, my task was to test different inhibitors of ACC and Fatty Acid Synthase (FASN), another important player concerning *de novo* lipogenesis, in context of the proliferation. As Soraphen A was shown to effectively inhibit proliferation of SKBR3, we decided to treat them with some more ACC inhibitors – TOFA and CP-640,186, as well as FASN inhibitors – Cerulenin, C75 and UCM05 to prove, that the reason of impaired proliferation is due to the decrease in *de novo* lipogenesis. Figure 7.3 shows, that all of them could inihibit the proliferation rate of those cells.
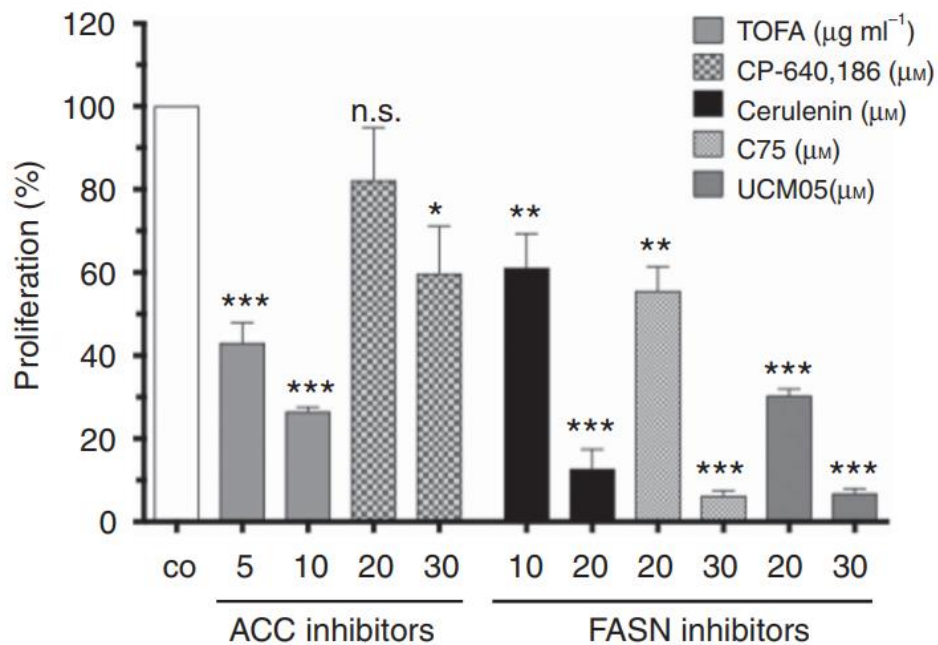
Figure 8.3. The proliferation of SKBR3 cells is inhibited upon the treatment with different doses of both ACC and FASN inhibitors. The proliferation rate was assessed after 72 hours of proliferation applying Cell-Titer Blue assay. The error bars show the standard deviation of three independent experiments. Significance was tested applying One-way ANOVA.

Moreover, we were able to prove, that this function is impaired via change in the composition of plasma membrane. We were able to rescue the effect of the inhibition of ACC by Soraphen A treatment applying the PI mix to the cells. This is shown in the Figure 7.4.
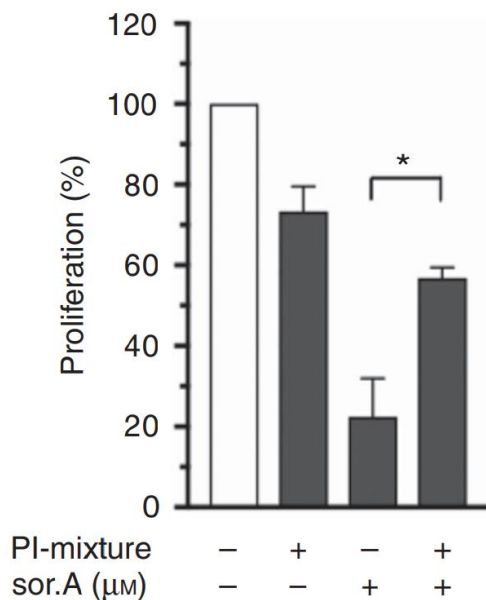
Figure 8.4. Treatment with PI mix rescued the effect of Soraphen A treatment on the proliferation. The error bars show the standard deviation between three independent experiments. Significance was tested applying the One-way ANOVA.

8.3 DISCUSSION

These studies show, that cellular membrane is an attractive target for cancer therapy. Treatment of cancer cells with the inhibitors of *de novo* lipogenesis led to impaired proliferation and migration. Dr. Katharina Stoiber could show, that these functions were connected to changes in the plasma membrane phospholipid composition, what led to increased membrane stiffness and resulted in inhibition of interaction between EGFR and HER2. Impaired signaling led to decrease in proliferation and migration of cancerous cells.

The issue of plasma membrane was already studied in the context of cancer (Zalba & Hagen, 2017). However, the membrane lipid therapy did not reach the clinic yet, even though it is described as a very promising new treatment approach (Escriba, 2017). Following the idea of targeting lipid metabolism, it is possible to inhibit a growth of cancer cells. This has been shown

for example using Orlistat, which is a fatty acid synthase (FASN) inhibitor, in combination therapies (Menendez et al., 2006; Wright et al., 2017). Also, acetyl-CoA carboxylase (ACC) has been shown as a good target to inhibit the proliferation of non-small-cell lung cancer *in vivo* using ND-646, an allosteric inhibitor of the ACC enzymes (Svensson et al., 2016).

To better understand the functional implications of the impaired phospholipid composition of cellular membrane, we used Soraphen A, which is a well-known ACC inhibitor, to analyze the crucial importance of phospholipid homeostasis on functions of cellular membrane. Even though the mechanism of action of this compound was not elucidated in detail so far, there is some data unraveling that targeting ACC leads to the changes in phospholipid composition of cellular membranes and its dynamics (Rysman et al., 2010). This also has been confirmed by our group and these data are available in the doctoral thesis of Dr. Katharina Stoiber. Moreover, in co-operation with Dr. Carla Perpeinter from the group of Prof. Dr. Jochen Feldmann (Photonics and Optoelectronics Group of Department of Physics and Center for Nanoscience, LMU) we could show, that treatment with Soraphen A leads to significant increase in stiffness of the membrane vesicles in comparison to the control group.

Cellular membrane is not only a barrier between a cell and environment. It also takes part in the signaling, for example via regulation of recycling process (Ray et al., 2016). We could confirm, that inhibition of ACC either with Soraphen A or siRNA directed against ACC1, changes the recycling of Transferrin receptor. In the doctoral thesis of Dr. Katharina Stoiber as well as in the publication of Braig et al. (Braig et al., 2015), it was also shown, that the localization and dimerization of the growth factors HER2 and EGFR was impaired upon the treatment with Soraphen A. As these two receptors are the important players in the process of cancer growth, changes in the membrane composition are affecting their lateral movement, what leads to the impaired downstream signaling and inhibition of cancer growth. Therefore, targeting the cellular membrane properties would be a promising therapeutic approach in cells where the classical compounds targeting growth factors receptors properties are limited due to mutations in the kinase domain of the receptor (Kobayashi et al., 2005). Moreover, this effect is amplified via the abrogated recycling process. The receptors, when activated, are internalized, sorted at the endosomes and, subsequently, they can be either degraded or recycled back to the plasma membrane to further promote proliferation. When this process is not functioning properly, the

dysregulated EGFR trafficking results in impaired cellular growth and cancer progression (Tomas et al., 2014). We could show, that the inhibition of the transferrin receptor recycling, which resulted from ACC inhibition, led to the accumulation of the receptor-ligand complex in the juxtanuclear area, what interfered with cancer-associated growth factor receptor signaling.

In summary, the work of Dr. Katharina Stoiber and me shows that altered properties of cellular membrane via interrogation of *de novo* lipogenesis impaired the characteristics of cellular membranes like its deformation and fluidity. This led to the decrease in the dimerization of EGFR and HER2, diminished receptor recycling capacity of cancer cells treated with ACC inhibitor and, finally, inhibition of proliferation. These data show, that targeting the membranes properties via inhibition of *de novo* lipogenesis is a promising approach concerning anti-cancer therapy.

9. REFERENCES

Abe F, Van Prooyen N, Ladasky JJ, Edidin M. *Interaction of Bap31 and MHC class I molecules and their traffic out of the endoplasmic reticulum.* J Immunol. 2009; 182(8): 4776-83

Amaravadi R, Kimmelman AC, White E. *Recent insights into the function of autophagy in cancer.* Genes Dev. 2016; 30: 1913–1930

Bayat Mokhtari R, Homayouni TS, Baluch N, Morgatskaya E, Kumar S, Das B, Yeger H. *Combination therapy in combating cancer.* Oncotarget. 2017; 8(23): 38022-38043

Best A, Dagliesh C, Ehrmann I, Kheirollahi-Kouhestani M, Tyson-Capper A and Elliott J. *Expression of Tra2β in cancer cells as a potential contributory factor to neoplasia and metastasis.* Int J Cell Biol. 2013; 2013:843781

Best A, James K, Dalgliesh C, Hong E, Kheirolahi-Kouhestani M, Curk T, Xu Y, Danilenko M, Hussain R, Keavney B, Wipat A, Klinck R, Cowell IG, Cheong Lee K, Austin CA, Venables JP, Chabot B, Santibanez Koref M, Tyson-Capper A, Elliott DJ. *Human Tra2 proteins jointly control a CHEK1 splicing switch among alternative and constitutivetarget exons.* Nat Commun. 2014; 5:4760

Bhat TA, Chaudhary AK, Kumar S, et al. *Endoplasmic reticulum-mediated unfolded protein response and mitochondrial apoptosis in cancer.* Biochim Biophys Acta. 2016; 1867(1):58-66

Braig S, Schmidt BUS, Stoiber K, Händel C, Möhn T, Werz O, Müller R, Zahler S, Koeberle A, Käs JA and Vollmar AM. *Pharmacological targeting of membrane rigidity: implications on cancer cell migration and invasion.* N J Phys. 2015; 17: 083007

Breckenridge DG, Stojanovic M, Marcellus RC, Shore GC. *Caspase cleavage product of BAP31 induces mitochondrial fission through endoplasmic reticulum calcium signals, enhancing cytochrome c release to the cytosol.* J Cell Biol. 2003; 160(7): 1115-27

Bryce NS, Hardeman EC, Gunning PW, Lock JG. *Chemical biology approaches targeting the actin cytoskeleton through phenotypic screening.* Curr Opin Chem Biol. 2019; 51: 40-47

Cano-González A, Mauro-Lizcano M, Iglesias-Serret D, Gil J, López-Rivas A. *Involvement of both caspase-8 and Noxa-activated pathways in endoplasmic reticulum stress-induced apoptosis in triple-negative breast tumor cells.* Cell Death Dis. 2018; 9(2): 134

Chen J, Guo H, Jiang H, Namusamba M, Wang C, Lan T, Wang T, Wang B. *A BAP31 intrabody induces gastric cancer cell death by inhibiting p27^{kip1} proteasome degradation.* Int J Cancer. 2019; 144(8): 2051-2062

Chen M, Lyu G, Han M, Nie H, Shen T, Chen W, Niu Y, Song Y, Li X, Li H, Chen X, Wang Z, Xia Z, Li W, Tian XL, Ding C, Gu J, Zheng Y, Liu X, Hu J, Wei G, Tao W, Ni T. *3′ UTR lengthening as a novel mechanism in regulating cellular senescence.* Genome Res. 2018 Feb 12

Chen SH, Lahav G. *Two is better than one; toward a rational design of combinatorial therapy.* Curr Opin Struct Biol. 2016; 41: 145–150

Chien CT, Bartel PL, Sternglanz R, Fields S. *The two-hybrid system: a method to identify and clone genes for proteins that interact with a protein of interest.* Proc Natl Acad Sci U S A. 1991; 88(21): 9578-82

Chonghaile TN, Sarosiek KA, Vo T-T, et al. *Pretreatment mitochondrial priming correlates with clinical response to cytotoxic chemotherapy.* Science 2011; 334(6059): 1129-1133

Clague MJ, Urbe S. *Ubiquitin: same molecule, different degradation pathways.* Cell. 2010; 143: 682–685

Clarke WR, Amundadottir L, James MA. *CLPTM1L/CRR9 ectodomain interaction with GRP78 at the cell surface signals for survival and chemoresistance upon ER stress in pancreatic adenocarcinoma cells.* Int J Cancer. 2019; 144(6): 1367-1378

Cooper GM. *The Cell: A Molecular Approach. 2nd edn.* Sinauer Associates: Sunderland, MA, USA

Dalloneau E, Pereira PL, Brault V, Nabel EG, Hérault Y. *Prmt2 regulates the lipopolysaccharide-induced responses in lungs and macrophages.* J Immunol. 2011; 187(9): 4826-34

Dang E, Yang S, Song C, Jiang D, Li Z, Fan W, Sun Y, Tao L, Wang J, Liu T, Zhang C, Jin B, Wang J, Yang K. *BAP31, a newly defined cancer/testis antigen, regulates proliferation, migration, and invasion to promote cervical cancer progression.* Cell Death Dis. 2018; 9(8): 791

Daoud R, Da Penha Berzaghi M, Siedler F, Hübener M, Stamm S. *Activity-dependent regulation of alternative splicing patterns in the rat brain.* European Journal of Neuroscience. 1999; 11:788–802

Dauwalder B, Amaya-Manzanares F, Mattox W. *A human homologue of the Drosophila sex determination factor transformer-2 has conserved splicing regulatory functions.* Proc Natl Acad Sci U S A. 1996; 93:9004–9

Decker P, Isenberg D, Muller S. *Inhibition of Caspase-3-mediated Poly(ADP-ribose) Polymerase (PARP) Apoptotic Cleavage by Human PARP Autoantibodies and Effect on Cells Undergoing Apoptosis.* The Journal of Biological Chemistry 2000; 275: 9043-9046

Diermeier S, Horváth G, Knuechel-Clarke R, Hofstaedter F, Szöllosi J, Brockhoff G. *Epidermal growth factor receptor coexpression modulates susceptibility to Herceptin in HER2/neu overexpressing breast cancer cells via specific erbB-receptor interaction and activation.* Exp Cell Res. 2005; 304(2): 604-19

Dufey E, Urraa H, Hetz C. *ER proteostasis addiction in cancer biology: Novel concepts.* Seminars in Cancer Biology 2015; 33: 40–47

ECIS - *European Cancer Information System* From https://ecis.jrc.ec.europa.eu, accessed on 03/04/2019 © European Union, 2019

Eirich J, Braig S, Schyschka L, Servatius P, Hoffmann J, Hecht S, Fulda S, Zahler S, Antes I, Kazmaier U, Sieber SA, Vollmar AM. *A Small Molecule Inhibits Protein Disulfide Isomerase and Triggers the Chemosensitization of Cancer Cells.* Angew Chem Int Ed Engl. 2014; 53(47): 12960-5

Elliott DJ., Best A., Dalgliesh C., Ehrmann I., and Grellscheid S., *How does Tra2beta protein regulate tissue-specific RNA splicing?* Biochemical Society Transactions 2012; 40: 784–788

Escriba PV, Busquets X, Inokuchi J, Balogh G, Torok Z, Horvath I, Harwood JL, Vigh L. *Membrane lipid therapy: Modulation of the cell membrane composition and structure as a molecular bas for drug discovery and new disease treatment.* Prog Lipid Res 2015; 59: 38-53

Escriba PV. *Membrane-lipid therapy: Modulation of the cell membrane composition and structure as a molecular base for drug discovery and new disease treatment.* Biochim Biophys Acta 2017; 1859: 1493-1506

Estornes Y, Aguileta MA, Dubuisson C, De Keyser J, Goossens V, Kersse K, Samali A, Vandenabeele P, Bertrand MJ. *RIPK1 promotes death receptor-independent caspase-8-mediated apoptosis under unresolved ER stress conditions.* Cell Death Dis. 2015; 6: e1798

Ferlay J, Colombet M, Soerjomataram I, Dyba T, Randi G, Bettio M, Gavin A, Visser O, Bray F. *Cancer incidence and mortality patterns in Europe: Estimates for 40 countries and 25 major cancers in 2018.* Eur J Cancer. 2018; 103:356-387.

Fields S & Song, O. *A novel genetic system to detect protein-protein interactions.* Nature 1989; 340: 245–247

Fukuda J, Kaneko T, Egashira M, Oshimi K. *Direct Measurement of CD34+ Blood Stem Cell Absolute Counts by Flow Cytometry.* Stem Cells 1998; 16: 294-300

Ganesh L, Yoshimoto T, Moorthy NC, Akahata W, Boehm M, Nabel EG, Nabel GJ. *Protein methyltransferase 2 inhibits NF-kappaB function and promotes apoptosis.* Mol Cell Biol. 2006; 26(10): 3864-74

Ghosh P, Grellscheid SN, Sowdhamini R. *A tale of two paralogs: human Transformer2 proteins with differential RNA-binding affinities.* J Biomol Struct Dyn. 2016; 34(9): 1979-86

Grellscheid S., Dalgliesh C., Storbeck M. et al*., Identification of evolutionarily conserved exons as regulated targets for the splicing activator Tra2β in development.* PLoS Genetics 2011; 7: 12, Article ID e1002390

Grimm S. *The ER–mitochondria interface: The social network of cell death.* Biochimica et Biophysica Acta 1823 (2012) 327–334

Guo J, Xia B, White E. *Autophagy-mediated tumor promotion.* Cell 2013; 155(6): 1216–1219

Haeussler M, Schönig K, Eckert H, Eschstruth A, Mianné J, Renaud JB, Schneider-MaunouryS, Shkumatava A, Teboul L, Kent J, Joly JS and Concordet JP. *Evaluation of off-target and on-target*

scoring algorithms and integration into the guide RNA selection tool CRISPOR. Genome Biology 2016; 17: 148

Hanahan D, Weinberg RA. *The hallmarks of cancer.* Cell. 2000; 100(1): 57-70

Hanahan D, Weinberg RA. *The hallmarks of cancer: the next generation.* Cell. 2011; 144(5):646-74

Holohan C, Van Schaeybroeck S, Longley DB, Johnston PG. *Cancer drug resistance: an evolving paradigm.* Nat Rev Cancer. 2013; 13(10): 714-26

Hsu PD, Scott DA, Weinstein JA, Ran FA, Konermann S, Agarwala V, Li Y, Fine JE, Wu X, Shalem O, Cradick TJ, Marraffini LA, Bao G & Zhang F. *DNA targeting specificity of RNA-guided Cas9 nucleases.* Nature Biotechnology 2013; 31: 827–832

Huo Y, Cai H, Teplova I, Bowman-Colin C, Chen G, Price S, Barnard N, Ganesan S, Karantza V, White E, et al. *Autophagy opposes p53-mediated tumor barrier to facilitate tumorigenesis in a model of PALB2-associated hereditary breast cancer.* Cancer Discov 2013; 3: 894–907

Ilan Y. Microtubules: *From understanding their dynamics to using them as potential therapeutic targets.* J Cell Physiol. 2019; 234(6): 7923-7937

Israël A. *The IKK Complex, a Central Regulator of NF-κB Activation.* Cold Spring Harb Perspect Biol. 2010; 2(3): a000158

Iwasawa R, Mahul-Mellier AL, Datler C, Pazarentzos E, Grimm S. *Fis1 and Bap31 bridge the mitochondria-ER interface to establish a platform for apoptosis induction.* EMBO J. 2011; 30(3): 556-68

Janczar S, Nautiyal J, Xiao Y, Curry E, Sun M, Zanini E, Paige AJ, Gabra H. *WWOX sensitises ovarian cancer cells to paclitaxel via modulation of the ER stress response.* Cell Death Dis. 2017; 8(7): e2955.

Jung CH, Ro SH, Cao J, Otto NM, Kim DH. *mTOR regulation of autophagy.* FEBS Lett. 2010; 584(7): 1287-95

Kajita K, Kuwano Y, Satake Y, Kano S, Kurokawa K, Akaike Y, Masuda K, Nishida K, Rokutan K. *Ultraconserved region – containing Transformer 2β4 controls senescence of colon cancer cells.* Oncogenesis. 2016; 5: e213

Kaneko M, Imaizumi K, Saito A, Kanemoto S, Asada R, Matsuhisa K, Ohtake Y. *ER Stress and Disease: Toward Prevention and Treatment.* Biol. Pharm. Bull. 2017; 40: 1337–1343

Kim KM., Adachi T., Nielsen P. J., Terashima M., Lamers M. C., Köhler G., and Reth M. *Two new proteins preferentially associated with membrane immunoglobulin D.* EMBO J. 1994; 13, 3793–3800.

Kobayashi S, Boggon TJ, Dayaram T, Janne PA, Kocher O, Meyerson M, Johnson BE, Eck MJ, Tenen DG, Halmos B *EGFR mutation and resistance of non-small-cell lung cancer to gefitinib*. *New Engl J Med.* 2005; 352: 786–792.

Ladasky JJ, Boyle S, Seth M, Li H, Pentcheva T, Abe F, Steinberg SJ, Edidin M. *Bap31 enhances the endoplasmic reticulum export and quality control of human class I MHC molecules.* J Immuno. 2006; 177(9): 6172-81

Lee E, Lee DH. *Emerging roles of protein disulfide isomerase in cancer.* BMB Rep. 2017; 50(8): 401–410

Levine B, Kroemer G. *Autophagy in the pathogenesis of disease*. Cell. 2008; 132: 27–42

Levy J, Cacheux W, Bara MA, L'Hermitte A, Lepage P, Fraudeau M, Trentesaux C, Lemarchand J, Durand A, Crain AM, et al. *Intestinal inhibition of Atg7 prevents tumour initiation through a microbiome-influenced immune response and suppresses tumour growth.* Nat Cell Biol 2015; 17: 1062–1073

Levy JM, Towers CG and Thorburn A. *Targeting Autophagy in Cancer.* Nat Rev Cancer. 2017; 17(9): 528–542

Li P, Nijhawan D, Budihardjo I, Srinivasula SM, Ahmad M, Alnemri ES, Wang X. *Cytochrome c and dATP-dependent formation of Apaf-1/caspase-9 complex initiates an apoptotic protease cascade.* Cell. 1997;91(4):479-89

Linjing Li, Xinyue Liu, Liye Zhou, Wei Wang, Zhuan Liu, Yan Cheng, Jing Li, and Hulai Wei. *Autophagy Plays a Critical Role in Insulin Resistance- Mediated Chemoresistance in Hepatocellular Carcinoma Cells by Regulating the ER Stress.* J Cancer. 2018; 9(23): 4314–4324

Ma C, Jin RM, Chen KJ, Hao T, Li BS, Zhao DH, Jiang H. *Low expression of B-Cell-Associated protein 31 is associated with unfavorable prognosis in human colorectal cancer.* Pathol Res Pract. 2018; 214(5): 661-666

Ma X, Dang C, Min W, Diao Y, Hui W, Wang X, Dai Z, Wang X, Kang H. *Downregulation of APE1 potentiates breast cancer cells to olaparib by inhibiting PARP-1 expression.* Breast Cancer Res Treat. 2019 Apr 15

Ma XH, Piao S, Wang D, McAfee QW, Nathanson KL, Lum JJ, Li LZ, Amaravadi RK. *Measurements of tumor cell autophagy predict invasiveness, resistance to chemotherapy, and survival in melanoma.* Clin Cancer Res 2011; 17: 3478–3489

Madden E, Logue SE, Healy SJ, Manie S, Samali A. *The role of the unfolded protein response in cancer progression: From oncogenesis to chemoresistance.* Biol Cell. 2019; 111(1): 1-17

Matlin AJ, Clark F, Smith CWJ. *Understanding alternative splicing: towards a cellular code.* Nat Rev Mol Cell Biol. 2005; 6:386–398

Menendez JA, Vellon L, Lupu R. *The antiobesity drug Orlistat induces cytotoxic effects, suppresses Her-2/neu (erbB-2) oncogene overexpression, and synergistically interacts with trastuzumab (Herceptin) in chemoresistant ovarian cancer cells.* Int J Gynecol Cancer 2006; 16: 219–221.

Mizushima N. *The role of the Atg1/ULK1 complex in autophagy regulation.* Curr Opin Cell Biol. 2010; 22: 132–139

Mowers EE, Sharifi MN and Macleod KF. *Autophagy in cancer metastasis.* Oncogene 2017; 36(12): 1619–1630

Muñoz-Pinedo C. and López-Rivas A. *A role for caspase-8 and TRAIL-R2/DR5 in ER-stress-induced apoptosis.* Cell Death Differ. 2018; 25(1): 226.

Nicoletti I, Migliorati G, Pagliacci MC, Grignani F, Riccardi C. *A rapid and simple method for measuring thymocyte apoptosis by propidium iodide staining and flow cytometry.* J Immunol Methods. 1991;139(2):271-9

Nicolson GL. *Cell Membrane Fluid–Mosaic Structure and Cancer Metastasis.* Cancer Res. 2015; 75(7): 1169-76

Paquette M, El-Houjeiri L, Pause A. *mTOR Pathways in Cancer and Autophagy.* Cancers (Basel) 2018; 10(1): 18

Park MH, Hong JT. Roles of NF-κB in Cancer and Inflammatory Diseases and Their Therapeutic Approaches. Cells 2016; 5(2): 15

Quaresma M, Coleman MP, Rachet B. *40-year trends in an index of survival for all cancers combined and survival adjusted for age and sex for each cancer in England and Wales, 1971-2011: a population-based study.* Lancet. 2015; 385(9974):1206-18.

Ran FA, Hsu PD, Wright J, Agarwala V, Scott DA and Zhang F. *Genome engineering using the CRISPR-Cas9 system.* Nat Protoc. 2013; 8(11): 2281–2308

Rauscher AÁ, Gyimesi M, Kovács M, Málnási-Csizmadia A. *Targeting Myosin by Blebbistatin Derivatives: Optimization and Pharmacological Potential.* Trends Biochem Sci. 2018; 43(9): 700-713

Ray S, Kassan A, Busija AR, Rangamani P, Patel HH. *The plasma membrane as a capacitor for energy and metabolism.* Am J Physiol Cell Physiol 2016; 310: C181-C192.

Remmerbach TW, Wottwah F, Dietrich J, Lincoln B, Wittekind C, Guck J. *Oral cancer diagnosis by mechanical phenotyping.* Cancer Res. 2009; 69: 1728-1732

Rysman E, Brusselmans K, Scheys K, Timmermans L, Derua R, Munck S, Van Veldhoven PP, Waltregny D, Daniëls VW, Machiels J, Vanderhoydonc F, Smans K, Waelkens E, Verhoeven G, Swinnen JV. *De novo lipogenesis protects cancer cells from free radicals and chemotherapeutics by promoting membrane lipid saturation.* Cancer Res 2010; 70: 8117–8126

Santanam U, Banach-Petrosky W, Abate-Shen C, Shen MM, White E, DiPaola RS. *Atg7 cooperates with Pten loss to drive prostate cancer tumor growth.* Genes Dev 2016; 30: 399–407

Satake Y, Kuwano Y, Nishikawa T, Fujita K, Saijo S, Itai M, Tanaka H, Nishida K, Rokutan K. *Nucleolin facilitates nuclear retention of an ultraconserved region containing TRA2β4 and accelerates colon cancer cell growth.* Oncotarget. 2018; 9(42): 26817-26833

Schamel WW, Kuppig S, Becker B, Gimborn K, Hauri HP, Reth M. *A high-molecular-weight complex of membrane proteins BAP29/BAP31 is involved in the retention of membrane-bound IgD in the endoplasmic reticulum.* Proc Natl Acad Sci U S A. 2003; 100(17): 9861-6

Seo SR, Lee HM, Choi HS, Kim WT, Cho EW, Ryu CJ. *Enhanced expression of cell-surface B-cell receptor-associated protein 31 contributes to poor survival of non-small cell lung carcinoma cells.* PLoS One. 2017; 12(11): e0188075

Shah PP, Dupre TV, Siskind LJ, Beverly LJ1. *Common cytotoxic chemotherapeutics induce epithelial-mesenchymal transition (EMT) downstream of ER stress.* Oncotarget. 2017; 8(14): 22625-22639.

Sherbet GV. *Membrane fluidity and cancer metastasis.* Exp Cell Biol. 1989; 57(4): 198-205

Shore GC, Papa FR, Oakes SA. *Signaling cell death from the endoplasmic reticulum stress response.* Curr Opin Cell Biol. 2011; 23(2): 143-149

Simmen T, Herrera-Cruz MS. *Cancer: Untethering Mitochondria from the ER?* Front Oncol. 2017; 7: 105

Svensson RU, Parker SJ, Eichner LJ, Kolar MJ, Wallace M, Brun SN, Lombardo PS, Van Nostrand JL, Hutchins A, Vera L, Gerken L, Greenwood J, Bhat S, Harriman G, Westlin WF, Harwood HJ Jr., Saghatelian A, Kapeller R, Metallo CM, Shaw RJ. *Inhibition of acetyl-CoA carboxylase suppresses fatty acid synthesis and tumor growth of non-small-cell lung cancer in preclinical models.* Nat Med 2016; 22: 1108–1119.

Swaminathan V, Mythreye K, O'Brien ET, Berchuck A, Blobe GC, Superfine R. *Mechanical stiffness grades metastatic potential in patient tumor cells and in cancer cell lines.* Cancer Res. 2011; 71(15): 5075-80

Tait SW, Green DR. *Mitochondria and cell death: outer membrane permeabilization and beyond.* Nature reviews Molecular cell biology 2010; 11(9): 621-632

Tan N, Liu Q, Liu X, Gong Z, Zeng Y, Pan G, Xu Q, He S. *Low expression of B-cell-associated protein 31 in human primary hepatocellular carcinoma correlates with poor prognosis.* Histopathology. 2016; 68(2): 221-9

Terziyska N, Alves CC, Groiss V, et al**.** *In vivo Imaging Enables High Resolution Preclinical Trials on Patients' Leukemia Cells Growing in Mice.* PLoS ONE. 2012;7(12): e52798

Tomas A, Futter CE, Eden ER. *EGF receptor trafficking: consequences for signaling and cancer.* Trends Cell Biol 2014; 24: 26–34.

Tong D, Liang YN, Stepanova AA, Liu Y, Li X, Wang L, Zhang F, Vasilyeva NV. *Increased Eps15 homology domain 1 and RAB11FIP3 expression regulate breast cancer progression via promoting epithelial growth factor receptor recycling.* Tumour Biol. 2017; 39:1010428317691010

Vatolin S, Phillips JG, Jha BK, Govindgari S, Hu J, Grabowski D, et al. *Novel Protein Disulfide Isomerase Inhibitor with Anticancer Activity in Multiple Myeloma.* Cancer Research 2016; 76(11): 3340-3350.

Vick B, Rothenberg M, Sandhöfer N, et al. *An advanced preclinical mouse model for acute myeloid leukemia using patients' cells of various genetic subgroups and in vivo bioluminescence imaging.* PLoS ONE. 2015;10(3): e0120925

Wakana Y, Takai S, Nakajima K, Tani K, Yamamoto A, Watson P, Stephens DJ, Hauri HP, Tagaya M. *Bap31 is an itinerant protein that moves between the peripheral endoplasmic reticulum (ER) and a juxtanuclear compartment related to ER-associated Degradation.* Mol Biol Cell. 2008; 19(5): 1825-36

Wang A, Zhang Y, Cao P. *Inhibition of BAP31 expression inhibits cervical cancer progression by suppressing metastasis and inducing intrinsic and extrinsic apoptosis.* Biochem Biophys Res Commun. 2019; 508(2): 499-506

Wang B, Nguyen M, Chang NC, Shore GC. *Fis1, Bap31 and the kiss of death between mitochondria and endoplasmic reticulum.* EMBO J. 2011; 30(3): 451-2

Watermann DO. *Splicing Factor Tra2-1 Is Specifically Induced in Breast Cancer and Regulates Alternative Splicing of the CD44 Gene.* Cancer Res. 2006; 66:4774–4780

White E. *Deconvoluting the context-dependent role for autophagy in cancer.* Nature reviews Cancer. 2012; 12: 401–410

Wijdeven RH, Pang B, Assaraf Y.G, Neefjes J. *Old drugs, novel ways out: Drug resistance toward cytotoxic chemotherapeutics.* Drug Resist Updat. 2016; 28: 65-81.

Wright C, Iyer AKV, Kaushik V, Azad N. *Anti-tumorigenic potential of a novel orlistat-AICAR combination in prostate cancer cells.* J Cell Biochem 2017; 118: 3834–3845

Xia Y, Shen S, Verma IM. *NF-κB, an active player in human cancers.* Cancer Immunol Res. 2014; 2(9): 823-30

Xu K, Han B, Bai Y, Ma XY, Ji ZN, Xiong Y, Miao SK, Zhang YY, Zhou LM. *MiR-451a suppressing BAP31 can inhibit proliferation and increase apoptosis through inducing ER stress in colorectal cancer.* Cell Death Dis. 2019; 10(3): 152

Xu S, Butkevich AN, Yamada R, Zhou Y, Debnath B, Duncan R, et al. *Discovery of an orally active small-molecule irreversible inhibitor of protein disulfide isomerase for ovarian cancer treatment.* Proceedings of the National Academy of Sciences 2012; 109 (40): 16348-16353.

Yadav N, Kumar S, Marlowe T, Chaudhary A, Kumar R, Wang J, et al. *Oxidative phosphorylation - dependent regulation of cancer cell apoptosis in response to anticancer agents.* Cell death & disease 2015; 6(11): e1969

Yang S, Wang X, Contino G, Liesa M, Sahin E, Ying H, Bause A, Li Y, Stommel JM, Dell'antonio G, et al. *Pancreatic cancers require autophagy for tumor growth.* Genes Dev 2011; 25: 717–729

Yu S, Wang F, Fan L, Wei Y, Li H, Sun Y, Yang A, Jin B, Song C, Yang K. *BAP31, a promising target for the immunotherapy of malignant melanomas.* J Exp Clin Cancer Res. 2015; 34:36

Zalba S. and Hagen TLM. *Cell membrane modulation as adjuvant in cancer therapy.* Cancer Treatment Reviews 2017; 52: 48–57

Zen K, Utech M, Liu Y, Soto I, Nusrat A, Parkos CA. *Association of BAP31 with CD11b/CD18. Potential role in intracellular trafficking of CD11b/CD18 in neutrophils.* J Biol Chem. 2004; 279(43): 44924-30

Zhang Z, Singh R, Aschner M. *Methods for the Detection of Autophagy in Mammalian Cells.* Curr Protoc Toxicol. 2017; 69: 20.12.1-20.12.26

Zhang Z, Zhang L, Zhou L, Lei Y, Zhang Y, Huang C. *Redox signaling and unfolded protein response coordinate cell fate decisions under ER stress.* Redox Biol. 2018: S2213-2317(18)30895-4

Zhang Z, Yu L, Dai G, Xia K, Liu G, Song Q, Tao C, Gao T, Guo W. *Telomerase reverse transcriptase promotes chemoresistance by suppressing cisplatin-dependent apoptosis in osteosarcoma cells.* Sci Rep. 2017; 7(1): 7070

Zheng HC. *The molecular mechanisms of chemoresistance in cancers.* Oncotarget. 2017; 8(35): 59950-59964

Zhou Y, Tozzi F, Chen J, Fan F, Xia L, Wang J. *Intracellular ATP levels are a pivotal determinant of chemoresistance in colon cancer cells.* Cancer Res. 2012; 72(1): 304–14.

Zhu X, Huang L, Gong J, Shi C, Wang Z, Ye B, Xuan A, He X, Long D, Zhu X, Ma N and Leng S. *NF-κB pathway link with ER stress-induced autophagy and apoptosis in cervical tumor cells.* Cell Death Discovery 2017; 3: 17059

Zou H, Henzel WJ, Liu X, Lutschg A, Wang X. *Apaf-1, a human protein homologous to C. elegans CED-4, participates in cytochrome c-dependent activation of caspase-3.* Cell. 1997;90(3):405-13

10. CURRICULUM VITAE

OLGA NAGŁO

Email: *olga.chojnacka@gmail.com*

EDUCATION

2016 – now,

Munich Ludwig Maximilian University of Munich / PhD studies

Doctoral studies at Ludwig Maximilian University of Munich, Faculty of Chemistry and Pharmacy, Department of Pharmacy – Center for Drug Research, Pharmaceutical biology

2011-2013,

Cracow Jagiellonian University / Master studies

Master studies at Jagiellonian University in Cracow, Faculty of Biology and Earth Sciences with specialization in Genetics and Biology of Reproduction

2008 – 2011,

Cracow Jagiellonian University / Bachelor studies

Bachelor studies at Jagiellonian University in Cracow, Faculty of Biology and Earth Sciences, field of Biology

2005 – 2008,

Strzelce Opolskie High School of the Departments Bilingual/ High school

High School of the Departments Bilingual, them. Władysław Broniewski, profile bio-chemical

PUBLICATIONS

Jagielska E, <u>Chojnacka O</u>, Sabała I. "*LytM fusion with SH3b-like domain restore its activity in physiological conditions*", Microb Drug Resist. 2016 Sep;22(6):461-9. doi: 10.1089/mdr.2016.0053.

Stoiber K, <u>Nagło O</u>, Pernpeintner C, Zhang S, Koeberle A, Ulrich M, Werz O, Müller R, Zahler S, Lohmüller T, Feldmann J, Braig S. "*Targeting de novo lipogenesis as a novel approach in anti-cancer therapy.*", Br J Cancer. 2018 Jan;118(1):43-51. doi: 10.1038/bjc.2017.374

Koczian F, <u>Nagło O</u>, Vomacka J, Vick B, Servatius P, Zisis T, Hettich B, Kazmaier U, Sieber SA, Jeremias I, Zahler S, Braig S. "*Targeting the ER-mitochondria interface sensitizes leukemia cells towards cytostatics.*", Haematologica. 2019 Mar;104(3):546-555. doi: 10.3324/haematol.2018.197368.

ACTIVITIES

2015 – 2019

Member of Polish Laboratory Animal Science Association (PolLASA)

2016 – 2019

Member of Life Science Munich (LSM) Graduate School

AWARDS

Deutscher Akademisher Austauschdienst (DAAD) scholarship

COURSES TAKEN

- ✓ Training for people taking care of experimental animals organized by Warsaw University: Department of Biology and Polish Laboratory Animal Science Association (PolLASA);
- ✓ Health and Colony Management of Laboratory Fish 2015, organized by MDI Biological Laboratory, Salisbury Cove, Maine, USA;

- ✓ German course at Ludwig Maximilian University of Munich – up to B2 level;
- ✓ Course on GraphPad software organized by Life Science Munich (LSM) graduate school;
- ✓ Good Manufacturer Practice (GMP) course organized by Life Science Munich (LSM) graduate school;

CONFERENCE PRESENTATIONS

32nd Euro Congress on Cancer Science & Therapy, Barcelona, Spain - poster presentation

LANGUAGES

Polish - native

English - fluent

German - good (B2)